

Phagocytosis and MHC II antigen presentation by human $\gamma\delta$ T cells

Luísa de Jesus Saraiva

Molecular Immunology Unit

UCL Institute of Child Health

London

A thesis submitted for the degree of Doctor of Philosophy

August 2014

Declaration

I, Luísa de Jesus Saraiva, confirm that the work presented in this thesis is my own. Where information has been derived from other sources, I confirm that this has been indicated in the thesis.

1 Abstract

$\gamma\delta$ T cells are a rare subset of T cells present in human blood and lymphoid tissues. Functionally, they stand at the interface of the innate and the acquired branch of the immune system as they express somatically rearranged antigen receptors but they also share many characteristics with NK cells. One of those is the ability to express CD16. CD16 is a cell-surface receptor that binds the Fc portion of IgG. In the isoform found on tissue macrophages and NK cells it is coupled to an intracellular signalling domain that allows it to initiate cellular processes leading to the internalisation of IgG-coated particles or cytotoxicity against IgG-coated cells. Therefore, it has a role in the clearance of IgG-coated complexes and the destruction of infected or malignant cells. In this thesis, I show that a population of $\gamma\delta$ T cells present in human blood from healthy donors express the CD16 receptor and implicate a role for this receptor in phagocytosis of IgG-coated bacteria and synthetic beads coated with recombinant influenza M1 protein. These cells were subsequently shown to activate influenza-specific T cells through MHC II presentation. Importantly, neither $\alpha\beta$ T cells nor NK cells were capable of significant phagocytosis. In addition, once CD11c⁺ cells had been removed from the NK fraction, neither $\alpha\beta$ T cells or NK cells were capable of MHC II antigen presentation of influenza M1 antigen. The CD16⁺ $\gamma\delta$ T cells displayed a phenotype of effector memory and late effector memory T cells suggesting a role for these cells in patrolling the blood and rapidly migrating to sites of inflammation for a combination of rapid effector and antigen presentation function.

Acknowledgments

First and foremost I would like to thank my supervisor Dr Kenth Gustafsson for taking me on as a student and for his endless enthusiasm and open-minded approach to science. This project would not have been possible without his patience and encouragement and many helpful intellectual discussions. I would also like to thank my co-supervisor Dr Siobhan Burns for taking me on first as a research assistant and then as a PhD student and for actively training me to become technically competent and providing guidance on the direction of research. I would also like to acknowledge the extensive contribution of Dr Conrad Vink as an editor throughout the re-drafting process, whose constructive criticism greatly improved the standard of this document.

I would like to thank Dr Yin Wu whose intellectual contributions made this project possible in the first place. In addition, I would like to acknowledge Dr Ayad Eddaoudi for technical assistance with flow cytometry and cell sorting and Dr Bertrand Vernais for technical assistance with confocal microscopy, Julien Record and Dr Dale Moulding for helping me with the granulocyte isolation, staining and microscopy, and Dr Giorgia Santilli for helping me with the NBT assays. I am also thankful to Flávio Saraiva for writing a randomising software to score microscopy data, to Dr Marlene Carmo for helping me with the chromium release assays, and to Dr Holly Stephenson for training me in the gentamicin protection assay.

A warm thank you to all the blood donors that contributed to this work and to the many members of MIU who make it a good place to work in. In particular, thank you to Dr João Metelo and João Nunes for patiently training me during the time I spend working with them and for their warm hospitality. Thanks to Aris whose 6 am thesis starts whilst doing army duty provided a standard no subsequent PhD student can hope to match. Thank you to Maria Manunta for enduring tango lessons whilst trying to ignore her foot needed medical attention. Thank you to Fran and Gavin for being the best desk neighbours. Thank you to Mus for his unshakable drive. Thank you to Sarah for her endless optimism and energy. Thank you to Ida for her encouragement and for showing us you can have it all. In addition, thank you to the rest of the MIU crowd in the upstairs offices for boozy Friday pub outings and over-ambitious cycling missions.

Thank you to the friends that keep me grounded and remind me of other times, scattered they may be around the world. A special thank you to Ana Luísa in Stockholm and Lina in Zurich. Thank you for your moral support, advice and laughter. Thank you also to Miguel, Catarina, Diana, Daniela, João Nascimento, Marta and Rita who liven up going back home.

Thank you to my mum for being such an inspiration throughout her life's struggles, and for completing her own PhD with three demanding children at her back. Thank you to my dad for his independent thinking and integrity and his selfless love and kindness. Thank you to my brother Flávio and my sister Inês for believing that there is no such thing as too much education!

To Conrad, thank you for keeping me sane and hopeful when times were rough and for making every day brighter.

List of Figures

Figure 4.1 – Detection of phagocytosis of opsonised green fluorescent <i>E. coli</i> by $\gamma\delta$ T cells using confocal microscopy	74
Figure 4.2 – Distinguishing intracellular <i>E. coli</i> from surface bound <i>E. coli</i> by confocal microscopy z-stacks	75
Figure 4.3 – Examples of confocal microscopy z-stacks where the distinction between intracellular <i>E. coli</i> and surface bound <i>E. coli</i> is ambiguous	76
Figure 4.4 – Discrimination between intra and extracellular <i>E. coli</i> associated with $\gamma\delta$ T cells using dual fluorescence flow cytometry.....	79
Figure 4.5 – Establishment of live GFP-expressing <i>E. coli</i> cultures as an alternative to lyophilised fluorescein-labelled <i>E. coli</i> for the study of phagocytosis in $\gamma\delta$ T cells.....	82
Figure 4.6 – Comparing phagocytosis of lyophilised fluorescein- <i>E. coli</i> and live GFP- <i>E. coli</i> by confocal microscopy	83
Figure 4.7 – Internalisation of opsonised live <i>E. coli</i> by $\gamma\delta$ T cells is detected in a standard gentamicin protection assay	86
Figure 4.8 – Comparative quantification of phagocytosis of highly purified leukocyte fractions using blind-scored confocal microscopy images	90
Figure 4.9 – A population of CD3+ $\gamma\delta$ TCR+ cells in whole blood can phagocytose opsonised GFP-expressing <i>E. coli</i>	94
Figure 4.10 – Characteristics of phagocytosing and non-phagocytosing CD3+ $\gamma\delta$ TCR+ cells in the whole blood phagocytosis assay	97
Figure 4.11 – Phagocytosing CD3+ $\gamma\delta$ TCR+ cells in whole blood produce reactive oxygen species.....	99
Figure 4.12 - Human blood $\gamma\delta$ T cells include cells with unusual dendritic-like extensions	100
Figure 4.13 – Phagocytosing CD3+ $\gamma\delta$ TCR+ cells in whole blood have unusual morphology.....	103
Figure 4.14 – Purity assessment of FACS sorted $\gamma\delta$ T cells by flow cytometry	107
Figure 4.15 – Purity of non-phagocytic and phagocytic FACS sorted $\gamma\delta$ T cells.....	108
Figure 4.16 – The CD3/ $\gamma\delta$ TCR complex is not expressed in human neutrophils or eosinophils.....	112
Figure 4.17 – The $\gamma\delta$ TCR is not expressed by polymorphonucleated cells	113
Figure 5.1 – Class II presentation of M1 influenza antigen by $\gamma\delta$ T cells.....	125
Figure 5.2 – $\gamma\delta$ T cells present significantly more M1 influenza antigen than other lymphocytes.....	128
Figure 5.3 – Antigen presentation was seen in some wells of NK cells directly isolated with CD56 beads but not when NK cells were isolated by depletion of non-NK cell types	132

Figure 5.4 – Comparison of antigen presentation by freshly isolated $\gamma\delta$ T cells and $\gamma\delta$ T cells which have undergone $\gamma\delta$ T APC maturation	135
Figure 5.5 – CD16, class II antigen presentation markers and co-stimulatory molecules on $\gamma\delta$ T cells	138
Figure 6.1 – Separate $\gamma\delta$ T cell populations identified by flow cytometry based on $\gamma\delta$ TCR versus CD3 staining	150
Figure 6.2 – CD16 is expressed on $\gamma\delta$ T cells in human blood.	153
Figure 6.3 – CD16+ $\gamma\delta$ T cells present in the blood of healthy donors preferentially display an effector memory T cell phenotype.	157
Figure 6.4 – Target cell antigen may be acquired by $\gamma\delta$ T cells through ADCC interactions	161
Figure 6.5 – mab2G12 binds HIV-1 gp120 on the surface of HIV-infected targets.....	164
Figure 6.6 – Development of a non-radioactive flow cytometry based cytotoxicity assay.	168
Figure 6.7 – Antibody-dependent cellular cytotoxicity was not detected with mab2G12 opsonised HIV-infected H9 targets.....	171
Figure 6.8 – $\gamma\delta$ T cells and NK cells show high cell-mediated cytotoxicity against the H9 lymphoma cell line.....	172
Figure 6.9 – HIV-1 RT is presented by MHC class II in monocytes after co-culture with opsonised HIV-1 infected targets.	175
Figure 6.10 – Activated MHC class II+ $\gamma\delta$ T cells did not present HIV-1 RT after co-culture with opsonised HIV-1 infected targets	176
Figure 6.11 - Comparison of MHC class II presentation of HIV-1 RT by freshly isolated $\gamma\delta$ T cells and monocytes from the same donor.	177

Table of Contents

Phagocytosis and MHC II antigen presentation by human $\gamma\delta$ T cells.....	1
Declaration.....	2
1 Abstract.....	3
Acknowledgments.....	4
List of Figures.....	6
Table of Contents.....	8
List of Tables.....	11
Abbreviations.....	12
2 Introduction.....	15
2.1 Phagocytosis.....	15
2.2 Cell-mediated cytotoxicity.....	21
2.3 Antigen presentation.....	25
2.4 $\gamma\delta$ T cells.....	27
2.4.1 $\gamma\delta$ TCR antigen recognition.....	28
2.4.2 The functions of $\gamma\delta$ T cells in the immune response.....	34
2.4.3 Phagocytosis by $\gamma\delta$ T cells.....	42
2.4.4 Antigen presentation by $\gamma\delta$ T cells to $\alpha\beta$ T cells.....	46
3 Materials and Methods.....	51
3.1 Materials.....	51
3.1.1 Cell isolation.....	51
3.1.2 Bacteria and bacterial growth media.....	51
3.1.3 Cell lines and cell culture media.....	52
3.1.4 Buffers and solutions.....	53
3.1.5 Antibodies.....	55
3.1.6 Kits and miscellaneous.....	57
3.2 Methods.....	58
3.2.1 Tissue culture.....	58
3.2.2 Flow cytometry.....	60
3.2.3 Fluorescence confocal microscopy.....	63

3.2.4	Microbiology	66
3.2.5	Nitroblue tetrazolium (NBT) test	68
3.2.6	Diff-Quick staining	69
3.2.7	Western blot.....	69
3.2.8	Chromium release assay.....	70
3.2.9	Antigen presentation assay.....	70
3.2.10	Statistical analysis.....	71
4	Phagocytosis by $\gamma\delta$ T cells	72
4.1	Aims	72
4.2	Introduction.....	72
4.3	Confocal microscopy of phagocytosis of opsonised fluorescein-labelled <i>E. coli</i> by $\gamma\delta$ T cells	73
4.4	Quantification of phagocytosis by $\gamma\delta$ T cells using a dual labelling flow cytometry assay	77
4.5	GFP-expressing live <i>E. coli</i> can be used to quantify phagocytosis	80
4.6	Internalisation of opsonised live <i>E. coli</i> by $\gamma\delta$ T cells can be detected in a standard gentamicin protection assay	84
4.7	Comparative quantification of phagocytosis of highly purified leukocyte fractions using blind scoring of confocal microscopy images.....	87
4.8	A population of CD3+ $\gamma\delta$ TCR+ cells in whole blood can phagocytose opsonised GFP-expressing <i>E. coli</i>	91
4.9	Phagocytosing CD3+ $\gamma\delta$ TCR+ cells in whole blood produce reactive oxygen species	98
4.10	Phagocytosing CD3+ $\gamma\delta$ TCR+ cells in whole blood have unusual morphology 100	
4.11	Purity assessment of FACS sorted fractions of CD3+ $\gamma\delta$ TCR+ cells	104
4.12	The $\gamma\delta$ TCR is not expressed on polymorphonucleated fractions in whole blood 109	
4.13	Summary.....	114
5	MHC class II antigen presentation by $\gamma\delta$ T cells.....	120
5.1	Aims	120
5.2	Introduction.....	120
5.3	$\gamma\delta$ T cells can present influenza M1 antigen to specific CD4 T cell hybridomas in a chloroquine-sensitive, HLA-DR restricted manner.....	123

5.4	$\gamma\delta$ T cells induce influenza M1-specific CD4 T cell responses significantly more than other T cells or NK cells	126
5.5	Antigen presentation signals seen in the NK fractions disappear when these are depleted of CD11c+ cells.....	129
5.6	Antigen presentation by freshly isolated versus activated $\gamma\delta$ T cells.....	133
5.7	Antigen presentation markers and CD16 on antigen presenting $\gamma\delta$ T cells.....	136
5.8	Summary.....	139
6	Cytotoxicity and antigen presentation by $\gamma\delta$ T cells in an HIV-1 model.....	141
6.1	Aims	141
6.2	Introduction.....	141
6.3	Sub-populations of $\gamma\delta$ T cells expressing different $\gamma\delta$ TCR/CD3 levels and different $\gamma\delta$ TCR/CD3 stoichiometry	148
6.4	Fc γ RIII (CD16) expression on $\gamma\delta$ T cells.....	151
6.5	Differentiation status of CD16+ $\gamma\delta$ T cells.....	154
6.6	Acquisition of target cell antigen through ADCC interactions.....	158
6.7	Opsonisation of HIV-1 infected cells with mab2G12.....	162
6.8	Development and validation of a non-radioactive flow cytometry based assay to test cell-mediated cytotoxicity against HIV-1 infected cells	165
6.9	Antibody-mediated cellular cytotoxicity against mab2G12 opsonised HIV-1 infected cells	169
6.10	MHC II presentation of antigen acquired from mab2G12 opsonised HIV-1 infected cells.....	173
6.11	Summary.....	178
7	Discussion.....	184
8	References.....	193

List of Tables

Table 1 – Human receptors mediating phagocytosis of pathogens, and their ligands.....	18
Table 2 – Selected ligands and human receptors capable of inducing cell-mediated cytotoxicity	23
Table 3 – $\gamma\delta$ TCR ligands in man and mouse.....	29
Table 4 – Reagents used for the isolation of cells from whole blood.....	51
Table 5 – Reagents used for the culture of mammalian cells	52
Table 6 – Buffers and solutions used throughout this study.....	53
Table 7 – Antibodies used throughout this study.....	55
Table 8 – Other reagents	57
Table 9 – Antibody staining for comparative flow cytometry phagocytosis assay.....	62
Table 10 – Antibody staining for FACS sorting of magnetically isolated fractions	65

Abbreviations

7-AAD – 7-amino-actinomycin	DCs – dendritic cells
ADCC – antibody-dependent cellular cytotoxicity	ddH ₂ O – double distilled water
Ag – antigen	DMA – 5-(N,N-Dimethyl)amiloride hydrochloride
APC – allophycocyanin	DMEM - Dulbecco's Modified Eagle Medium
APCs – antigen presenting cells	DNA – deoxyribonucleic acid
BAT3 – human leukocyte antigen B-associated transcript 3	DPBS – Dulbecco's phosphate buffered saline
B-LCL – B lymphoblastoid cell line	DTT - dithiothreitol
BSA – bovine serum albumin	<i>E. coli</i> – <i>Escherichia coli</i>
CCR5 – C-C chemokine receptor type 5	EDTA - ethylene diamine triacetic acid
CCR6 – C-C chemokine receptor type 6	ELISA - enzyme-linked immunosorbent assay
CCR7 – C-C chemokine receptor type 7	Env – human immunodeficiency virus envelope protein
CD40L – CD40 ligand	ER – endoplasmic reticulum
CD62L – CD62 ligand	FACS - fluorescence activated cell sorter
CDR3 – complementary determining region 3	F-actin – filamentous actin
CFSE – carboxyfluorescein succinimidyl ester	FCS – fetal calf serum
CFU – colony forming units	FITC – fluorescein isothiocyanate
CGD – chronic granulomatous disease	FSC – forward light scatter
CL3 – containment level 3	GFP – green fluorescent protein
CLIP – class II-associated peptide	HA – hemagglutinin
CMV – human cytomegalovirus	HH – human immunodeficiency virus-infected H9 cells
CXCR3 – CXC chemokine receptor type 3	HIV – human immunodeficiency virus
DAPI – 4',6-Diamidino-2-Phenylindole	

HIV-1 RT – human immunodeficiency virus 1 reverse transcriptase

HLA-DR – human leukocyte antigen-D related

HMB-PP – (E)-4-hydroxy-3-methyl-but-2-enyl pyrophosphate

HRP – horseradish peroxidase

ICAM-1 – Intercellular adhesion molecule 1

IFN- γ – interferon γ

Ig – immunoglobulin

IgG – immunoglobulin G

IgM – immunoglobulin M

IL-17A – interleukin 17A

IL-1 β – interleukin 1 β

IL-2 – interleukin 2

IL-23 – interleukin 23

IL-6 – interleukin 6

IPP – isopentenyl pyrophosphate

IPTG - isopropyl β -D-thiogalactopyranoside

ITAM – immunoreceptor tyrosine-based activation motif

LB – Luria broth

M1 – influenza matrix protein 1

MACS – magnetic activated cell sorting

MFI – mean fluorescence intensity

MHC – major histocompatibility complex

MICA/B – major histocompatibility complex-class-I chain-related molecules A and B

NBT – nitroblue tetrazolium

NK – natural killer

NKAT2 – natural killer-associated transcript 2

NKG2A – natural killer group 2A

NKG2C – natural killer group 2C

NKG2D – natural killer group 2D

OD – optical density

o.n. – overnight

PAMPs – pathogen-associated molecular patterns

PAX-5 – paired box transcription factor 5

PBMCs – peripheral blood mononuclear cells

PBS – phosphate buffered saline

PCNA – proliferating cell nuclear antigen

PE – phycoerythrin

PFA – paraformaldehyde

PfEMP-1 – *Plasmodium falciparum* erythrocyte binding protein

PI – propidium iodine

PMN – polymorphonucleated cells

PPD – *Mycobacterium tuberculosis*-purified protein derivative (PPD)

RBC – red blood cells

RIPA – radio immunoprecipitation assay

ROS – reactive oxygen species

RPMI – Roswell Park Memorial Institute medium

RT – room temperature

SDS – sodium dodecyl sulfate

SSC – side light scatter

TAP – transporter associated with antigen presentation

TCM – central memory T cells

TCR – T cell receptor

TEM – effector memory T cells

TEMRA – terminally differentiated effector memory T cells

TGF- β – transforming growth factor β

TLRs – Toll-like receptors

Tnaïve – naïve T cells

TNF – tumour necrosis factor

TNF- α – tumour necrosis factor α

T α T – tetanus toxoid

ULBPs – UL16-binding proteins

UNF – uninfected

WASP – Wiskott-Aldrich syndrome protein

2 Introduction

Millions of years of co-habitation with microorganisms have generated formidable defences against infection. The first line of defence against human pathogens are the physical and chemical barriers that separate us from the outside world, that is, the linings of the skin, the enzymes in our tears and saliva, the acidic pH in our stomach. These defensive barriers are evolutionarily very ancient and provide us with protection against a broad and largely unforeseen spectrum of pathogens. When a pathogen breaches these first lines of defence, the cells of the innate immune system come into play. Macrophages are cells of the innate immune system and reside in tissues. They have receptors on their surface that recognise common patterns found on the bacterial surface called pathogen-associated molecular patterns (PAMPs). They use these receptors to bind and engulf and then destroy these microorganisms. Macrophages activated by pathogen products produce soluble mediators called cytokines that recruit other cells of the immune system from the blood stream, notably neutrophils and immature dendritic cells. When at the site of injury, neutrophils quickly engulf and destroy large amounts of bacteria. Immature dendritic cells, however, process the pathogen intracellularly into smaller pieces, called antigens. They then display these on their cell surface on specific receptors called MHC molecules. Antigens displayed on MHC class I and MHC class II molecules activate CD8 and CD4 T cells, respectively. These cells are part of the adaptive branch of the immune system, that appeared later in evolutionary terms, and added an enormous diversity to the types of pathogens to which the organism could be protected from. In addition, adaptive immunity included a method by which the organism can learn from previous infections, and generate a faster and stronger immune response against a second infection with the same pathogen. In this introduction I will detail the mechanisms by which cells of the immune system use phagocytosis, cytotoxicity and antigen presentation to control infection. Afterwards, I will describe human $\gamma\delta$ T cells and what is known about them in these fields.

2.1 Phagocytosis

The mechanisms of recognition, uptake and degradation of particles by professional phagocytes have been thoroughly reviewed recently by Flannagan and Jaumouille et al (1). Cells of the immune system use phagocytosis to clear pathogens like bacteria or fungi from a site of infection. It is also important for the engulfment of apoptotic bodies which is

crucial for tissue homeostasis and remodelling. Phagocytosis was first observed by Elias Metschnikoff more than a century ago (2) and is defined as the ingestion of relatively large ($\geq 0.5 \mu\text{m}$) particles by a process that is both receptor-mediated and actin-dependent. Unlike macropinocytosis, it involves the recognition and binding of particles by specific receptors on the surface of the phagocytic cell. Although there are different phagocytic receptors as well as different cells capable of phagocytosis, there are key principles that govern all phagocytic processes. These key principles are the requirement for a coordinated signalling cascade induced by particle binding, the need for cytoskeletal rearrangement and the occurrence of membrane remodelling (1).

Phagocytosis is mostly performed by macrophages and neutrophils. Also part of the myeloid phagocyte system are inflammatory monocytes and immature dendritic cells (3). Macrophages mature continuously from monocytes in the bloodstream that migrate into tissues and become tissue resident macrophages. Neutrophils are polymorphonucleated cells (PMN) that are abundant in the blood but short-lived. They make up the vast majority (around 70%) of leukocytes, or white blood cells, in human blood. Macrophages are the first to encounter a pathogen because they are usually present at the site of infection, but they are soon met by neutrophil reinforcements. Phagocytes recognise pathogens by means of their cell-surface receptors and can discriminate between host and pathogen surface markers.

Phagocytic receptors include receptors that recognise foreign bodies and receptors that recognise apoptotic bodies. Pathogens often display molecules not found in the host cells. These are called pathogen-associated molecular patterns (PAMPs) and can be detected by several receptors, in particular Toll-like receptors (TLRs) but also some phagocytic receptors. Table 1 lists phagocytic receptors that recognise pathogens and are found in human phagocytes. For instance, the lipopolysaccharide (LPS) displayed by gram-negative bacteria is detected by the scavenger receptor A (4). Pathogens can also be recognised indirectly through soluble molecules that coat them and are found in circulation in the blood and interstitial fluids. These molecules are called opsonins and include immunoglobulins and components of the complement cascade. The best characterised opsonic receptors bind the Fc portion of immunoglobulin G (IgG) (5) or the complement component iC3b (6). Receptors for apoptotic bodies, on the other hand, usually recognise

phosphatidylserine exposed on the surface of apoptotic cells. This lipid is usually restricted to the inner leaflet of the plasma membrane in healthy cells and is therefore not detected by phagocytes (7-9).

Table 1 – Human receptors mediating phagocytosis of pathogens, and their ligands

Adapted from Flannagan RS, Jaumouille V, Grinstein S. The cell biology of phagocytosis. *Annu Rev Pathol* 2012;7:61-98.

Receptors	Ligands	References
Pattern-recognition receptors		
<i>Mannose receptor (CD206)</i>	Mannan	(10)
<i>Dectin-1 (CLEC7A)</i>	β 1,3-glucan	(11)
<i>CD14</i>	Lipopolysaccharide-binding protein	(12)
<i>Scavenger receptor A (CD104)</i>	Lipopolysaccharide, lipoteichoic acid	(4;13)
<i>CD36</i>	Plasmodium falciparum-infected erythrocytes	(14)
<i>MARCO</i>	Bacteria	(15)
Opsonic receptors		
<i>FcγRI (CD64)</i>	IgG1 = IgG3 > IgG4	(5)
<i>FcγRIIa (CD32a)</i>	IgG3 \geq IgG1 = IgG2	(5)
<i>FcγRIIIa (CD16a)</i>	IgG	(5)
<i>FcαRI (CD89)</i>	IgA1, IgA2	(16)
<i>FcϵRI</i>	IgE	(17)
<i>CR1 (CD45)</i>	Mannan-binding lectin, C1q, C4b, C3b	(18)
<i>CR3 (α_Mβ₂, CD11b/CD18, Mac-1)</i>	iC3b	(6)
<i>CR4 (α_Vβ₂, CD11c/CD18, gp150/95)</i>	iC3b	(6)
<i>α₅β₁</i>	Fibronectin, vitronectin	(19)

Recognition of pathogens through phagocytic receptors is just the first step in phagocytosis. Receptor binding leads to the activation of intracellular signalling cascades. The best-understood model is the internalisation of IgG coated particles by Fc γ receptor-mediated phagocytosis in macrophages. In conceptual terms, the process takes three consecutive steps. First the Fc γ receptors bind the IgG coated particle. Then the Fc γ receptors cluster together triggering an intracellular signalling cascade. The signalling cascade drives actin polymerisation and the engulfment of the particle.

Clustering of the Fc γ receptors brings the cytosolic domain of these receptors in close proximity. The receptors contains a region called immunoreceptor tyrosine-based activation motif (ITAM). Receptor clustering leads to phosphorylation of tyrosines in ITAM motifs by tyrosine kinases, particularly of the Src family. Receptor phosphorylation is followed by the recruitment of adaptor proteins and the resulting signalling cascade activates the actin nucleation complex Arp2/3 which elicits actin polymerization and drives the extension of pseudopods that surround the foreign particle. Arp2/3 supports actin polymerization in Fc γ receptor-mediated phagocytosis (20). It can be activated by Wiskott-Aldrich syndrome protein (WASP). In fact, macrophages from patients with Wiskott-Aldrich syndrome, that have defective WASP, show impaired Fc γ receptor-mediated phagocytosis (21).

Although there are differences between the mechanisms of action of different phagocytic receptors, all receptor-mediated phagocytosis involves the engulfment of the particle in a membrane-bound vacuole called the phagosome. Once inside the cell, the phagocyte can manipulate the conditions inside the phagosome to promote the destruction of the trapped organism. Conversely, some pathogens have evolved remarkable strategies to manipulate phagosome maturation. A notable example is *Mycobacterium tuberculosis*, the causative agent of human tuberculosis. Once inside the macrophage phagosome, *Mycobacterium tuberculosis* arrests phagosome maturation at an early stage where it can survive inside the host (22). In normal settings, the phagosome interacts in succession with various endocytic compartments, to generate vacuoles of increasingly microbicidal power. As a result, the mature phagosome is markedly acidic (pH \approx 4.5), highly oxidative and enriched with hydrolytic enzymes that all contribute to the destruction of the particle.

Of note, phagosome maturation is different in dendritic cells and in neutrophils and macrophages. Although neutrophils and macrophages primarily serve to destroy the pathogen, the main function of dendritic cells (DCs) is to activate primary and secondary adaptive immune responses. The initiation of adaptive immune responses requires CD4 and CD8 T cells to recognise short peptides associated with MHC class II or class I molecules present on the surface of DCs. For this reason, it makes sense that the pH in the phagosome in dendritic cells remains neutral throughout phagosome maturation since this could promote the recovery of a variety of different antigens from an engulfed body, as opposed to its quick degradation (23).

The unique microbicidal and degradative capacities of the mature phagosome are the result of the concerted effort of not only its acidic pH, but the presence of hydrolytic enzymes, oxidants and cationic peptides, acquired through the earlier fusion with lysosomal vesicles. The low pH is also required to activate lysosomal hydrolases such as cathepsins that function optimally in acidic conditions. However, the various contributions of the different lytic effector mechanisms is, as mentioned earlier, variable among the different types of phagocytes, depending on their primary function. In neutrophils, the fusion with endocytic vesicles is replaced by fusion with neutrophil granules that carry multiple antimicrobial molecules. Some of these molecules are specific to neutrophils, such as the antibiotic peptides of the defensin and cathelicidin families (24). Phagocytosis induces a respiratory burst where reactive oxygen species are produced that help destroy the pathogen. Neutrophils are particularly strong at producing reactive oxygen species (ROS) (25). The most important of these are nitric oxide (NO), the superoxide anion (O_2^-) and hydrogen peroxide (H_2O_2) which are toxic to bacteria. Nitric oxide is produced by the nitric oxide synthase iNOS2. Superoxide is generated through the NADPH oxidase complex. Mutations affecting genes encoding subunits of the NADPH oxidase complex in chronic granulomatous disease (CGD) lead to impairment of ROS production and patients suffer from recurrent infections by numerous bacterial and fungal pathogens (26).

Phagocytosis ultimately culminates in the destruction of the internalised pathogen. Subsequently, antigens recovered from the digested pathogen can be presented by antigen presenting cells to activate CD4 and CD8 T cells and initiate an adaptive immune response.

2.2 Cell-mediated cytotoxicity

The extracellular milieu is a particular inhospitable place for a pathogen and many of them have chosen to infect the cells of the host. In addition, cells of the host can turn cancerous. These cells will need to be removed in order to control infection and prevent the development of a tumour. The mechanisms by which cells of the immune system destroy infected or “altered” cells generally involve either a granule exocytosis pathway or a “death receptor” pathway. The recognition process that initiates these events depends on the nature of the effector cell. It can be divided into TCR-mediated recognition, Fas/Fas ligand recognition or recognition by Natural Killer (NK) receptors, although cells other than NK cells can express “NK receptors” particularly $\gamma\delta$ T cells and activated CD8 T cells as recently reviewed (27). Recognition of the infected or tumour cell can also occur in an indirect manner, through antibodies bound to its cell surface and Fc receptors on the surface of the effector cell. Cellular effectors of antibody-dependent cytotoxicity (ADCC) are NK cells, $\gamma\delta$ T cells, activated CD8 T cells, monocytes, macrophages and dendritic cells. Neutrophils and eosinophils can also mediate ADCC but require cytokine activation.

A glimpse of the receptor-ligand interactions that can activate cytotoxicity is shown in Table 2. These receptors bind to and are activated by molecules expressed on the surface of infected or distressed cells. NK cells quickly recognise and respond to targets via germline encoded receptors. Activating receptors present in NK cells include the Fc γ receptor CD16, NKG2D, and the natural cytotoxicity receptors NKp30, NKp44 and NKp46, as well as many others (28). The activation of NK cell cytotoxicity is the consequence of the integration of signals from both the activating and inhibitory receptors (29). Inhibitory receptors recognise MHC class I molecules, expressed by all cells of the body except erythrocytes. Therefore, engagement of MHC class I molecules by NK cell receptors leads to an inhibitory signal that prevents the NK cell from being activated and spares the healthy cell from being killed. However, many tumour cells downregulate MHC class I molecules and in the absence of inhibitory signals the NK cell will become activated and kill the target. Even activating receptors can be manipulated by the pathogen to prevent NK cell activation. Human cytomegalovirus (CMV) for instance encodes proteins that mimic MHC class I and bind the NK cell inhibitory receptor, LIR-1, with a higher affinity than host MHC class I, and proteins that decrease the expression of CD155, a ligand for

NK cell activating receptors (30). The CMV main tegument protein pp65 can also inhibit NK cell activation via binding to NKp30 (31). Similarly, the proliferating cell nuclear antigen (PCNA) which is overexpressed by cancer cells, binds to and inhibits NKp44 (32). Finally, NKG2D, expressed by NK cells, $\gamma\delta$ T cells and CD8 T cells, recognises the stress ligands MHC-class-I chain-related molecules A and B (MICA/B) and UL16-binding proteins leading to an activation signal.

Table 2 – Selected ligands and human receptors capable of inducing cell-mediated cytotoxicity

Receptors	Ligands	Source	References
<i>CD8 – TCR complex</i>	MHC class I – peptide complex	All types of pathogen-derived protein antigens	(33)
<i>Fas / CD95</i>	Fas ligand	Various cell types	(34)
<i>NKG2D</i>	MICA, MICB and UL16-binding proteins (ULBPs)	Stressed cells	(35)
<i>NKp30</i>	<i>Plasmodium falciparum</i> erythrocyte binding protein (<i>PfEMP-1</i>)	<i>Plasmodium falciparum</i> infected cells	(36)
	Human leukocyte antigen B-associated transcript 3 (BAT3)	Tumour cells	(37)
<i>NKp44</i>	Viral haemagglutinins	Virus infected cells	(38)
<i>NKp46</i>	Hemagglutinin (HA) proteins of the influenza and vaccinia virus	Virus infected cells	(38;39)
	Vimentin	<i>Mycobacterium tuberculosis</i> infected cells	(40)
<i>Fc receptors</i>	IgG, IgA and IgE bound particles	Antibody-coated target cells	(41)

CD8 T cells, or cytotoxic T cells, are able to recognise an incredible variety of antigens via their T cell receptor (TCR). This recognition is stabilised by the interaction between CD8 on the cytotoxic T cell and MHC class I expressed on the target cell. The MHC class I complex presents foreign proteins derived from antigen processing. A second signal is provided by CD28 engagement on the cytotoxic T cell by CD80 or CD86 on the antigen presenting cell. The enormous repertoire of antigens recognised by T cells is due to the evolution of a process called V(D)J recombination where V, D and J gene segments are somatically rearranged to construct an immense diversity of possible T cell receptors from the same set of genes. Each T cell will express only one of these possible combinations in their TCR and will expand when their specific antigen is encountered during the course of an immune response.

Another way by which cell death can be induced is through Fas – Fas ligand interactions. Fas can be upregulated in various immune and non-immune cells and its engagement leads to the induction of programmed cell death, or apoptosis, in the target cell. It is particularly important in the resolution of an immune response, as Fas – Fas ligand interactions are used to eliminate T cells that have expanded during the course of the immune response but that are no longer necessary. The importance of the FAS pathway in the regulation of the immune response is evident by the autoimmunity caused by genetic defects in the FAS gene in severe autoimmune lymphoproliferative syndrome (ALPS) (42;43).

Last but not least, cell-mediated cytotoxicity can be induced indirectly by the binding of Fc receptors on the effector cell with the Fc portion of an antibody-coated target cell. This process is called antibody-dependent cytotoxicity (ADCC). When target bound antibodies crosslink activating Fc receptors, a cytotoxic pathway is initiated. Therefore, the specificity of ADCC is conferred by target-bound antibody which means monoclonal antibody therapy may be an attractive option for cancers over-expressing specific antigens (44). The main effector cells for ADCC are NK cells although other Fc receptor-expressing cells can mediate ADCC. The role of ADCC in host immunity is strongly highlighted by the impact of Fc γ receptor polymorphisms on the clinical outcome of cancer patients. The Fc γ receptor IIIA, or CD16A, is expressed by NK cells, $\gamma\delta$ T cells, activated $\alpha\beta$ T cells and macrophages. The CD16A gene exhibits a polymorphism due to a single nucleotide change leading to the presence of either a valine or a phenylalanine at position 158. The presence

of a 158V genotype results in a stronger binding to human IgG1 and has been associated with a better outcome in non-Hodgkin lymphomas treated with the anti-CD20 IgG1 antibody rituximab (45;46).

Although the manner in which cytotoxic responses are activated by different effectors may be different, owing to the different receptors expressed, two common cytotoxicity methods are shared: the granule exocytosis pathway and the Fas pathway. The granule exocytosis pathway utilizes perforin to traffic granzymes to appropriate locations in the target cells, where they cleave critical substrates that initiate DNA fragmentation and apoptosis. This is mediated by a calcium-dependent polarised exocytotic process at the lytic synapse. The lytic synapse involves the reorganisation of the actin cytoskeleton and the clustering of membrane receptors at the site of contact with the target cell. Perforin, released from granules in the effector cell, inserts and polymerises within the target cell membrane, allowing access of granzymes to the target cell cytosol. The importance of perforin is highlighted by the severe immunodeficiency caused by the lack of a functional perforin gene that predisposes a child to overwhelming viral infection in familial hemophagocytic lymphohistiocytosis type 2 (47). In addition, crosslinking of the Fc receptor CD16 on NK cells induces the expression of Fas ligand, enabling them to kill Fas⁺ targets. Therefore, the two cytotoxicity pathways can be used by the same cell to mediate killing of targets.

2.3 Antigen presentation

Innate cells are involved in the induction of adaptive immune responses. Microbial antigens typically enter through the skin and gastrointestinal tracts, where they are captured by dendritic cells (DCs) and trafficked into afferent lymph nodes. At the lymph node, the dendritic cell encounters T cells and specifically activates them via TCR-MHC interactions and co-stimulation. Alternatively, antigens that enter the blood stream are captured by antigen presenting cells in the spleen. When a dendritic cell takes up a pathogen, it becomes activated, and matures into a highly effective antigen presenting cell (33). Maturation leads to downregulation of phagocytic receptors like Fc receptors and mannose receptors. Conversely, maturing dendritic cells upregulate molecules related to T cell activation, including the co-stimulation molecules CD80, CD86 and ICAM-1 and the cytokine IL-12, and increase both the number of MHC class II molecules on their cell surface and their half-life (48).

The three major types of antigen-presenting cells are dendritic cells, macrophages and B cells. Antigen presentation by mature dendritic cells at peripheral lymphoid organs leads to the activation of naïve T cells, i.e., T cells that have never encountered antigen before. Activation induces clonal expansion and differentiation into effector T cells. Effector T cells combat the infection by producing cytokines that activate other cells or by cell-mediated cytotoxicity. These are mainly CD4 T cells and CD8 T cells, respectively. In particular, inflammatory CD4 T cells activate macrophages to destroy phagocytosed microbes through the production of IFN- γ and interactions of CD40 ligand (CD40L) expressed on their surface with CD40 on the macrophage. In addition, they also play an important role in stimulating antibody production by B cells that recognise the same antigen by providing a second signal with CD40-CD40L interactions when they recognise a specific peptide-MHC complex presented on the B cell surface. This leads to the proliferation and differentiation of B cells into antibody-producing plasma cells. An alternative co-stimulation signal can be provided by common microbial constituents like bacterial polysaccharides encountered by the B cell, in the absence of T cells.

Peptides can be presented on MHC class I molecules or on MHC class II molecules, and are recognised by CD4 T cells or CD8 T cells, respectively. Peptides can originate from different sources, intracellular for MHC class I or exogenous for MHC class II. In addition, cross-presentation can also occur where exogenous antigen is presented by MHC class I molecules. In this way, exogenous antigen can also prime CD8 T cells. This circumvents a conceptual problem with naïve T cell activation. Naïve T cells, whether CD4+ or CD8+, need to be activated by professional APCs, usually dendritic cells. In the case where a pathogen does not infect APCs or interferes with its MHC class I pathway, or even when a tumour arises in a non-APC cell type, naïve CD8 T cells would not be activated to exert their cytotoxic function. Cross-presentation circumvents these problems by allowing antigen acquired exogenously, such as in the form of infected cell debris, to be presented on MHC class I allowing the priming of CD8 adaptive immunity (49). In addition, endogenous proteins can be presented on MHC class II when they are degraded by autophagy (50). Autophagy is a process used during cellular homeostasis to salvage amino acids from proteins and organelles at the end of their life.

MHC class I molecules are expressed by all nucleated cells. In MHC class I presentation, antigens are degraded by cytosolic and nuclear proteasomes. The resulting peptides are translocated into the endoplasmic reticulum (ER) by transporter associated with antigen presentation (TAP). In the ER, peptide and MHC class I molecules are assembled and the complexes leave for expression at the cell surface (51). MHC class II molecules are encoded by three polymorphic genes (*HLA-DR*, *HLA-DQ* and *HLA-DP* in humans) that bind to different peptides. Many MHC class II alleles are strong genetic markers for several autoimmune disorders like rheumatoid arthritis, multiple sclerosis and type 1 diabetes although the mechanisms underlying the association are not clearly understood (52). MHC class II molecules are primarily expressed by professional antigen presenting cells (APCs) such as DCs, macrophages and B cells. The transmembrane α and β chains of MHC class II are assembled in the ER and associate with the invariant chain (Ii). The resulting complex is transported into a late endosomal compartment where Ii is digested, leaving a residual class II-associated peptide (CLIP) in the peptide-binding groove. CLIP is then exchanged for a peptide derived from antigen processing and the loaded MHC class II molecule is transported to the cell membrane for presentation to CD4 T cells.

2.4 $\gamma\delta$ T cells

$\gamma\delta$ T cells are non-conventional T cells characterised by the presence of a CD3/TCR complex composed of γ and δ variable chains, instead of α and β chains. Their serendipitous discovery dates back to the first attempts at cloning the $\alpha\beta$ TCR in 1984 (53). In humans, they are present mainly in peripheral blood and in gut epithelia and small numbers of $\gamma\delta$ T cells can also be found in the spleen and in the liver (54). In human blood, they typically make up to 5% of the total T cell pool whereas in the gut they constitute 25-60% of total intraepithelial lymphocytes (IELs). $\gamma\delta$ T cells in human and primate blood typically express the V γ 9V δ 2 TCR whereas tissue-associated $\gamma\delta$ T cells are mostly V δ 1+ with V δ 3+ a smaller additional population. In mice, $\gamma\delta$ TCR+ IELs are common in the skin where they are part of the dendritic epidermal T cell (DETC) compartment. Mouse $\gamma\delta$ T cells seem to preferentially locate to body surfaces in contact with the outside world and are common in the tongue, the gut, the genital tract and the lung.

2.4.1 $\gamma\delta$ TCR antigen recognition

The $\gamma\delta$ TCR, similarly to the $\alpha\beta$ TCR and the immunoglobulin chains (Igs) of the B cell receptor (BCR) is generated through somatic rearrangement of V(D)J genes. V(D)J recombination generates antigen receptor diversity. However, $\gamma\delta$ TCRs differ from $\alpha\beta$ TCRs in the mechanism of antigen recognition and some respond to unique antigens. Unlike most $\alpha\beta$ TCRs, $\gamma\delta$ TCRs are not restricted to engaging a peptide presented on an MHC molecule. Structural clues suggest in fact that $\gamma\delta$ TCRs may be more similar to Igs than to $\alpha\beta$ TCRs in the way that they bind antigen, which could explain why they can respond to antigen in the absence of an antigen presenting molecule. The CDR3 loops (complementarity determining region 3) of the TCR α and β chain are nearly identical in length and their length is constrained. This generates a 3-dimensional structure which binds both peptide and MHC molecule on an antigen presenting cell. However, the CDR3s of Ig heavy chains are long and variable, and those of Ig light chains are short and constrained which allow B cells to recognise a variety of antigens without the need for an antigen presenting molecule. Similarly, the CDR3 length of the TCR δ chain is also long and variable whereas that of the TCR γ chain is short and constrained (55). Therefore, the predicted structure of the antigen binding moiety, suggests that $\gamma\delta$ TCR-antigen interactions may be more similar to antibody-antigen interactions than $\alpha\beta$ TCR-peptide/MHC complex interactions.

In contrast to $\alpha\beta$ T cells, and in agreement with predicted Ig-like recognition by the $\gamma\delta$ TCR, $\gamma\delta$ T cells are generally double negative for both CD4 and CD8 and accordingly are not restricted by either MHC class II or MHC class I molecules in their ability to recognise their cognate antigen (56). Human and murine $\gamma\delta$ TCRs are activated by a variety of molecules, including peptides, lipids, small phosphorylated prenyl metabolites and large protein antigens. These antigens have been recently reviewed by Chien et al (57) and are listed in Table 3.

Table 3 – $\gamma\delta$ TCR ligands in man and mouse

Adapted from Chien Y et al (57) and Vantourout P et al (58)

<i>Antigen</i>	<i>$\gamma\delta$ subset</i>	<i>Context</i>	<i>References</i>
<i>Human $\gamma\delta$ T cells</i>			
<i>MICA/B</i>	V δ 1	Stress-induced ligands expressed on intestinal epithelium and epithelial tumours	(59;60)
<i>ULBP4</i>	V δ 2	Stress-induced ligand expressed by tumour cells	(61)
<i>CD1c</i>	V δ 1 (clones)	CD1c expressed by APCs, upregulation of CD1c in the absence of foreign antigen could be a danger signal	(62)
<i>CD1d-sulfatide</i>	V δ 1	Myelin glycosphingolipid, relevant in multiple sclerosis (MS) pathology	(63)
<i>Endothelial protein C receptor</i>	V γ 4V δ 5 (clone)	Recognition of CMV-infected endothelial cells and epithelial tumours	(64)
<i>Phytoerythrin (PE)</i>	0.025% of $\gamma\delta$ T cells	Microbial recognition	(65)
<i>Phosphoantigens</i>	V γ 9V δ 2	Broad recognition of tumours, bacteria and protozoa parasites	(66)
<i>Histidyl-tRNA synthetase</i>	V γ 1.3V δ 2	Muscle infiltrating $\gamma\delta$ T cells in autoimmune myositis patient	(67)
<i>Listeriolysin O</i>	PBMC $\gamma\delta$ T cells (clone)	Recognition of bacterium-derived toxins	(68)

<i>Antigen</i>	<i>γδ subset</i>	<i>Context</i>	<i>References</i>
<i>Mouse γδ T cells</i>			
<i>T10/T22</i>	0.1-1% of γδ T cells	Recognition of infected lymphocytes with an activation-induced phenotype, immunoregulation	(69-72)
<i>I-E^k</i>	Vγ2Vδ5 (clone)	Alloreactivity	(70)
<i>Herpes Simplex Virus glycoprotein I</i>	Vγ2Vδ8 (clone)	Herpes Simplex Virus infection	(73)
<i>Cardiolipin, apolipoprotein H</i>	Vγ1 (clones)	Recognition of cardiolipin+ bacteria and apoptotic eukaryotic cells	(74)
<i>Phytoerythrin (PE)</i>	0.02-0.4% of γδ T cells	Microbial recognition	(65)
<i>Insulin peptide (B:9-23)</i>	Vγ1 (clones)	αβ T cells and B cells that recognise the same peptide mediate diabetes in non-obese diabetes (NOD) mice	(75;76)

The $\gamma\delta$ TCR repertoire suggests a role for $\gamma\delta$ T cells in “lymphocyte stress surveillance” because they recognise molecules that are induced on “stressed” cells as a result of infection or transformation. This is similar to the role of patrolling macrophages and DCs whereas $\alpha\beta$ T cells, on the other hand, recognise antigens processed and presented by myeloid antigen presenting cells and therefore fit in to the immune response at a later time. Another important group of molecules recognised by $\gamma\delta$ TCRs seem to be autoantigens such as a myelin glycosphingolipid, histidyl-tRNA synthetase and a processed insulin peptide which imply a role for $\gamma\delta$ T cells in the onset of autoimmunity.

Antigens recognised by $\gamma\delta$ TCRs include host molecules that are induced on activated, stressed or cancerous cells such as T10 and T22 in the mouse (69-72), and MICA, MICB and ULBP4 in the human (59-61). Another MHC related molecule that is recognised by $\gamma\delta$ TCRs, specifically V δ 1+ clones, is CD1c (62), which can present self and microbial lipid-based antigen and is upregulated during inflammation-induced monocyte differentiation to DCs. Therefore, the recognition of CD1c and other MHC related molecules may be part of a common mechanism of stress surveillance by $\gamma\delta$ T cells which seems to be primarily a function of V δ 1+ cells in humans.

Human V δ 1+ cells expand and exert anti-viral responses during CMV infection (77-82) and the TCR of a $\gamma\delta$ T cell clone from a cytomegalovirus (CMV)-infected patient was found to directly bind endothelial protein C receptor (EPCR), which allowed the $\gamma\delta$ T cells to recognise both endothelial cells targeted by cytomegalovirus and epithelial tumours (64). Therefore, these $\gamma\delta$ TCRs recognise stressed human cells by engaging stress-regulated self-antigens.

In healthy individuals, V δ 1+ cells, which are more prevalent in tissues than in peripheral blood, have been found to react to CD1d loaded with sulfatide (63), a glycosphingolipid present in myelin. V δ 1+ cells have also been found to recognise cardiolipin complexed with apolipoprotein H (74). Cardiolipin is a lipid present in many bacteria and in the inner mitochondria membrane. During early apoptosis it translocates to the eukaryotic cell membrane where it is bound by serum apolipoprotein H. This complex was found to be recognised by V γ 1+ clones. It could allow $\gamma\delta$ T cells to recognise apoptotic eukaryotic cells and perhaps promote their clearing by releasing proinflammatory cytokines to recruit macrophages. Additionally, murine $\gamma\delta$ T cell clones also respond to a processed insulin

peptide without the need for an MHC molecule (75). Recently, the microbial antigen phycoerythrin (PE) was found to be recognised by a large percentage of naïve human and mouse $\gamma\delta$ T cells (65). A $\gamma\delta$ T cell clone has also been identified that responds to a herpes simplex virus glycoprotein (73).

However, the antigens that have been better studied so far belong to a group collectively called “phosphoantigens”. These phosphorylated small molecular weight moieties activate the majority of $\gamma\delta$ T cells present in human and primate blood. Surprisingly, given their ubiquity in human blood, these $\gamma\delta$ T cells are not found outside the primate world. They are characterised by a TCR composed of V γ 9 and V δ 2 chains. V γ 9V δ 2 T cells, in most healthy individuals, make up nearly 90% of all $\gamma\delta$ T cells in peripheral blood (83-85). The other main subset in humans pairs with V δ 1 chains and is the predominant $\gamma\delta$ T cell subset found at mucosal sites. This striking lack of diversity is thought to arise from a large expansion of the V γ 9V δ 2 subset early in life (86).

The V γ 9V δ 2 pairing recognises the microbial metabolite (E)-4-hydroxy-3-methyl-but-2-enyl pyrophosphate (HMB-PP) which is present in many pathogenic, opportunistic and commensal microbes (87). In this way the V γ 9V δ 2 pairing functions almost as a pattern-recognition receptor and allows for a rapid immune response without the need for prior selection and expansion that is necessary to generate $\alpha\beta$ T cell responses. In fact, substantial expansion of human V γ 9V δ 2+ cells is found in the acute phase of a large number of bacterial (88-101) and protozoan (95;102-109) infections, including some with the highest burden of disease worldwide such as malaria and tuberculosis, and food-borne pathogens common in the developing world such as *Listeria monocytogenes* and *Toxoplasma gondii*. The V γ 9V δ 2 pairing also responds to an endogenously produced phosphoantigen called isopentenyl pyrophosphate (IPP). IPP is an intermediate generated in the mevalonate pathway of isoprenoid synthesis and is a precursor in cholesterol synthesis and cholesterol derivatives (steroid hormones, vitamin D, bile salts, and lipoproteins). Both stressed and transformed cells frequently have a dysregulated mevalonate pathway and accumulate high amounts of IPP which marks them for recognition (and killing) by V γ 9V δ 2 T cells (110) which has implications for both cancer and autoimmunity. V γ 9V δ 2 T cells quickly home to perturbed human skin such as inflamed psoriatic lesions (111). Their clinical importance can also be highlighted by the fact that low numbers of circulating V γ 9V δ 2 T cells are a

negative biomarker in prognostic scoring for ovarian cancer (112). Interestingly, the endogenous levels of IPP can be manipulated using clinically relevant drugs. Aminobisphosphonates such as zoledronate, which are used to treat osteoporosis and some types of bone cancer increase the intracellular accumulation of IPP by inhibiting the IPP-processing enzyme farnesyl pyrophosphatase (FPP) synthase. As a consequence, treatment of tumour cells with aminobisphosphonates increases their susceptibility to $\gamma\delta$ T cell-mediated killing, which has generated a lot of interest in cell-based immunotherapies. Clinical trials have used either *ex vivo* expanded autologous V γ 9V δ 2 T cells or the administration of aminobisphosphonate drugs to patients alone. Partial tumour remissions have been reported for the *in vivo* drug administration trials. (113). A separate class of compounds - alkylamines - also activate V γ 9V δ 2 T cells (114) through the same mechanism. These compounds are found in dietary plants such as tea (114;115), apples (116) and wine (117). However, their potency in activating V γ 9V δ 2 T cells is 500-fold lower than that of aminobisphosphonates, owing to a much weaker inhibition of FPP synthase (118). Finally, in addition to activating V γ 9V δ 2 T cells in a TCR-dependent manner (119), phosphoantigens also require cell-cell contact (120) and fail to bind soluble V γ 9V δ 2 TCR (121). These features are all suggestive of an antigen presenting molecule but its identity has remained elusive until recently. A report by Vavassori et al, recently published in *Nature Immunology*, identifies butyrophilin 3A1 (CD277) as the long sought after cell surface-bound antigen-presenting molecule for phosphoantigens to V γ 9V δ 2 T cells (122). This molecule is ubiquitously expressed which explains why V γ 9V δ 2 T cells themselves were found to present phosphoantigens to other V γ 9V δ 2 T cells (120).

Another interesting aspect of $\gamma\delta$ T cells that sets them apart from conventional $\alpha\beta$ T cells is their striking lack of TCR diversity. Although the potential for diversity generated through V(D)J recombination is similarly high in both $\gamma\delta$ T cells and $\alpha\beta$ T cells, the $\gamma\delta$ TCR antigen specificities and the frequency of these antigen specific cells described so far suggest that the $\gamma\delta$ TCR antigen repertoire could be considerably smaller than that of the $\alpha\beta$ TCR. The actual $\alpha\beta$ T cell antigen-specific repertoire has been estimated at approximately 10^6 different antigens. In contrast, the $\gamma\delta$ TCR repertoire was estimated by Chien et al based on the list of $\gamma\delta$ TCR ligands described so far to be in the range of 10^3 - 10^4 different antigens, similar to the B cell antigen-specific repertoire (57).

This striking lack of TCR diversity is particularly visible in human blood where oligoclonal populations expressing the V γ 9V δ 2 TCR make up the overall majority of $\gamma\delta$ T cells. This surprising dominance is not present at birth but develops during childhood and then persists throughout adulthood. In fact, by 1 year of age less than 5% of V γ 9V δ 2 T cells are naïve, in contrast to the majority of V δ 1+ cells (123). One possible explanation for this could be extensive clonal expansion as a consequence of the continuous exposure to environmental microbial ligands during childhood (86) since the V γ 9V δ 2 TCR responds to common bacterial antigens.

In conclusion, $\gamma\delta$ TCRs recognise a variety of antigens, some of which are exclusive to $\gamma\delta$ T cells and therefore widen the scope of immune responsiveness provided by $\alpha\beta$ TCRs. They suggest a role for $\gamma\delta$ T cells in the monitoring of tissues to look for stress-induced molecules that could signal transformation or infection. Importantly, the scope of $\gamma\delta$ TCR recognition also implies a role for $\gamma\delta$ T cells in the pathology of autoimmunity.

2.4.2 The functions of $\gamma\delta$ T cells in the immune response

$\gamma\delta$ T cells have multiple roles in the immune response. They respond rapidly to danger signals and are among the earliest producers of inflammatory cytokines in many infection settings. They are also potent cytotoxic effectors against infected or tumour cells and murine models deficient in $\gamma\delta$ T cells seem more prone to developing some types of cancer. Additionally, $\gamma\delta$ T cells located in tissues such as the gut and the skin maintain immune homeostasis through the promotion of tolerance, wound healing and the removal of infected or transformed cells. They are particularly important during pregnancy in promoting tolerance to the developing fetus and protecting it from CMV. They are also particularly prevalent and relevant in early life where the $\alpha\beta$ T cell compartment is typically impaired. Evidence from early life and other states where $\alpha\beta$ T cell functions are impaired such as in children with immunodeficiencies and $\alpha\beta$ T cell (-/-) murine models suggests that $\gamma\delta$ T cells can compensate for $\alpha\beta$ T cells particularly in B cell help promoting antibody production. However, the specificity of the antibodies produced is often against self and in these cases $\gamma\delta$ T cells may cause autoimmunity. At last, evidence from $\gamma\delta$ T cell deficient mice suggests that $\gamma\delta$ T cells may have a role in terminating the immune response as these mice commonly have exacerbated $\alpha\beta$ T cell activity resulting in tissue damage.

In this section, current knowledge of the main roles of $\gamma\delta$ T cells in the immune response will be discussed. At the end, potential roles for $\gamma\delta$ T cells in phagocytosis and antigen presentation to $\alpha\beta$ T cells will be introduced in more detail.

2.4.2.1 Early producers of inflammatory cytokines

In terms of functional properties, $\gamma\delta$ T cells have well established roles as cytotoxic effectors against infected and tumour cells, as well as inflammatory cytokine producing cells, particularly IFN- γ and TNF- α . Their capacity to recognise antigens that are displayed after infection or other forms of stress and to respond rapidly to these without the need for extensive clonal expansion, equips $\gamma\delta$ T cells for the early stages of the immune response.

$\gamma\delta$ T cells produce inflammatory cytokines that are involved in protective immunity against viruses and intracellular pathogens (IFN- γ and TNF- α), extracellular bacteria and fungi (IL-17A) and extracellular parasites (IL-4, IL-5 and IL-13). In infections, $\gamma\delta$ T cells respond earlier than $\alpha\beta$ T cells. For instance, they are the major initial producers of IFN- γ after *Listeria monocytogenes* infection and of IL-4 after *Nippostrongylus brasiliensis* infection and appear days before the $\alpha\beta$ T cell response develops (124). $\gamma\delta$ T cells are also early non-redundant producers of IFN- γ *in vivo* after *Mycobacterium tuberculosis* (Mtb) infection in mice which enhances IL-12 production by dendritic cells in the lung and stimulates DCs to prime Mtb-specific CD8+ $\alpha\beta$ T cells more efficiently in the lung (125). In addition, $\gamma\delta$ T cells contribute to pathogen clearance directly, by producing bacteriostatic or lytic molecules, such as granulysin and defensins (126;127). They are also non-redundant players in controlling vaccinia virus infection, as $\gamma\delta$ T cell-deficient mice infected with this virus show increased mortality and higher virus titres compared to WT mice (128).

In the mouse, $\gamma\delta$ T cells are the primary source of the neutrophil-attracting cytokine IL-17A both helping to clear bacterial infections and exacerbating autoimmune pathologies. This rapid IL-17A production has been demonstrated in various mouse models of bacterial infection (129-131) and autoimmunity (132-135) including rheumatoid arthritis (132), psoriasis (136), type 1 diabetes (137) and progressive renal failure (138). In lung allergy models, IL-17A production by $\gamma\delta$ T cells has conflictingly been attributed to the resolution of airway inflammation (139;140). In humans however, IL-17-producing $\gamma\delta$ T cells are not

readily detected typically making up less than 1% of the V γ 9V δ 2+ cells in the peripheral blood of healthy donors (141;142). However, they make up the majority of $\gamma\delta$ T cells found in the blood and cerebrospinal fluid of children suffering from bacterial meningitis and they can be generated in *in vitro* cultures from naïve V γ 9V δ 2+ cells with the polarising cytokines IL-1- β , TGF- β , IL-6, and IL-23 (143). IL-17-producing $\gamma\delta$ T cells have also been found in HIV patients where they belong to the V δ 1 subset (144).

2.4.2.2 Cell-mediated cytotoxicity

$\gamma\delta$ T cells use cell-mediated cytotoxicity to kill infected, activated or transformed cells. Although NK cells are notorious MHC-unrestricted cytotoxic killers there is evidence to suggest a non-redundant role for $\gamma\delta$ T cells in certain settings. For instance, $\gamma\delta$ T cell-deficient mice develop cutaneous tumours faster than WT mice challenged with the mutagen methylcholanthrene or skin tumour cell lines (145;146). This protection in WT mice is mediated by both the early production of IFN- γ (146) and direct lysis of transformed cells (145) by $\gamma\delta$ T cells.

Cytotoxic pathways used by $\gamma\delta$ T cells are the same as those used by CD8 T cells and NK cells, namely the engagement of death-inducing receptors, such as Fas and other members of the TNF-family, and the release of cytotoxic molecules such as perforin and granzymes (126;147). Cytotoxicity through the granule exocytosis pathway can be induced by the recognition of tumour or infected cells through the $\gamma\delta$ TCR or through NK receptors. In particular, NKG2D is expressed on the vast majority of $\gamma\delta$ T cells and can trigger cytotoxicity either alone or as a co-stimulatory signal following V γ 9V δ 2 TCR recognition (148). The importance of NKG2D is supported by the various strategies used by viruses and tumours to evade it (149;150). Cytotoxicity in $\gamma\delta$ T cells seems to be mainly confined to the CD16+ and/or CD56+ subset (151;152). These cells are thought to develop quickly from the differentiation of more common CD16- CD56- central memory $\gamma\delta$ T cells (153). Finally, the induction of cytotoxicity in $\gamma\delta$ T cells can also be mediated by CD16-IgG opsonised target interactions much in the same way as for NK cells (154).

Antibody-dependent cytotoxicity (ADCC) by $\gamma\delta$ T cells has been demonstrated by different groups. Tokuyama et al showed that $\gamma\delta$ T cells expanded from healthy donors and subjects with malignancy were ADCC effectors with trastuzumab coated HER2-overexpressing

breast cancer cells, and with rituximab coated CD20+ lymphoma cell lines (Daudi, Raji and Ramos) (152). A different group used expanded $\gamma\delta$ T cells from healthy donors and follicular lymphoma patients to demonstrate ADCC with a novel anti-CD20 monoclonal antibody called GA101 and primary follicular lymphoma cells (155). Another group reported that expanded $\gamma\delta$ T cells from healthy donors or HIV patients were efficient ADCC effectors against a head and neck cancer cell line – 012SCC – in the presence of cetuximab, an anti-epidermal growth factor receptor monoclonal antibody (156). The same authors gave an oral presentation at the 16th International Symposium on HIV and Emerging Infectious Diseases about as yet unpublished findings that $\gamma\delta$ T cells from elite HIV controllers have retained ADCC potential as compared to normal HIV patients and that expanded $\gamma\delta$ T cells from these elite HIV controllers are able to kill Env-decorated targets in the presence of opsonising antibody (157). In addition, cross-linking of CD16 on $\gamma\delta$ T cells can also result in TNF- α (158) or IFN- γ (155;159;160) production. Interestingly, *in vivo* CMV-expanded $\gamma\delta$ T cells from transplantation recipients with CMV infections expressed CD16 but their anti-CMV action was not mediated by ADCC and instead was due to IFN- γ production after cross-linking of CD16 by IgG-opsonised virions (160). The authors hypothesize the lack of ADCC effector function could be due to the low levels of anti-CMV IgGs found in the patients. In addition, it should be mentioned that the previous ADCC studies focused on phosphoantigen-expanded V γ 9V δ 2 T cells whereas CMV-expanded $\gamma\delta$ T cells are predominantly of the V δ 1 subtype (80). IFN- γ production by $\gamma\delta$ T cells was additionally enhanced by IL-12 and IFN- α and inhibited CMV multiplication.

2.4.2.3 Tissue homeostasis

Tissue-associated $\gamma\delta$ T cells are commonly V δ 1+ with V δ 3+ and V δ 5+ being additional minor populations (161) and their main role is maintaining immune homeostasis in the local microenvironment (162). They have an important role in wound healing through the production of epithelial growth factors, remove distressed or transformed epithelial cells and dampen excessive inflammation (163-166). In the intestinal tract they play a non-redundant role in maintaining tolerance to food antigens as well as the intestinal flora (164;167). An increased number of $\gamma\delta$ TCR+ IEL is also observed in humans in celiac disease (168-172) and inflammatory bowel syndrome (173) and there is evidence that they

dampen inflammation by suppressing $\alpha\beta$ TCR+ IEL function (167). V δ 1+ cells are also particularly important in pregnancy and early life.

During pregnancy a heightened immune tolerance and protection from infection need to be balanced to both prevent rejection of the semiallogeneic embryo and successfully support its growth for 9 months. $\gamma\delta$ T cells have been observed at the maternal/fetal interface throughout pregnancy in humans, mice (174) and sheep(175). In humans, V δ 1+ cells are recruited to the maternal/fetal interface (176) and are the most frequent type of $\gamma\delta$ T cells found in the blood in healthy pregnancy. Strikingly, in women that have suffered from recurrent abortions (177) or are deemed at risk due to clinical symptoms (178) the V γ 9V δ 2 subset remains the most frequent in the blood during pregnancy. These observations strongly support a role for V δ 1+ cells in maintaining immunotolerance to the fetus which is further supported by findings that these cells produce IL-10 and TGF- β in the human decidua (179).

2.4.2.4 Interactions with other immune cells

$\gamma\delta$ T cells modulate the behaviour of other cells through the release of soluble intermediates or cell-cell contact. For instance, *in vitro* studies show that V γ 9V δ 2 T cells can induce maturation of DCs through a cell-cell contact dependent production of IFN- γ and TNF- α (180;181), and reciprocally, immature DCs induce activation of V γ 9V δ 2 T cells (182).

$\gamma\delta$ T cells may also play a part in the termination of the immune response. For instance, in murine influenza virus infection, $\gamma\delta$ T cells emerge late after pathogen numbers have declined (183). These late $\gamma\delta$ T cell responses could contribute to the resolution of inflammation since $\gamma\delta$ T cell-deficient mice develop larger and longer lasting inflammatory lesions when challenged with intracellular bacteria (184). In a different murine model, mice lacking $\gamma\delta$ IELs displayed an exaggerated immunopathology to *Eimeria vermiformis* gut infection, as a result of failure to control $\alpha\beta$ T cell responses (185). Therefore, $\gamma\delta$ T cells could act late in the immune response to dampen $\alpha\beta$ T cell responses.

$\gamma\delta$ T cells may also have an important role in B cell function which is apparent from studies with $\alpha\beta$ T cell deficient mice and immunocompromised individuals.

During the humoral immune response, antigen is transported into secondary lymphoid organs. Here, T cells expressing CXCR5 respond to the chemokine B-cell-attracting chemokine 1 (BCA-1/CXCL13) by migrating to the B cell region and interact resulting in germinal centre (GC) formation. It is at these structures that the processes of somatic hypermutation, class switch recombination and affinity maturation of activated B cells occur which result in the generation of memory B cells and antibody secreting plasma cells (186). In the absence of T cell help, antigen priming leads to B cell apoptosis (187). Follicular helper T cells (T_{FH}) are defined by their follicular location and by the high expression of specific markers: CXCR5, the inhibitory receptor PD-1 and the costimulatory molecule ICOS, which interact with specific ligands on B cells, and the cytokine IL-21 which acts on B cells (188). In secondary lymphoid organs, such as the tonsils, CD4+ $\alpha\beta$ T cells compose the majority of CXCR5+ T cells. However, small subsets of CD8+ $\alpha\beta$ T cells (189) and invariant NK T cells (190-192) can also provide B cell help albeit to a lesser extent. Interestingly, $\alpha\beta$ TCR-deficient mice develop normal germinal centres and class-switched antibodies which suggests that a different cell type such as $\gamma\delta$ T cells could compensate for the lack of these cells (193-195). However, the antibodies produced in these mice are mostly against self-antigens, strongly supporting a role for $\gamma\delta$ T cells in autoimmunity.

In healthy humans, CXCR5+ $\gamma\delta$ T cells can be found in small numbers in circulation and are able to provide B cell help *in vitro* (196). In addition, V γ 9V δ 2 T cells can be driven to a T_{FH} phenotype after phosphoantigen stimulation in the presence of IL-21 (197-199). These *in vitro* derived $\gamma\delta$ T_{FH} produce large amounts of BCA-1, which in addition to its chemotactic role for CXCR5+ cells also promotes the upregulation of molecules that promote follicular dendritic cell maturation (200). *In vivo*, lessons from immunocompromised individuals strongly support the ability of $\gamma\delta$ T cells to provide B cell help and suggest a link to autoimmunity. This may be particularly relevant in diseases characterised by a reduced $\alpha\beta$ T cell compartment such as AIDS which are often associated with autoimmunity.

No $\gamma\delta$ T cell (-/-) individual has been identified so far which would suggest that the phenotype is either embryonic lethal or so mild as to not cause significant complications. However, some patients have been described with severely reduced numbers of $\alpha\beta$ T cells

but normal numbers of $\gamma\delta$ T cells. Together, their phenotypes suggest an important role for $\gamma\delta$ T cells in modulating the behaviour of other immune cells. 9 cases so far have been observed with a hypomorphic mutation in the recombinase activating gene 1 (*RAG1*) that leads to a partial RAG-1 deficiency and severe combined immunodeficiency (SCID) (www.orpha.net). Two RAG-1-deficient SCID reports were published in the same issue of the Journal of Clinical Investigation. One of them presented a patient with severely reduced $\alpha\beta$ T cell numbers but normal $\gamma\delta$ T cell numbers with a diversified oligoclonal repertoire and predominance of $V\gamma4V\delta3+$ cells (201). Several of the $\gamma\delta$ T cell clones displayed reactivity against CMV. Specific antibodies against vaccines, infections, and also autoantibodies could be found despite minimal B cell numbers. The other publication reported RAG1-deficient SCID in 4 patients from separate families. The phenotype consisted of oligoclonal expansion of CMV-reactive $\gamma\delta$ T cells combined with $\alpha\beta$ T cell lymphopenia and autoimmunity. The patients all displayed autoimmune cytopenias (anemia in 3 patients and neutropenia in 1) and had either anti-red blood cell or anti-polymorphonuclear autoantibodies (202). These phenotypes support a role for $\gamma\delta$ T cells in providing B cell help to stimulate antibody production and in promoting autoimmunity. In support of this role in autoimmunity, elevated levels of $\gamma\delta$ T cells are observed in children with autoimmune thrombocytopenic purpura, a disorder characterised by immune-mediated antiplatelet destruction. (203). The levels of $\gamma\delta$ T cells in these children correlate with the degree of thrombocytopenia and the $\gamma\delta$ T cells are mainly of the $V\gamma9V\delta2$ TCR subset. Interestingly, *in vitro* studies with $\gamma\delta$ T cells from healthy adults also report that a subset of $\gamma\delta$ T cells present in human blood can promote B cell function and these cells express the $V\gamma9V\delta2$ TCR (196). However, the RAG1-deficient patients did not have an overrepresentation of the $V\gamma9V\delta2$ subset in the blood which is typical of their young age and will be enhanced by CMV-induced expansion of other subsets.

Other genetic disorders can cause a similar phenotype to RAG1 deficiency. Partial CD3 δ and TCR α defects have been described that result in combined immunodeficiency with severely reduced numbers of $\alpha\beta$ T cells, but normal numbers of $\gamma\delta$ T cells, B cells and NK cells (204;205). Although these patients suffered from immune dysregulation and autoimmunity they did not succumb to infection and remained relatively healthy for some years on antibiotic prophylaxis. They were able to produce class-switched antibodies and

to mount antibody responses to both vaccination and auto-antigens. Therefore, evidence from these immunodeficiency patients again suggests that $\gamma\delta$ T cells can play an important role in promoting autoimmunity by promoting the production of autoantibodies.

2.4.2.5 Importance in early life

$\gamma\delta$ T cells may be particularly important in early life. In all embryonic animal models where it was investigated, $\gamma\delta$ T cells are the first type of T cell to be detected in the thymus and the first to leave and populate the periphery (206-209). They can be detected in the murine thymus by embryonic day 14 (210) and by week 8 in humans (211). Their ontogeny is similar to $\alpha\beta$ T cells. Bone marrow precursor cells migrate to the thymus where they rearrange their TCR- γ , TCR- δ and TCR- β loci in an attempt to generate a productive $\gamma\delta$ TCR or pre-TCR (TCR- β paired with an invariant pre-TCR- α). This competition, combined with the signal strength of TCR signalling, directs the cell towards a $\gamma\delta$ T cell or $\alpha\beta$ T cell fate (212). As $\alpha\beta$ T cells emerge from the thymus, the relative proportion of $\gamma\delta$ T cells in circulation start to decrease. Interestingly, unlike $\alpha\beta$ T cells, which are nearly exclusively dependent on the thymus for their development and maturation, some $\gamma\delta$ T cells seem to be generated in extrathymic sites. In particular, V δ 1+ cells are present in athymic mice (213) and it is interesting that a skewed V δ 1+/V δ 2+ ratio is found in the blood of HIV-1 patients since this infection is characterised by a loss of thymic function (214).

The prevalence of $\gamma\delta$ T cells in early life suggests that they may contribute preferentially to neonatal protection, when $\alpha\beta$ T cell responses are functionally impaired and DCs are immature. Evidence for the role of $\gamma\delta$ T cells in neonatal protection is further discussed with particular emphasis on CMV.

Human cytomegalovirus (CMV) is the most common cause of congenital infection, affecting around 0.64% of live births (215). CMV can translocate the placental barrier and infect the developing fetus and it can also infect the baby through maternal breast milk. Infection is usually asymptomatic in adults but may cause serious sequelae in the neonate including hearing loss, vision loss and mental retardation. In the adult immune system there is compelling evidence for CMV-specific CD4 T cells as critical controllers of CMV infection (216;217). However, the immune system of the neonate is qualitatively different

from the adult. A dramatic expansion of fetal V δ 1+ cells is seen in human cytomegalovirus (CMV) infection *in utero* (79) and these cells differentiate into strong IFN- γ producing effectors. It is therefore possible that $\gamma\delta$ T cells *in utero* functionally replace the CD4 T cell Th1 responses that are characteristically low in pregnancy and newborns (218;219). Fetal $\gamma\delta$ T cells in congenital CMV had upregulated cytotoxic mediators including granzymes, perforin, granulysin, FasL and TRAIL which equipped them for cell-mediated cytotoxicity. In addition, clones from CMV-infected newborns efficiently killed CMV-infected cells and limited CMV replication *in vitro*. Therefore, there is strong evidence that $\gamma\delta$ T cells mediate protection in the developing fetus in congenital CMV.

Additional evidence of the competence of $\gamma\delta$ T cells to protect the host in early life are found in a study comparing $\gamma\delta$ T cells and $\alpha\beta$ T cells from the blood of neonates (220). The authors found neonate $\gamma\delta$ T cells showed stronger *in vitro* cytokine responses upon stimulation particularly for IFN- γ which is typically impaired in neonate $\alpha\beta$ T cells and mediates protection against intracellular parasites, bacteria and certain viruses. Therefore, $\gamma\delta$ T cells are well equipped to contribute to immunoprotection in the neonate, possibly compensating for the selective immaturity of the $\alpha\beta$ T cell compartment during this critical period. In addition, in two mouse models of parasite gut infection, $\gamma\delta$ T cells were found to be required for the protection of young but not adult mice (221;222). $\gamma\delta$ T cells may therefore contribute disproportionately to immunity in young animals.

2.4.3 Phagocytosis by $\gamma\delta$ T cells

Lymphocytes are not usually considered phagocytic cells. Our general understanding of immunology is that the phagocytic response is both an early and a late event in the immune response and that the main players are neutrophils, macrophages and dendritic cells. Although all cells in the body can sample their extracellular environment to some extent, these professional phagocytes share among them tools that allow them to recognise and engulf pathogens and cell debris highly efficiently. They share among them machinery that allows them to destroy engulfed pathogens and then to alert other immune cells of their presence. In 2009, a group presented evidence of professional phagocytosis performed by $\gamma\delta$ T cells from the blood of healthy donors (223). The authors used freshly isolated $\gamma\delta$ T cells to demonstrate phagocytosis of opsonised particles and also antigen presentation to $\alpha\beta$ T cells after co-stimulation with phosphoantigens and B-LCL help. Wu et al showed

detailed microscopic evidence of internalised *Escherichia coli* and 1 μm beads by freshly isolated human peripheral blood $\gamma\delta$ T cells. Why have other groups not reported similar observations? Phagocytosis in $\gamma\delta$ T cells may not be an obvious feature because of three facts: first, the lack of abundant phagocytic receptors on $\gamma\delta$ T cells, second, constraints of cell size, and third, competition with professional phagocytes. These particular constraints will be examined followed by a discussion of the possible relevance of phagocytosis by $\gamma\delta$ T cells in the immune response.

Phagocytosis is a receptor-mediated process and T cells do not have an abundance of phagocytic receptors. However, a proportion of $\gamma\delta$ T cells in the blood express the cell-surface receptor CD16, although with considerable variability among different donors and different reports (158-160;223-226). Although this receptor is also found on NK cells, where it mediates antibody-dependent cytotoxicity, it is a phagocytic receptor in macrophages. It can also induce phagocytosis if transduced into COS-1 cells that were previously not phagocytic (227). Importantly, CD16 binds IgG-coated particles and therefore cells expressing only this phagocytic receptor can only exhibit phagocytosis towards IgG-opsonised targets. Accordingly, blocking of CD16 substantially decreased antigen presentation from phagocytosed particles in Wu et al's original work (223).

Secondly, there are constraints of cell size. The restrictions on phagocytosis may be mechanical as phagocytes need to have a sufficient volume of cytoplasm to accommodate the phagocytosed particle. Steady-state lymphocytes typically have a very high nucleus to cytoplasm ratio unlike professional phagocytes. For example, B cells are not phagocytic (228) but malignant B cells transform into cells with a large macrophage-like morphology that are capable of ingesting large particles by phagocytosis (229-231). Nonetheless, bovine activated $\gamma\delta$ T cells acquire a different morphology to resting T cells, with an enlarged cytoplasm and occasional membrane protrusions similar to dendritic cells (232). Moser's group described a similar morphology in *in vitro* activated human V γ 9V δ 2 T cells (233). In addition, Wu et al detailed the presence of $\gamma\delta$ T cells with a dendritic-like morphology in small numbers in the blood of healthy donors without any deliberate *in vitro* activation or active infection (223). Therefore, although most $\gamma\delta$ T cells have the morphology of small lymphocytes, with a small round body and a very small cytoplasm to nucleus ratio, small numbers of larger dendritic-like $\gamma\delta$ T cells may be present among circulating cells in

peripheral blood (223). In addition, isolated $\gamma\delta$ T cells quickly acquire a similar morphology upon activation (232;233).

Finally, phagocytosis by $\gamma\delta$ T cells may not be evident due to competition by professional phagocytes. In phagocytosis experiments containing mixed populations of leukocytes, professional phagocytes such as neutrophils and monocytes may take up microbes much more efficiently than $\gamma\delta$ T cells, as they display a variety of phagocytic receptors on their surface. In addition, they are present in significantly higher numbers in the blood whereas $\gamma\delta$ T cells are a minor population in human blood in the absence of infection. The vast majority of leukocytes in the blood are neutrophils (around 70%) and about 10% of PBMCs are monocytes, whereas only around 1-5% of T cells generally express a $\gamma\delta$ TCR.

For all these reasons conventional professional phagocytes have a significant competitive advantage over $\gamma\delta$ T cells in their opportunity to phagocytose and can make use of a variety of different receptors to recognise their target. Therefore, they will be preferentially seen to phagocytose in mixed populations of cells.

However, it is interesting to think of the possibility of phagocytosis in $\gamma\delta$ T cells from an evolutionary point of view. Curiously, the 3D structure of $\gamma\delta$ TCRs is more similar to immunoglobulins (Ig) than to $\alpha\beta$ TCRs. The CDR3 loops in the γ and δ chains, the key components for antigen recognition, very closely resemble the CDR3 regions of Ig light chains and heavy chains, as opposed to those of the α and β chains in $\alpha\beta$ TCRs (234-236). This was taken to suggest that the recognition of antigen by $\gamma\delta$ T cells may be more similar to the binding of antibody to antigen than the MHC/peptide complex recognised by $\alpha\beta$ T cells, but in addition, it may also suggest a separate evolution of $\gamma\delta$ and $\alpha\beta$ TCRs. Phylogenetic studies of the constant region of T cell receptors suggest that TCR γ and δ sequences are more ancient than TCR α and β sequences, implying that the ancestral immune cell was more like a modern $\gamma\delta$ T cell than a modern $\alpha\beta$ T cell (237). According to this phylogenetic analysis, the $\gamma\delta$ T cell-like ancestor then gave rise to $\alpha\beta$ T cells and B cells. In this way, $\gamma\delta$ T cells are thought to predate $\alpha\beta$ T cells and B cells in evolution. Since phagocytosis arose long before adaptive immunity, the initial $\gamma\delta$ T cell-like ancestor may have shared innate and adaptive immunity properties. Phagocytosis may therefore be a feature retained to some extent by modern $\gamma\delta$ T cells. Another argument in line with the

possibility of phagocytic cells in the modern $\gamma\delta$ T cell population is that not all developing $\gamma\delta$ T cells depend on the same molecular switch for lineage commitment. This raises the possibility that phenotypically distinct $\gamma\delta$ T cell lineages may co-exist (238) and that therefore a distinct $\gamma\delta$ TCR+ lineage may have retained the ability for phagocytosis.

The best supporting evidence for an evolutionary explanation for $\gamma\delta$ T cell phagocytosis would be the presence of phagocytic $\gamma\delta$ T cells in evolutionarily more primitive animals. Although no such studies have been reported for $\gamma\delta$ T cells, a report in *Nature Immunology* highlighted the surprising high phagocytic ability of B cells from the rainbow trout and catfish (239). The uptake of bacteria was followed by phagolysosome formation and intracellular killing. These animals are teleost fish, which were the first animal species to evolve adaptive immunity (240). This report therefore shows evidence of phagocytic ability in one of the earliest evolved adaptive immune cells. Notably, phagocytic IgM+ lymphocytes represented 62% of all peripheral blood phagocytes and so were not a minor population which suggests that phagocytosis co-existed in the first evolved adaptive immune cells.

The earlier report of professional phagocytosis in $\gamma\delta$ T cells (223) leaves important questions that the work leading to this thesis has tried to address. For instance:

- Is phagocytosis a feature of a particular type of $\gamma\delta$ TCR+ cell?
- What proportion of $\gamma\delta$ T cells phagocytose?
- How does this compare to other cells of the immune system?
- Do $\gamma\delta$ T cells produce microbicidal products after bacterial engulfment?

The answers to these questions would help frame what role $\gamma\delta$ T cell phagocytosis could play in the immune response. For instance, $\gamma\delta$ T cell phagocytosis could play a role locally at infection sites after B cell humoral responses. $\gamma\delta$ T cells, being one of the earliest players in the immune response, would initially exert cytotoxicity and produce inflammatory cytokines while neutrophils and tissue macrophages phagocytosed. Later, after the generation of specific antibodies, $\gamma\delta$ T cells at the infection site might help clear the infection more quickly through the recognition and uptake of antibody coated pathogens or pathogen fragments. In this case, experimental phagocytosis should find phagocytosis

restricted to the Fc receptor expressing subset of $\gamma\delta$ T cells. Since some $\gamma\delta$ T cells have been shown to produce bacteriostatic substances (126;127) they may also be able to destroy the engulfed pathogen, therefore controlling the spread of infection. Additionally, $\gamma\delta$ T cells could play a role in modulating the antigen-specific $\alpha\beta$ T cell response enhancing it locally by presenting engulfed pathogen antigens and inducing the expansion of previously selected antigen specific $\alpha\beta$ T cells. Presentation after phagocytosis in $\gamma\delta$ T cells could perhaps even dampen the immune response and help terminate it if phagocytosis and antigen processing and presentation happens temporally late and antigen is presented in the absence of co-stimulation. A cell type simultaneously capable of cytotoxicity, phagocytosis and of stimulating antigen-specific $\alpha\beta$ T cell responses could prove a useful tool in cancer immunotherapy and V γ 9V δ 2 T cells can be readily expanded *ex vivo* for reinfusion (241).

2.4.4 Antigen presentation by $\gamma\delta$ T cells to $\alpha\beta$ T cells

At the time of the beginning of this thesis, there were two isolated reports of professional antigen presentation in human $\gamma\delta$ T cells (223;233). In addition, there were reports of MHC class II antigen presentation in bovine (232), porcine (242), and murine (243) $\gamma\delta$ T cells. The field has since grown with additional insights on the ability of human $\gamma\delta$ T cells to cross-present microbial, virus and tumour antigen to CD8+ $\alpha\beta$ T cells (244-246). In addition, the mechanism for cross-presentation seems to involve the cytosolic pathway (247) and activation signals required for professional antigen presentation function have been identified (233;246). Therefore, there is hope that these insights can be applied to improve $\gamma\delta$ T cell-based tumour immunotherapy approaches (248).

The first report of professional antigen presentation was in Science in 2005 by Brandes et al (233). Activated V γ 9V δ 2 T cells rapidly acquired features of professional antigen presenting cells including the expression of the class II antigen presentation molecule HLA-DR and the co-stimulatory molecules CD80/86 and CD40, as well as the lymph node homing molecule CCR7. In addition, the morphology of the $\gamma\delta$ T cells changed and they developed a markedly activated appearance often with long membrane projections. Phase contrast images of $\gamma\delta$ T cell cultures showed cells with the appearance of being highly motile. These characteristics are very reminiscent of the prototypical antigen presenting cell – the mature dendritic cell. Immature dendritic cells are specialised to internalise and

process antigens, and keep MHC class II molecules in endocytic compartments (249). Upon stimulation, they mature into powerful inducers of T cell immunity. These express high levels of surface MHC class II (249) and have the appearance of large, nonadherent, stellate and motile cells (250). Mature DCs express an abundance of T cell adhesive and co-stimulatory molecules. The authors showed that upon activation with a TCR agonist and IL-2, in the presence of B-LCL feeder cells, V γ 9V δ 2 T cells rapidly altered their morphology and phenotype towards that of mature dendritic cells. Functionally, activated V γ 9V δ 2 T cells could induce primary $\alpha\beta$ T cell responses to the same extent as LPS-matured DCs. They could also process and present the soluble protein antigens tetanus toxoid (TT) and the complex protein mixture *Mycobacterium tuberculosis*-purified protein derivative (PPD). Activation of TT- and PPD-specific CD4 T cells was blocked by chloroquine and with a blocking anti-HLA-DR antibody, demonstrating requirements for both active processing and presentation via HLA-DR for $\alpha\beta$ T cell activation. It should be noted that simply stimulating freshly isolated $\gamma\delta$ T cells with phosphoantigen and IL-2 does not equip them with antigen presentation properties, as was shown recently by a study using transcriptome analysis that did not find APC markers on phosphoantigen-activated $\gamma\delta$ T cells (251). This points to an interesting and as yet undefined role for B-LCL help in the induction of an APC phenotype in these cells.

Wu et al added to these findings by describing a mechanism by which $\gamma\delta$ T cells could acquire antigen for presentation (223). The authors showed that human $\gamma\delta$ T cells were capable of taking up *Escherichia coli* and influenza M1 protein coated 1 μ m beads when these were specifically opsonised with IgG antibodies. The authors therefore infer that human $\gamma\delta$ T cells are capable of Fc-mediated phagocytosis. Accordingly, presentation of M1 antigen was disrupted in the presence of an anti-CD16 blocking antibody, in addition to being sensitive to chloroquine and HLA-DR blocking.

Subsequent studies have focused on cross-presentation, or the ability of these cells to degrade exogenous protein and load it on MHC class I (244;245;247;248). Cross-presentation by $\gamma\delta$ T cells could have important implications as $\gamma\delta$ T cells are highly cytotoxic and a functional link between cytotoxicity and antigen presentation could amplify the immune response to cancer or infection. In addition, as mentioned previously, cross-presentation is particularly important for naïve T cell activation, in the case where a

pathogen does not infect APCs or even when a tumour arises in a non-APC cell type (49). The anti-tumour cytotoxicity of $\gamma\delta$ T cells is well established in the literature. Therefore, if antigen is acquired locally from tumour cell debris then $\gamma\delta$ T cells could be potent inducers of anti-tumour adaptive immunity. Since $\gamma\delta$ T cells can be readily expanded *ex vivo* to large numbers (252-254), they could potentially be used in novel approaches to tumour immunotherapy.

Activated V γ 9V δ 2 T cells outperformed dendritic cells in cross-presentation of exogenous particulate antigen, which was shown to occur via macropinocytosis (247). Macropinocytosis is used by immature dendritic cells as part of their normal function to sample the local environment and to induce tolerance to self-antigens. A substantial portion of internalised particulate antigen in activated V γ 9V δ 2 T cells was exported to the cytosol and degraded by the proteasome. $\gamma\delta$ T cells were also capable of cross-presenting cellular debris and displayed delayed endosomal acidification, which is thought to contribute to the preservation of antigens in DCs. This data suggests the cytosolic pathway as a mechanism for cross-presentation of particulate antigens in $\gamma\delta$ T cells.

Our own group investigated the regulation of professional antigen presentation in cross-presenting human $\gamma\delta$ T cells (246). In addition to the previously described requirements for TCR ligation, IL-2 and B-LCL help, the authors showed a potent, reversible second signal via CD16 ligation to opsonised tumour cells. The presence of opsonised tumour cells was sufficient to induce a level of cross-presentation similar to mature DCs. The same effect could not be seen in the presence of antibody, tumour cells alone, or non-binding antibody and tumour cells. This signalling was termed “licensing”, drawing parallels from the licensing for potent antigen presentation in DCs through CD40-CD40L ligation by CD40L-expressing CD4 T cells (255-257). The effect was reversible as separating $\gamma\delta$ T cells and opsonised tumour cells resulted in a loss of the ability of these cells to cross-present, accompanied by a loss of surface co-stimulatory molecules. This study raises the possibility that we could improve on current $\gamma\delta$ T cell immunotherapy trials (113) by combining the capacity of $\gamma\delta$ T cells for ADCC (152;155-157) with a concomitant stimulation of cross-presentation of tumour associated antigens (244-246) and improve anti-cancer immunity.

In the work described in this thesis the MHC class II antigen presentation experiments established by Wu et al were replicated (223). In addition, $\gamma\delta$ T cells were compared with other lymphocytes in the blood to further establish whether professional antigen presentation function is a unique feature of V γ 9V δ 2 T cells activated in this way. Also, because CD16 was demonstrated in the original work by Wu et al to be important in antigen uptake for presentation, and this same receptor is known to mediate ADCC in $\gamma\delta$ T cells (152;155-157), I investigated whether ADCC, as opposed to direct cytotoxicity, could be used as an efficient mechanism of antigen uptake for class II presentation in $\gamma\delta$ T cells. Of note, relevant studies had been published with NK cells, where incubation of NK cells with NK-sensitive but not NK-insensitive tumour cell targets led to the transient activation of MHC class II antigen presentation function by the NK cells (258;259). A similar study with $\gamma\delta$ T cells had been conducted *ex vivo* by following an *in vivo* bovine foot-and-mouth disease virus infection (260). In this study, $\gamma\delta$ T cells were shown to exert high cytotoxicity and concomitantly acquired MHC class II antigen presentation function transiently during the acute phase of infection. These studies suggest that cytotoxic effectors can be activated through NK cell receptors to acquire antigen presentation function and aid anti-virus and anti-tumour immunity.

The experiments described in this thesis aim to help clarify the extent of phagocytosis in human $\gamma\delta$ T cells and the settings in which it could play a role (ADCC, after humoral responses). In addition, I have tried to include other relevant lymphocytes ($\alpha\beta$ T cells and NK cells) in the experimental design, to investigate whether phagocytosis and subsequent antigen presentation is unique to $\gamma\delta$ T cells or whether other lymphocyte subsets share a similar plasticity.

In summary, in addition to phagocytosis, this thesis studies MHC class II presentation of exogenous antigen by $\gamma\delta$ T cells. The main aims of the antigen presentation experiments described in this thesis are:

- To replicate the original work by Wu et al (223) describing class II presentation of influenza M1 antigen by $\gamma\delta$ T cells but additionally include $\alpha\beta$ T cells and NK cells in the same experiments in order to elucidate whether class II presentation is a unique feature of these cells among similar lymphocyte subsets

- To investigate whether antigen can be acquired by $\gamma\delta$ T cells from infected target cells coated with antibody and whether this antigen is later presented by the $\gamma\delta$ T cell via MHC class II

The answers to these questions may help clarify what role phagocytosis and class II antigen presentation by $\gamma\delta$ T cells could play in the immune response.

3 Materials and Methods

3.1 Materials

3.1.1 Cell isolation

The following materials were used to isolate PBMC or PMN fractions from whole blood and to isolate different cell types from PBMCs.

Table 4 – Reagents used for the isolation of cells from whole blood

Reagent	Supplier	Cat no.
<i>Ficoll-Paque</i>	GE Healthcare	17-1440-03
<i>Dextran</i>	Sigma	D4876
<i>anti-$\gamma\delta$ TCR microbead kit</i>	Miltenyi Biotec	130-050-701
<i>anti-PE microbeads</i>	Miltenyi Biotec	130-048-801
<i>anti-CD56 microbeads</i>	Miltenyi Biotec	130-050-401
<i>NK cell isolation kit</i>	Miltenyi Biotec	130-092-657
<i>anti-CD14 microbeads</i>	Miltenyi Biotec	130-050-201
<i>LS columns</i>	Miltenyi Biotec	130-042-401
<i>MS columns</i>	Miltenyi Biotec	130-042-201

3.1.2 Bacteria and bacterial growth media

Escherichia coli strain DH5 α containing the plasmid pAKgfp1 were acquired from Addgene (plasmid #14076). The bacteria were grown in LB broth (20g Luria broth base (Sigma #L3022) + 1L ddH₂O + autoclaving) supplemented with 100 μ g/ml ampicillin (Sigma #A9518) and 1mM IPTG (Sigma #I1284), or in bacterial plates made with LB agar (35g LB agar (Sigma #19344) + 1L ddH₂O + autoclaving) supplemented with 100 μ g/ml ampicillin.

3.1.3 Cell lines and cell culture media

Primary cells and cell lines were grown in either complete RPMI media or complete DMEM media as described in the following table.

Table 5 – Reagents used for the culture of mammalian cells

Media	Cells	Description
<i>Complete RPMI</i>	Human T cells, NK cells, monocytes, neutrophils, Daudi, K562, B-LCL	RPMI (Gibco #61870) 10% (v/v) heat-inactivated FCS (Sigma #F7524) 1% (v/v) penicillin/streptomycin (Gibco #15140)
<i>Hybridoma media</i>	A1C5 hybridoma	DMEM (Gibco #61965) 10% (v/v) heat-inactivated FCS 1% (v/v) penicillin/streptomycin 1% (v/v) non-essential amino acids (Gibco #11140-035) 1% (v/v) pyruvate (Gibco #11360-039) 50 μ M β -mercaptoethanol (Gibco #31350-010)
<i>Freezing media</i>	Various	90% FCS 10% DMSO

3.1.4 Buffers and solutions

All dilutions volume/volume (v/v) for liquids and weight/volume (w/v) for solids unless otherwise stated.

Table 6 – Buffers and solutions used throughout this study

Buffers/Solutions	Recipe/Manufacturer
<i>Dulbecco's phosphate buffered saline (DPBS)</i>	Gibco #14190-094
<i>Phosphate buffered saline (PBS)</i>	10x PBS tablets were dissolved in ddH ₂ O
<i>PBS-T</i>	PBS + 0.05% Tween 20
<i>0.1% Triton</i>	PBS + 0.1% Triton X
<i>4% paraformaldehyde</i>	diluted from 16% stock from Alfa Aesar #43368
<i>ELISA blocking buffer</i>	PBS-T + 5% BSA
<i>ELISA stop solution</i>	1M Sulfuric acid
<i>ELISA substrate</i>	Becton Dickinson #555214
<i>FACS buffer</i>	DPBS + 0.5% FCS + 2mM EDTA
<i>MACS buffer</i>	DPBS + 0.5% FCS + 2mM EDTA, 0.2 µm sterile filtered
<i>RIPA buffer</i>	25mM Tris-HCl pH 7.6, 150mM NaCl, 1% NP-40, 1% sodium deoxycholate, 0.1% SDS
<i>Laemmli's buffer (2x)</i>	0.5M Tris-HCl pH 6.8, 10% glycerol, 2% SDS and bromophenol blue, 100mM DTT
<i>Western blocking buffer</i>	PBS-T + 5% BSA
<i>Western ECL reagent</i>	SuperSignal West Pico Chemiluminescent Substrate, Thermo Scientific #34080
<i>Western running buffer</i>	diluted from 20x NuPAGE MOPS SDS running buffer (Invitrogen #NP0001)

<i>Western transfer buffer</i>	diluted from 20x NuPAGE transfer buffer (Invitrogen #NP0006)
<i>Talon buffer</i>	50 mM Na-phosphate, pH 8.0 + 300 mM NaCl + 0.01% Tween 20
<i>Fix & lyse buffer for comparative phagocytosis assay</i>	diluted from 10x stock from Glycotope Biotechnology's PHAGOTEST kit
<i>Fix & lyse buffer for general flow cytometry</i>	eBioscience #00-5333-54
<i>saline</i>	0.9% NaCl
<i>Fast green methanol</i>	Medion Diagnostics #F04660/90
<i>Eosin Y in PBS</i>	Medion Diagnostics #F04662/90
<i>Thiazine dye</i>	Medion Diagnostics #F04663/90

3.1.5 Antibodies

A list of all the antibodies used in this study is provided in Table 6, together with their use and working dilution. For flow cytometry, antibody dilutions are commonly described as μl of antibody added per test. A test is defined as the amount of antibody used to stain a cell sample in a final volume of 100 μl . Cell number can range from 10^5 to 10^8 cells/test.

Table 7 – Antibodies used throughout this study

Antibodies	Supplier	Cat no.	Dilution
<i>Magnetic cell isolation</i>			
<i>$\alpha\beta$ TCR-PE</i>	eBioscience	12-9986	20 μl /test
<i>Flow Cytometry</i>			
<i>$\gamma\delta$ TCR-FITC</i>	eBioscience	11-9959	5 μl /test
<i>$\gamma\delta$ TCR-PE</i>	eBioscience	12-9959	5 μl /test
<i>$\gamma\delta$ TCR-APC</i>	Becton Dickinson	555718	5 μl /test
<i>CD3-eFluor450</i>	eBioscience	48-0038	5 μl /test
<i>CD3-APC</i>	Biolegend	300412	5 μl /test
<i>$\alpha\beta$ TCR-APC</i>	Biolegend	306717	5 μl /test
<i>CD56-APC</i>	Becton Dickinson	555518	20 μl /test
<i>CD14-APC</i>	Becton Dickinson	561708	20 μl /test
<i>CD27-PE</i>	eBioscience	12-0271	0.7 μl /test
<i>CD45RA-APC</i>	eBioscience	17-0458	5 μl /test
<i>CD16-eFluor450</i>	eBioscience	48-0168	5 μl /test
<i>CD16-APC</i>	eBioscience	17-0168	5 μl /test
<i>CD16-PerCP-Cy5.5</i>	Biolegend	302027	5 μl /test
<i>HLA-DR-APC</i>	eBioscience	17-9956	5 μl /test
<i>CD80-PE</i>	eBioscience	12-0809	5 μl /test
<i>CD86-PE</i>	Becton Dickinson	555665	20 μl /test
<i>mouse IgG1-eFluor450 isotype control</i>	eBioscience	48-4714	5 μl /test
<i>mouse IgG1-FITC isotype control</i>	Becton Dickinson	555748	20 μl /test

<i>mouse IgG1-PE isotype control</i>	eBioscience	12-4714	5 µl/test
<i>mouse IgG1-APC isotype control</i>	eBioscience	17-4714	5 µl/test
<i>mouse IgG1-PerCP-Cy5.5 isotype control</i>	eBioscience	45-4714	5 µl/test
<i>biotin anti-human IgG</i>	Vector Laboratories	BA-3000	1:200
<i>fluorescein streptavidin</i>	Vector Laboratories	SA-1200	1:100
<i>Alexa Fluor 405-conjugated anti-rabbit IgG</i>	Invitrogen	A31556	1:1000
Fluorescence Confocal Microscopy			
<i>anti-γδ TCR mouse IgG1</i>	Becton Dickinson	555716	0.1 µg/ml
<i>Cy5-conjugated anti-mouse IgG</i>	Invitrogen	M35011	0.25 µg/ml
Western blot			
<i>anti-γδ TCR mouse IgG1</i>	Beckman Coulter	PN IM1349	1 µg/ml
<i>anti-GAPDH rabbit polyclonal IgG</i>	Santa Cruz Biotech	FL-335	1 µg/ml
<i>HRP-conjugated anti-mouse IgG</i>	Invitrogen	626520	1:1000
<i>HRP-conjugated anti-rabbit IgG</i>	Dako	P 0448	1:2000
Functional cell assays			
<i>mab2G12</i>	NIBSC	EVA 3064	10 µg/ml
<i>Rituximab</i>	Roche	-	10 µg/ml
<i>human IgG1 isotype control</i>	Calbiochem	400120	10 µg/ml
<i>anti-HLA-DR blocking antibody</i>	Becton Dickinson	347360	10 µg/ml
<i>mouse IgG2α isotype control</i>	Becton Dickinson	554126	10 µg/ml

3.1.6 Kits and miscellaneous

Table 8 – Other reagents

Item	Supplier	Cat no.
<i>Mouse IL-2 ELISA</i>	R&D	DY402
<i>Dynabeads</i>	Invitrogen	10103D
<i>SeeBlue Plus2 Prestained Standard</i>	Invitrogen	P/N100006636
Fluorescent cell labelling		
<i>CFSE</i>	Invitrogen	C34554
<i>Dil</i>	Invitrogen	V-22886
<i>PKH26</i>	Sigma	MINI26
<i>Live/Dead Fixable Far Red Dead Cell Stain</i>	Invitrogen	L10120
<i>Alexa Fluor 555-labelled phalloidin</i>	Invitrogen	A34055
Chemicals		
<i>Isopentenyl pyrophosphate (IPP)</i>	Sigma	I0503
<i>Recombinant human IL-2</i>	PeproTech	200-02
<i>Cytochalasin D</i>	Sigma	C8273
<i>Dimethyl amiloride (DMA)</i>	Sigma	A 4562
<i>Chloroquine</i>	Sigma	C6628
<i>Nitroblue tetrazolium</i>	Sigma	84010
<i>Gentamicin</i>	Sigma	G1272
<i>Protease inhibitor</i>	Sigma	P8340

3.2 Methods

3.2.1 Tissue culture

3.2.1.1 Blood collection

Blood was collected from healthy volunteers by venopuncture using a blood collection set (Greiner bio-one #450153) into conical tubes containing 3 IU/ml of heparin (AppliChem #A3004,0250). Blood was kept at room temperature (RT) until processing and was routinely used within 2h of collection.

3.2.1.2 PBMC isolation

PBMCs were isolated from the peripheral blood of healthy volunteers using a standard Ficoll-Paque separation. Briefly, collected blood was diluted 1:2 in Dulbecco's PBS (DPBS) and layered over 15 ml of Ficoll-Paque in conical tubes. The blood was spun at 350 g for 20 min at RT, with the centrifuge brake off. The white buffy layer was aspirated and washed once in DPBS at 300 g for 5 min before magnetic separation.

3.2.1.3 Isolation of polymorphonucleated cells from whole blood

PMN fractions were isolated from whole blood with a dextran sedimentation step followed by a Ficoll-Paque separation. 2 ml of 10% dextran (in saline) and 2 ml of 1x saline were added to 10 ml of freshly collected blood in a conical tube. The tube was mixed by inversion and allowed to settle for 30-45 min at RT. The top plasma layer was removed. The remainder was layered over an equal volume of Ficoll-Paque and spun at 400 g for 10 min at RT. The supernatant was aspirated. The pellet was quickly resuspended in 10 ml of ddH₂O to lyse the red blood cells and immediately mixed with 10 ml of 2x saline to restore isotonicity. The cells were spun for 180 g for 7 min to pellet the cells and resuspended in warm complete RPMI.

3.2.1.4 Magnetic separation

$\gamma\delta$ T cells were routinely isolated from PBMCs using a positive magnetic isolation kit. In a routine isolation 50 ml of blood were used to separate PBMCs. PBMC pellets were resuspended in 200 μ l of ice-cold MACS buffer and 50 μ l of the anti- $\gamma\delta$ TCR hapten antibody included in the kit were added. The cells were incubated on ice for 10 min. After that time, 150 μ l of ice-cold MACS buffer were added, followed by 100 μ l of anti-hapten

FITC magnetic beads included in the kit. The cells were incubated on ice for 15 min. The cells suspension was topped up to 10 ml with ice-cold MACS buffer and spun at 300 g for 5 min at 4°C. The supernatant was carefully aspirated and the remaining pellet was resuspended in 500 µl of ice-cold MACS buffer and loaded onto a freshly prepared LS column. 3 washes were made with 3 ml of ice-cold MACS buffer. The cells were eluted by removing the column from the magnet and plunging 5 ml of ice-cold MACS buffer through. The cells were pelleted at 300 g for 5 min at 4°C. The pellet was resuspended again with 500 µl of buffer and loaded onto a freshly prepared MS column. The column was rinsed three times in buffer and the cells were eluted in 1 ml of buffer.

To check for purity, the cells suspension was mixed by pipetting and 95 µl were taken and incubated with 5 µl of CD3-eFluor450 antibody. The cells were stained in the fridge for 20 min in polystyrene FACS tubes. The cells were washed once at 300 g for 5 min at 4°C. The supernatant was removed and the cells were resuspended in 100 µl. The cells were placed on ice and taken to the flow cytometry facility to check for purity. Purity was assessed as the % of CD3+ $\gamma\delta$ TCR+ cells and was routinely 96-98%.

Monocytes were isolated in a similar way by positive magnetic isolation with a different kit. NK cells were generally isolated using a negative magnetic isolation kit to deplete non-NK cell types (Miltenyi Biotec #130-092-657). A positive isolation kit was used when mentioned in results chapter 5 (Miltenyi Biotec #130-050-401). $\alpha\beta$ T cells were isolated with a PE-conjugated pan- $\alpha\beta$ TCR antibody followed by anti-PE magnetic beads and one MS column.

3.2.1.5 Activation of $\gamma\delta$ T cells

When indicated, $\gamma\delta$ T cells were activated according to Moser's original protocol for $\gamma\delta$ T APC maturation (233). Briefly, 1×10^6 allogeneic non-HLA-DRB1*0101 B-LCL cells were irradiated at 80 Gy and seeded into 0.5 ml of complete RPMI, supplemented with IPP (50 µM) and IL-2 (100 IU/ml). The feeder cells were rested in the incubator during the $\gamma\delta$ T cell magnetic isolation. Freshly isolated $\gamma\delta$ T cells isolated from 50 ml of peripheral blood were resuspended in prewarmed media and added to the well. The cells were co-cultured for 18h at 37°C 5%CO₂.

3.2.1.6 Hybridoma cell culture

The hybridoma cell line A1C5 was a kind gift from Dr David Canaday from Case Western Reserve University, Cleveland, US (261). The hybridoma cells were kept at a concentration of $0.2-1 \times 10^6$ cells/ml. Cell concentration is crucial with this cell line so hybridoma cells were thawed 3-4 days before an antigen presentation assay, and the cell concentration was adjusted daily with fresh media to $0.2-0.5 \times 10^6$ cells/ml.

3.2.2 Flow cytometry

3.2.2.1 Basic assessment of surface markers

PBMCs, magnetically isolated cells or whole blood were incubated with fluorochrome-conjugated antibodies or the matched isotype control at the appropriate volumes as listed in Table 6. All antibodies were stained for 20 min at 4°C in polystyrene FACS tubes. The cells were washed once with approximately 2 ml of FACS buffer at 300 g for 5 min at 4°C and resuspended and analysed within the hour in a BD LSRII flow cytometer. Alternatively, cells were fixed with 1 ml of lyse& fix reagent for 20 min at RT, which also lyses red blood cells in whole blood samples. Samples were analysed on a BD LSRII flow cytometer. Generally, 10 000 events of the cell type of interest were acquired. The results were analysed with FlowJo (version 7.6.5.).

3.2.2.2 Dual-labelling phagocytosis assay

$\gamma\delta$ T cells were freshly isolated by magnetic selection as previously described. The cell viability was confirmed by trypan blue exclusion and the cell number was counted with a haemocytometer chamber. 200 000 cells were seeded in polystyrene FACS tubes in 200 μl of complete RPMI. Opsonised fluorescein-labelled *E. coli* were prepared as previously described. $\gamma\delta$ T cells and bacteria were incubated on separate tubes for 10 min on ice. 20 μl of opsonised bacterial suspension was added to the well at an approximate ratio of 100 bacteria: 1 $\gamma\delta$ T cell. The tubes were incubated at 37°C for 45 min in a waterbath with gentle swirling halfway through. A squirt bottle containing DPBS was chilled in the fridge at 4°C , and the centrifuge was pre-cooled. After 45 min, all tubes were placed on ice. The samples were washed in approximately 2 ml of cold DPBS and spun at 300g for 5 min at 4°C . The supernatant was removed with an aspirator and the remaining pellet was resuspended in the remaining liquid with a P200 pipette. A 1:1000 dilution of Alexa Fluor

405-conjugated anti-rabbit IgG antibody was added. The antibody should bind the rabbit IgG portion in the opsonised non-engulfed bacteria. The samples were incubated for 20 min at 4°C. The samples were washed once in approximately 2 ml of cold DPBS and spun at 300g for 5 min at 4°C. The supernatant was removed with an aspirator and the remaining pellet was resuspended in the remaining liquid with a P200 pipette. The samples were placed on ice and taken to the Flow Cytometry facility where they were analysed within the hour in a BD LSRII flow cytometer. The results were analysed with FlowJo (version 7.6.5).

3.2.2.3 Comparative phagocytosis assay in whole blood

GFP-expressing *E. coli* were grown in 3 ml of sterile LB media supplemented with ampicillin and IPTG at 37°C overnight. The bacteria were washed once in DPBS and then opsonised with 25 µl of opsonising reagent for 30 min at 37°C. A blood sample was collected from a healthy donor during this incubation period. The heparinised blood sample was split into separate polystyrene FACS tubes. After the bacterial opsonisation, the bacteria were washed in 1 ml DPBS and spun at 14 000 g for 2 min at RT. The bacteria were resuspended thoroughly in 20 µl and then in a further 180 µl. FACS tubes and bacteria were pre-chilled separately for 10 min on ice. The bacteria were mixed by vortexing. 20 µl of the bacteria suspension were added per tube while the tubes were on ice. Bacteria and leukocytes were mixed by briefly vortexing. The tubes were placed in a 37°C waterbath except for one which was kept on ice as a control. The tubes were swirled halfway through the incubation time. A squirt bottle with DPBS was chilled at 4°C. The centrifuge was pre-chilled. After 30 min in the waterbath, all tubes were transferred to ice. Approximately 2 ml of cold DPBS were added per tube and they were spun at 300 g for 5 min at 4°C. The tubes were placed again on ice. The supernatant was removed down to the red pellet with a bench aspirator and a P200 pipette leaving the leukocytes in a residual volume of approximately 200 µl. Antibodies were added as described in Table 8 and the cells were mixed by gentle vortexing.

Table 9 – Antibody staining for comparative flow cytometry phagocytosis assay

<i>Tube</i>	<i>Label</i>	<i>Antibodies</i>
1	$\gamma\delta$ T cells	10 μ l $\gamma\delta$ TCR-APC 10 μ l CD3-eFluor450
2	$\alpha\beta$ T cells	10 μ l $\alpha\beta$ TCR-APC 10 μ l CD3-eFluor450
3	NK cells	40 μ l CD56-APC 10 μ l CD3-eFluor450
4	monocytes	40 μ l CD14-APC
5	ice control	-

The cells were stained for 20 min at 4°C. The tubes were placed again on ice and washed with ice-cold DPBS at 300 g for 5 min at 4°C. The supernatant was removed, the cells were resuspended with gentle vortexing and 2 ml of lyse & fix reagent were added per tube (10x stock from GlycoTope Biotechnology's PHAGOTEST kit, diluted 2 ml in 19 ml of ddH₂O). The cells were mixed with a P1000 pipette. The cells were incubated for 20 min at RT in the dark. The tubes were spun at 300 g for 5 min at 4°C. The cells were placed on ice and analysed by flow cytometry in a BD LSRII flow cytometer within an hour. The results were analysed with FlowJo (version 7.6.5.).

3.2.2.4 Cell-mediated cytotoxicity assay

Effector cells were seeded at the mentioned E:T ratios with a constant target cell number of 10 000 targets. When an E:T ratio is not mentioned, an E:T=10 with 100 000 effector cells was used per well. Effector cells were seeded in 100 μ l in complete RPMI in a U bottom 96-well plate. The plate was kept in the incubator at 37°C 5%CO₂ while the targets were prepared. 3 ml of target cell culture containing between 1.5-3x10⁶ cells were transferred to a 15 ml conical tube. Targets cells used were either K562, H9 or HH cells, as mentioned. The cells were spun at 300 g for 2 min at RT. The cells were washed 1x in 10 ml of DPBS to remove all traces of protein in the supernatant which is crucial for PKH26 staining. The cells were resuspended in 200 μ l of diluent C (part of PKH26 kit). In a separate tube, 2 μ l of PKH26 were mixed with 400 μ l of diluent C to make a 2x stock. 200 μ l of this 2x stock was immediately mixed with the cell suspension and incubated for

3 min at RT in the dark. The staining was quenched with 400 μ l of FCS, prewarmed to RT, and incubated for 1 min. The cells were spun at 300 g for 2 min at RT. The supernatant was aspirated and the cells were washed once in 10 ml of DPBS. The cells were resuspended in 1 ml of complete RPMI and counted. For direct cytotoxicity assays, the target cells were resuspended at 1×10^5 cells/ml and 100 μ l were added per well. For antibody-dependent cytotoxicity assays, target cells were incubated with 10 μ g/ml of mab2G12 or human IgG1 for 30 min at RT in microcentrifuge tubes. After 30 min, the antibody coated cells were added to the wells with no washing step. The plate was spun at 200 g for 1 min at RT and carefully placed in the incubator. The cells were co-cultured for 4h at 37°C 5%CO₂. After 4h the plate was spun at 300 g for 5 min. A sample of PKH26-labelled targets was snap frozen in the absence of a cryoprotectant to use as a control to set the “dead targets” gate. Untouched PKH26-labelled target cells were also used as a control to visualise “live targets”. The supernatant was aspirated and the cells were resuspended in 150 μ l of DPBS. The plate was spun again and the cells were resuspended in 50 μ l of DPBS. A 1:500 dilution of Live/Dead Fixable Far Red dye was prepared and 50 μ l were added per well. The wells were mixed with pipetting and the cells were stained for 30 min at RT, protected from light. The plate was spun again. The supernatant was decanted. The cells were washed once in DPBS and resuspended in 2% paraformaldehyde. The cells were fixed for 15 min at RT and placed in the fridge o.n. before being analysed by flow cytometry in a BD LSRII flow cytometer. The results were analysed with FlowJo (version 7.6.5.).

3.2.3 Fluorescence confocal microscopy

Cells were analysed by fluorescence confocal microscopy in polylysine coated slides (Vector Laboratories #H-4000). The cells were added to 1 cm³ wells drawn with a wax pen (Thermo Scientific #J2800AMNZ). The cells were incubated in a volume of approximately 150 μ l of complete RPMI at 37°C 5%CO₂ for different times depending on the assay. Afterwards, the slides were taken out of the incubator, rinsed in PBS and fixed in 100 μ l/well of 4% paraformaldehyde for 15 min at RT. The slides were rinsed 3x in PBS and permeabilised in 100 μ l/well of 0.1% Triton (10 ml PBS + 10 μ l Triton) for 7 min at RT. The slides were rinsed 3x in PBS and blocked in 100 μ l/well of 3% BSA (0.3g BSA + 10 ml PBS) for 30 min at RT. The slides were rinsed 3x in PBS and stained with 1° antibodies as mentioned in the assays in 100 μ l of PBS for 30 min at RT. The slides were rinsed 3x in

PBS and stained with 2° antibodies for 30 min at RT. The slides were rinsed 3x in PBS and 1x in ddH₂O and mounted. Mounting media ProLong Gold antifade reagent with DAPI (Invitrogen #P36935) was allowed to warm to RT for 10 min before use. Excess moisture from the slides was removed by tapping the side of the slide on a clean paper towel. One drop of mounting media per well was added and the well was sealed with a coverglass (Heathrow Scientific #HEA159879H). The samples were cured overnight (o.n.) at RT in the dark. The next day, the edge of the coverslips was sealed with nail polish and the sample was stored at 4°C until examination with a fluorescence confocal microscope (Zeiss LSM 710).

3.2.3.1 Phagocytosis assays

Oponised fluorescein-labelled *E. coli* were prepared as the following description. Fluorescein-labelled killed *Escherichia coli* (K-12 strain) and opsonising reagent were acquired from Invitrogen (#E-2861 and #E-2870, respectively). The opsonising reagent is derived from purified rabbit polyclonal IgG antibodies specific for *E. coli*. and both products are supplied as lyophilised powders. The *E. coli* vial contains 10 mg at approximately 3x10⁸ *E. coli* per mg of solid. This vial was reconstituted at 20 mg/ml in DPBS. The tubes were capped and the particles were gently swirled into suspension, followed by vigorous vortexing. Reconstituted suspensions were stored at 4°C in the dark until use. The opsonising reagent is sufficient to opsonise 10 mg of the matching lyophilised *E. coli*. The opsonising reagent was reconstituted in 500 µl of sterile ddH₂O and stored at -20°C in single-use aliquots. *E. coli* suspensions were freshly opsonised before each experiment in the following way. Equal volumes of opsonising reagent and the 20 mg/ml suspension of *E. coli* were mixed in a sterile 1.5 ml microcentrifuge tube and incubated for 30 min at 37°C in a waterbath, in the dark. The opsonised bacteria were washed 1x with 1 ml of DPBS at 14 000 g for 2 min. The pellet was resuspended in DPBS and added to the γδ T cells.

γδ T cells were freshly isolated by magnetic selection as previously described. The cell viability was confirmed by trypan blue exclusion and the cell number was counted with a haemocytometer chamber. 20 000 – 40 000 γδ T cells and opsonised fluorescein-labelled *E. coli* were seeded per well on polylysine slides. The slides were kept in the incubator at 37°C 5%CO₂ for 45 min. After that incubation period, the slides were fixed, permeabilised,

blocked, stained and mounted as mentioned earlier. The 1° antibody used was 1 µg/well of mouse IgG1 anti-γδ TCR antibody diluted in 100 µl of PBS. As a 2° antibody, 2.5 µg/well of Cy5-conjugated anti-mouse IgG antibody were diluted in 100 µl of PBS. Together with the 2° antibody, F-actin was stained with 1:100 Alexa Fluor 555-labelled phalloidin. Pictures were taken using a Zeiss LSM710 fluorescence confocal microscope.

To compare phagocytosis across different cell types, a slightly different phagocytosis assay was performed. γδ T cells, αβ T cells, NK cells and monocytes were isolated by magnetic isolation from PBMCs as previously described. For each experiment, 50 ml of blood were drawn from a healthy donor. PBMCs were isolated by Ficoll separation and resuspended in 50 ml of DPBS. Of these, 7 ml were transferred to a separate tube for monocyte isolation, 7 ml for NK cell isolation and 2 ml for αβ T cell isolation. The remaining volume was used for γδ T cell isolation. After magnetic isolation, the samples were resuspended in 100 µl of MACS buffer and fluorochrome-conjugated monoclonal antibodies were added as described in Table 9. The samples were stained for 20 min at 4°C and washed once in MACS buffer before cell sorting on a MoFlo XDP flow cytometer.

Table 10 – Antibody staining for FACS sorting of magnetically isolated fractions

Sample	Magnetic isolation staining	Further staining for FACS sorting
<i>γδ T cells</i>	γδ TCR-FITC	5 µl CD3-APC
<i>αβ T cells</i>	αβ TCR-PE	5 µl CD3-APC
<i>NK cells</i>	-	5 µl CD3-APC 20 µl CD56-PE
<i>monocytes</i>	-	20 µl CD14-APC

The FACS sorted cells were seeded onto 1 cm³ wells drawn in polylysine slides. Opsonised fluorescein-labelled *E. coli* or opsonised GFP-expressing *E. coli* were prepared as described previously, and added to the slides at a ratio of 100 bacteria to 1 leukocyte. The slides were incubated at 37°C 5%CO₂ for 45 min. The slides were then fixed, permeabilised, blocked, stained and mounted as previously mentioned. No antibodies were used so that the pictures could remain anonymous throughout scoring. However, in order to visualise the cell body, F-actin was stained with 1:100 Alexa Fluor 555-labelled phalloidin. 100 pictures were taken

per well. The pictures were anonymised and randomised using the purpose build “RenameRandom” software before being analysed. Each picture was scored using the “cell counter” plugin in the microscopy analysis software Image J.

3.2.3.2 Acquisition of target cell antigen

Magnetically isolated $\gamma\delta$ T cells were stained with CFSE. For CFSE labelling, the cells were resuspended at 1×10^6 /ml in prewarmed PBS/0.1% BSA. One vial of CFSE powder was reconstituted in 18 μ l of DMSO to make a CFSE stock. 2 μ l of CFSE stock were added per ml of cell suspension. The cells were incubated for 10 min at 37°C. CFSE staining was quenched by the addition of 5 volumes of ice cold complete RPMI and incubation on ice for 5 min. The cells were spun at 300 g for 5 min at RT and resuspended in 10 ml of complete RPMI. The cells were washed 3x in media and rested in the incubator at 37°C 5%CO₂ while the Daudi cells were stained. Daudi cells were stained with the lipophilic orange-red fluorescent dye Vybrant DiI. Daudi cells were resuspended at 1×10^6 cells/ml in prewarmed serum-free RPMI. 5 μ l of DiI were added per ml of cell suspension. The cells and dye were mixed gently by pipetting and incubated for 5 min at 37°C. The cells were spun at 300 g for 5 min at RT and resuspended in warm complete RPMI. The cells were washed 3x in complete RPMI. Afterwards, the cells were pelleted and incubated in a 1.5 ml microcentrifuge tube with 10 μ g/ml of Rituximab. The cells and antibody were incubated for 15 min at RT. $\gamma\delta$ T cells and Daudi cells were mixed and seeded onto polylysine slides. The cells were co-cultured for 1h at 37°C 5%CO₂. When indicated, the $\gamma\delta$ T cells and Daudi cells were pre-incubated with 250 μ M DMA or 5 μ M Cytochalasin D, or both. The slides were mounted with a hard-set mounting media (Vector Labs #H-1400) as the mounting media usually used is not compatible with DiI.

3.2.4 Microbiology

3.2.4.1 GFP- E. coli culture

GFP-expressing *E. coli* were grown fresh before each experiment in 3 ml of LB media supplemented with ampicillin and IPTG at 37°C overnight.

3.2.4.2 Construction of a GFP-E. coli growth curve

GFP-expressing *E. coli* were inoculated from a colony in a plate in 3 ml of LB media supplemented with ampicillin and IPTG at 37°C. A sample of 150 μ l of the culture was

taken every hour for 8h. The sample was mixed by vortexing and 100 µl were diluted with 900 µl of sterile DPBS (= -1 dilution). The sample was diluted a further 5 times in the same way and 100 µl of the -6 dilution were seeded in duplicate ampicillin plates. The optical density at 600 nm (OD 600) was measured in a spectrophotometer. For the first and second hours, OD 600 was measured with the -1 dilution. For the following hours the -6 dilution was used. In this way, photometric measurements were taken in the linear range (0.1 and 0.5 OD 600). Ampicillin plates were incubated at 37°C overnight. The next day, colonies were counted using a colony counter. The concentration of the bacterial cultures was calculated from the number of colonies on the plate according to the following equation:

$$\frac{CFU}{ml} = \frac{\text{no. colonies} \times \text{dilution factor}}{\text{volume plated}}$$

3.2.4.3 Gentamicin protection assay

For the gentamicin protection assay, leukocyte cones were used instead of freshly drawn blood as the number of $\gamma\delta$ T cells needed exceeds what can reasonably be obtained from 50 ml of blood. A leukocyte cone derives from a pint (568 ml) donation of blood. Leukocyte cones were obtained from the National Blood Service. PBMCs were isolated from leukocyte cones in the same way as previously described for fresh blood except instead of the blood being diluted 1:2 in DPBS, leukocyte cones containing around 8 ml of concentrated blood product were diluted to 50 ml in DPBS. After isolation of the PBMCs, the cell viability was confirmed by trypan blue exclusion and the cell number was counted with a haemocytometer chamber. Magnetic isolation of monocytes, $\gamma\delta$ T cells and $\alpha\beta$ T cells was performed in parallel from 100×10^6 , 20×10^6 and 20×10^6 PBMCs from the same sample. The cells were resuspended at 1×10^6 /ml in complete RPMI without antibiotics and seeded at 100 000 cells/well in triplicate. Monocytes were seeded in flat-bottom 96-well plates and T cells were seeded in U bottom 96-well plates to prevent cell loss during the washing steps. The number of GFP-expressing *E. coli* in the bacterial culture was estimated from the OD 600 to achieve an approximate ratio of 100 bacteria: 1 leukocyte. The bacteria were pelleted at 14 000 g for 2 min at RT in a microcentrifuge tube. The pellet was resuspended with 25 µl of opsonising reagent and incubated for 30 min at 37°C in a waterbath. The bacteria were washed 1x in 1ml of DPBS. The bacteria were resuspended in complete RPMI without antibiotics and 20 µl were added per well. A sample was seeded

onto ampicillin plates to confirm the bacteria: leukocyte ratio. The leukocytes and bacteria were incubated for 45 min at 37°C 5%CO₂. The plates were spun at 300 g for 5 min at 4°C to pellet the cells. Supernatants were very carefully removed with a P200 pipette so as not to disturb the pellet. The pellets were resuspended in 200 µl of cold DPBS/well and spun at 300 g for 5 min at 4°C. This step is crucial as it removes excess bacteria in suspension. Bacteria do not pellet well at 300 g unlike leukocytes which means the majority of them will be removed. The pellets were resuspended in 150 µg/ml of gentamicin diluted in complete RPMI without antibiotics. The cells were incubated in gentamicin media for 1 h at 37°C 5%CO₂ to kill any remaining non-engulfed bacteria. After the incubation period, a sample of gentamicin supernatant was seeded onto ampicillin plates to confirm bacterial killing. Afterwards, the cells were washed 3x in 200 µl DPBS/well at 300g 5 min 4°C spins to remove any remaining traces of gentamicin. The supernatant was carefully removed from all the wells and the pellets were resuspended in 100 µl of 0.1% Triton in DPBS/well (10 ml DPBS + 10 µl Triton). The lysis buffer was incubated for 15 min at RT to lyse eukaryotic cells and release phagocytosed bacteria. Lysis was confirmed by light microscopy. The entire contents of each well (100 µl) were diluted in 900 µl of sterile DPBS. The samples were thoroughly mixed by vortexing and 100 µl were seeded onto ampicillin agar plates. The plates were incubated o.n. at 37°C and colonies were counted the next day with a colony counter.

3.2.5 Nitroblue tetrazolium (NBT) test

A phagocytosis assay with opsonised GFP-expressing *E. coli* and whole blood was performed as described previously with CD3/γδ TCR staining with the only difference that the cells were not fixed in the last step and instead resuspended in FACS buffer for sorting. The cells were FACS sorted on a MoFlo XDP. FACS sorted phagocytic and non-phagocytic CD3+ γδ TCR+ cells and neutrophils were collected on flat-bottom 96-well plates. 1 µg/ml of NBT reagent was added to all wells and incubated at 37°C 5%CO₂. After 30 min of incubation, the wells were examined on a light microscope and pictures were taken with an attached digital camera. Cells with blue formazan precipitates were scored as NBT positive.

3.2.6 Diff-Quick staining

A phagocytosis assay with opsonised GFP-expressing *E. coli* and whole blood was performed as described previously with CD3/ $\gamma\delta$ TCR staining. FACS sorted phagocytic and non-phagocytic CD3+ $\gamma\delta$ TCR+ cells were collected on 1.5 ml microcentrifuge tubes. The cells were cytopun onto microscopy slides. The slides were fixed in fast green methanol for 1 min at RT, stained in Eosin Y in PBS for 1 min at RT and then stained in Thiazine dye in PBS for 1 min at RT. The slides were blotted for excess dye in between steps. The slides were blotted and allowed to air dry. Pictures were taken with a light microscope with a digital camera attached. The cells were scored according to morphology.

To confirm the presence of eosinophils and neutrophils in a PMN fraction from whole blood I used the exact same staining procedure. Neutrophils can be identified by their purple multi-lobed nuclei and light cytoplasm and eosinophils stain orange-red for eosin granules and have bi-lobed nuclei.

3.2.7 Western blot

1×10^6 cells were pelleted in 1.5 ml microcentrifuge tubes at 300 g for 10 min at 4°C. Lysis buffer was prepared fresh by diluting 100 μ l of protease inhibitor with 900 μ l of RIPA buffer and kept on ice. After the cells were pelleted, the supernatant was removed and the cells were resuspended in 40 μ l of ice-cold lysis buffer. The cells were lysed for 30 min on ice and spun at 14 000 g for 10 min at 4°C. The supernatants were transferred to new microcentrifuge tubes and stored on ice. 2x Laemmli's buffer was added to the supernatants, mixed and incubated at 85°C for 5 min. The samples and the SeeBlue Plus2 Prestained Standard were separated by electrophoresis in a Novex 4-12% Bis-Tris gel in 1x MOPS buffer at 200V for 35 min. The separated proteins were wet-transferred onto a methanol-activated Immobilon-P PVDF membrane using the X-Cell II Blot Module and 1x NuPAGE Transfer buffer containing 10% methanol at 30V for 1h. The membrane was blocked in PBS-T + 5% BSA for 1h at RT. Primary antibody staining was performed for 1h with 1 μ g/ml of anti- $\gamma\delta$ TCR mouse IgG1 and 1 μ g/ml of anti-GAPDH rabbit polyclonal IgG. The membrane was washed 3x with PBS-T and stained with HRP-conjugated anti-mouse IgG (1:1000) and HRP-conjugated anti-rabbit IgG (1:2000) for 1h at RT. The membrane was washed three times in PBS-T and peroxidase activity was visualised with a Western ECL reagent and UviChemi chemiluminescence detection.

3.2.8 Chromium release assay

A classic chromium release assay was used to validate the flow cytometry-based cytotoxicity assay developed for the CL3 lab. I tested PBMCs from the same donor in parallel with the two assays. The assays were performed in U bottom 96-well plates. The first 3 rows of columns A to G were seeded with 100 µl of complete RPMI. PBMCs were isolated and resuspended at 2.5×10^6 cells/ml. 200 µl were seeded in the first column and serially diluted with 100 µl volumes and a P200 multipipette until column F so that the maximum E:T ratio had 250 000 PBMCs/well. Columns A to F correspond to different E:T ratios, whereas no effectors are added to column G. The plate was kept at 37°C 5%CO₂ while the targets cells were prepared. K562 cells were counted and 2×10^6 K562 cells were pelleted at 300 g for 5 min at RT. The cells were resuspended in 180 µl of fresh warm complete RPMI. 20µl of chromium-51 (Perkin Elmer #NEZ030002MC) were added and the cells were incubated in a waterbath at 37°C for 1h. Chromium-labelled K562 cells were washed 3x in DPBS and resuspended in complete RPMI. The cells were counted and the concentration was adjusted to 5×10^4 cells/ml. 100 µl of targets were added to all the wells including an extra 3 rows of column I. The plate was spun at 200 g for 1 min at RT to promote effector and target cell contact. The plate was carefully removed from the centrifuge and 100 µl of 2% Triton were added to column I. The cells were carefully placed in the incubator at 37°C 5%CO₂ for 4h. 50 µl of the supernatants were added to 150 µl of scintillation fluid (Perkin Elmer #1200-439) in a 96-well plate and radioactivity was read the next day. Specific lysis was calculated according to the following formula, where spontaneous lysis refers to wells with target cells in the absence of effectors and maximum lysis refers to target cells in the absence of effectors in the presence of 1% Triton:

$$\% \text{ Specific Lysis} = \frac{(\text{Sample cpm} - \text{Spontaneous Lysis Control cpm})}{(\text{Maximum Lysis Control cpm} - \text{Spontaneous Lysis Control cpm})} * 100\%$$

3.2.9 Antigen presentation assay

Antigen presenting cells were isolated from the PBMCs of healthy HLA-DRB1*0101 donors by magnetic isolation. Cells were seeded at 20 000 cells/well in 20 µl of hybridoma media in triplicate. The cells were rested in the incubator at 37°C 5%CO₂ while the antigen coated beads were prepared. Selected wells were incubated with 50 µg/ml of chloroquine in hybridoma media for 1h.

The beads were prepared as follows: 50 μ l of Dynabeads were transferred to a 1.5 ml microcentrifuge tube, the beads were washed 3x with 700 μ l of cold Talon buffer using a Miltenyi biotec magnet to separate the magnetic beads from the supernatant. 50 μ l of recombinant his-tagged M1 protein (2.2 mg/ml) were mixed with the beads and incubated on a roller for 5 min at RT. The beads were washed again 3x with cold Talon buffer. The beads were mixed with 50 μ l of anti-M1 rabbit polyclonal serum and incubated for 5 min at RT. M1 protein and anti-M1 serum were a kind gift from Dr Paul Digard, University of Cambridge. The beads were washed 3x with 700 μ l of Talon buffer and resuspended in 140 μ l of warm hybridoma media and 5 μ l were added per well. Antigen presenting cells were incubated with the beads for 1h.

Selected wells then received a blocking anti-HLA-DR antibody or matched isotype control for 30 min. The hybridoma cells were pelleted at 300 g for 5 min at RT. The cells were resuspended in warm hybridoma media and the concentration was adjusted to 1×10^6 cells/ml. 20 μ l of the hybridoma cell suspension were added per well. The cells were co-cultured for 24h at 37°C 5%CO₂. After 24h, the plates were spun at 300 g for 5 min at RT and the supernatants were collected. The supernatants were frozen at -20°C and read the next day with a mouse IL-2 ELISA and half-area ELISA plates (costar #3690).

3.2.10 Statistical analysis

Statistical analysis was performed with GraphPad Prism. Data were analysed with a one-way ANOVA followed by Tukey's correction for multiple comparisons. A p value ≤ 0.05 was taken as statistically significant: $p \leq 0.05 = *$, $p \leq 0.01 = **$, $p \leq 0.001 = ***$. For all bar graphs, the mean \pm SD is plotted.

4 Phagocytosis by $\gamma\delta$ T cells

4.1 Aims

- Observation of $\gamma\delta$ T cell phagocytosis by confocal microscopy
- Quantification of $\gamma\delta$ T cell phagocytosis by comparison with other leukocytes by
 - gentamicin protection assay
 - confocal microscopy
 - flow cytometry
- Characterisation of phagocytic $\gamma\delta$ T cells in terms of features shared with classical phagocytes in the blood such as reactive oxygen species production
- Identification of distinguishing features between phagocytic and non-phagocytic $\gamma\delta$ T cells such as cell surface markers and morphology

4.2 Introduction

Phagocytosis is a specialised process restricted to professional phagocytes. Professional phagocytes include monocytes, macrophages and dendritic cells and also polymorphonucleated cells such as neutrophils and eosinophils.

Phagocytosis is an active endocytic process used for the uptake of particles more than 0.5 μm in diameter. It is receptor-mediated and requires actin polymerization and reorganization (228;262). Phagocytic receptors include Fc γ receptors, complement receptors and mannose receptors. After internalisation the phagocytosed particle is contained in a phagosomal vesicle that fuses with lysosomes containing a variety of hydrolytic enzymes that kill and degrade microbes (263). Phagocytosis is used to clear pathogens such as bacteria or yeast, or large debris such as the remnants of dead cells (228).

Phagocytosis was recently reported in a population of human blood $\gamma\delta$ T cells (223). This intriguing observation supports the notion that $\gamma\delta$ T cells may be evolutionarily ancient lymphocytes and could have implications on their role in the control of infection and cancer. This chapter describes experiments designed to better understand the relevance of phagocytosis by $\gamma\delta$ T cells through the quantification of phagocytosis in these cells in parallel with other immune cells and attempting to isolate and characterise the phagocytic $\gamma\delta$ T cell fraction.

4.3 Confocal microscopy of phagocytosis of opsonised fluorescein-labelled *E. coli* by $\gamma\delta$ T cells

Confocal microscopy is a useful tool for detecting $\gamma\delta$ T cell phagocytosis as it allows for the direct observation of cell-scale processes and the staining of $\gamma\delta$ TCR receptors. Both confocal microscopy and electron microscopy were previously used to evidence phagocytosis in freshly isolated $\gamma\delta$ TCR⁺ cells (223). Since our lab did not have direct access to an electron microscope I decided to replicate the original qualitative confocal microscopy assay before developing it further as a quantitative one. In brief, $\gamma\delta$ T cells were isolated to high purity (96-98%) by double column direct magnetic isolation from freshly isolated PBMC from healthy donors. They were mixed with fluorescein-labelled *E. coli* opsonised with anti-*E. coli* IgG antibodies and incubated on microscopy slides for 45 min at 37°C. The cells were stained for $\gamma\delta$ TCR (magenta) and F-actin (red). In Figure 4.1 I show representative images of a phagocytosis experiment. This experiment was repeated in six donors with similar results (data not shown).

Phagocytosis defined as green bacteria fully within the red actin border on z-stacks was observed in only a small proportion of $\gamma\delta$ T cells. $\gamma\delta$ T cells were frequently associated with bacteria, but most of these appeared to be bound to the cell surface (Figure 4.1, asterisks). Individual cells were imaged across several z-stacks to determine whether bacteria were inside the $\gamma\delta$ T cell. On most z-stacks it was difficult to determine whether bacteria were surface-bound or internalised (Figure 4.3) but some appeared to show that the bacteria had been phagocytosed (Figure 4.2, white arrow). $\gamma\delta$ TCR staining (magenta) was typically punctate which might be due to clustering of the anti- $\gamma\delta$ TCR magnetic beads during the magnetic isolation procedure. In addition, $\gamma\delta$ TCR staining was weaker on some cells. This is perhaps due to lower levels of $\gamma\delta$ TCR expressed on some $\gamma\delta$ T cell populations (as shown later in Figure 5.1) or the fact that most of the surface $\gamma\delta$ TCR epitopes may already be occupied by the anti- $\gamma\delta$ TCR magnetic beads used during the cell isolation step.

In conclusion, evidence of phagocytosis as defined by internalisation of bacteria could be detected in $\gamma\delta$ T cells freshly isolated from the blood of healthy donors. However, the proportion of $\gamma\delta$ T cells found to phagocytose was small. In order to improve quantification of phagocytosis by $\gamma\delta$ T cells I decided to explore the use of flow cytometry as described in the next section.

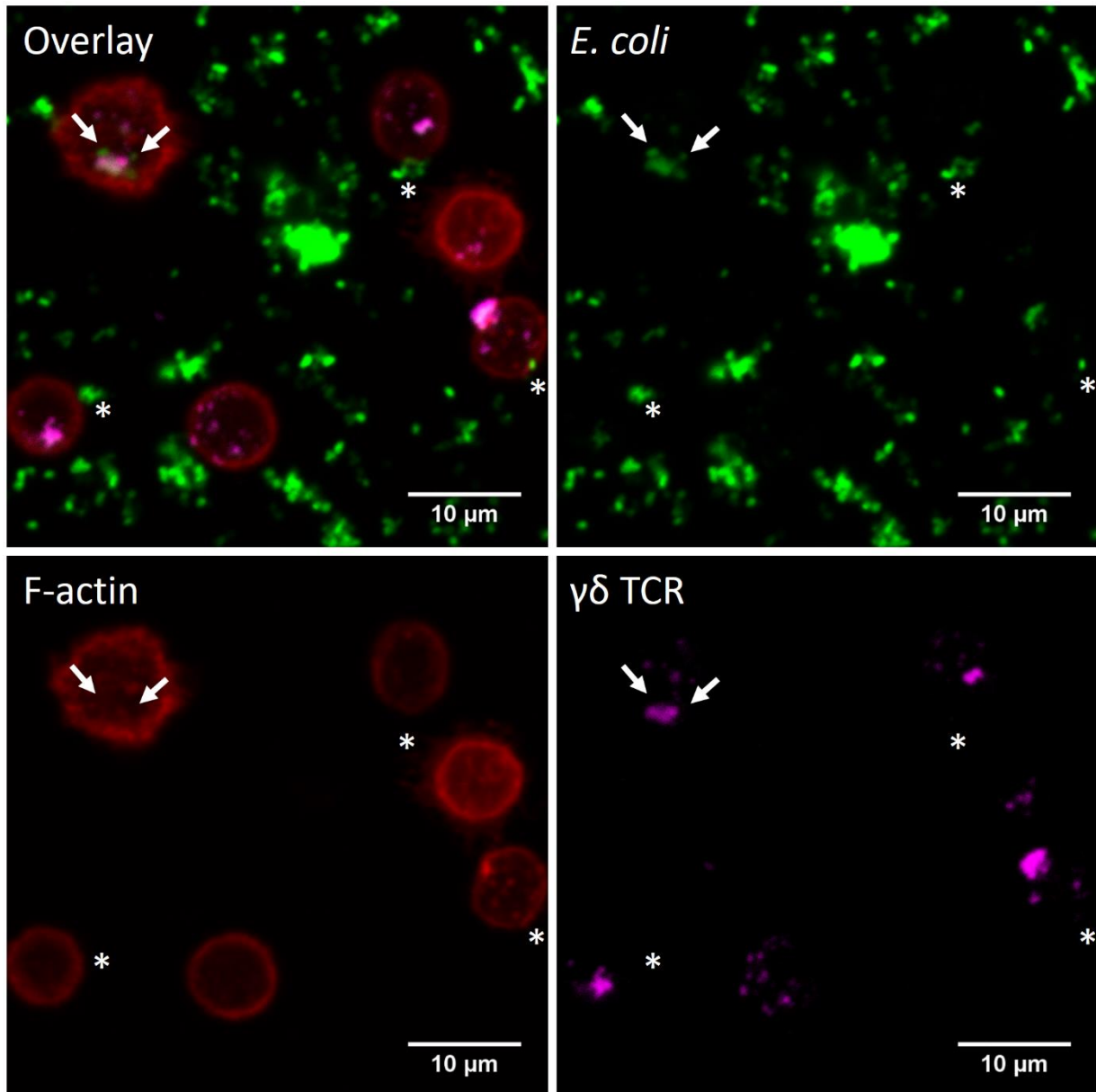


Figure 4.1 – Detection of phagocytosis of opsonised green fluorescent *E. coli* by $\gamma\delta$ T cells using confocal microscopy

To investigate whether human blood $\gamma\delta$ T cells can phagocytose, freshly MACS isolated $\gamma\delta$ T cells were incubated with IgG-opsonised fluorescein-labelled *E. coli* for 45 min at 37°C in polylysine coated slides in complete RPMI. The slides were then fixed, permeabilised and stained for $\gamma\delta$ TCR (magenta) and F-actin (red) to visualise by fluorescence confocal microscopy. Individual cells can be identified by their fluorescent red cytoskeleton. Punctate $\gamma\delta$ TCR staining can be observed in magenta in all cells. White arrows indicate phagocytosed *E. coli*. Asterisks denote bacteria bound to the $\gamma\delta$ T cells but not internalised.

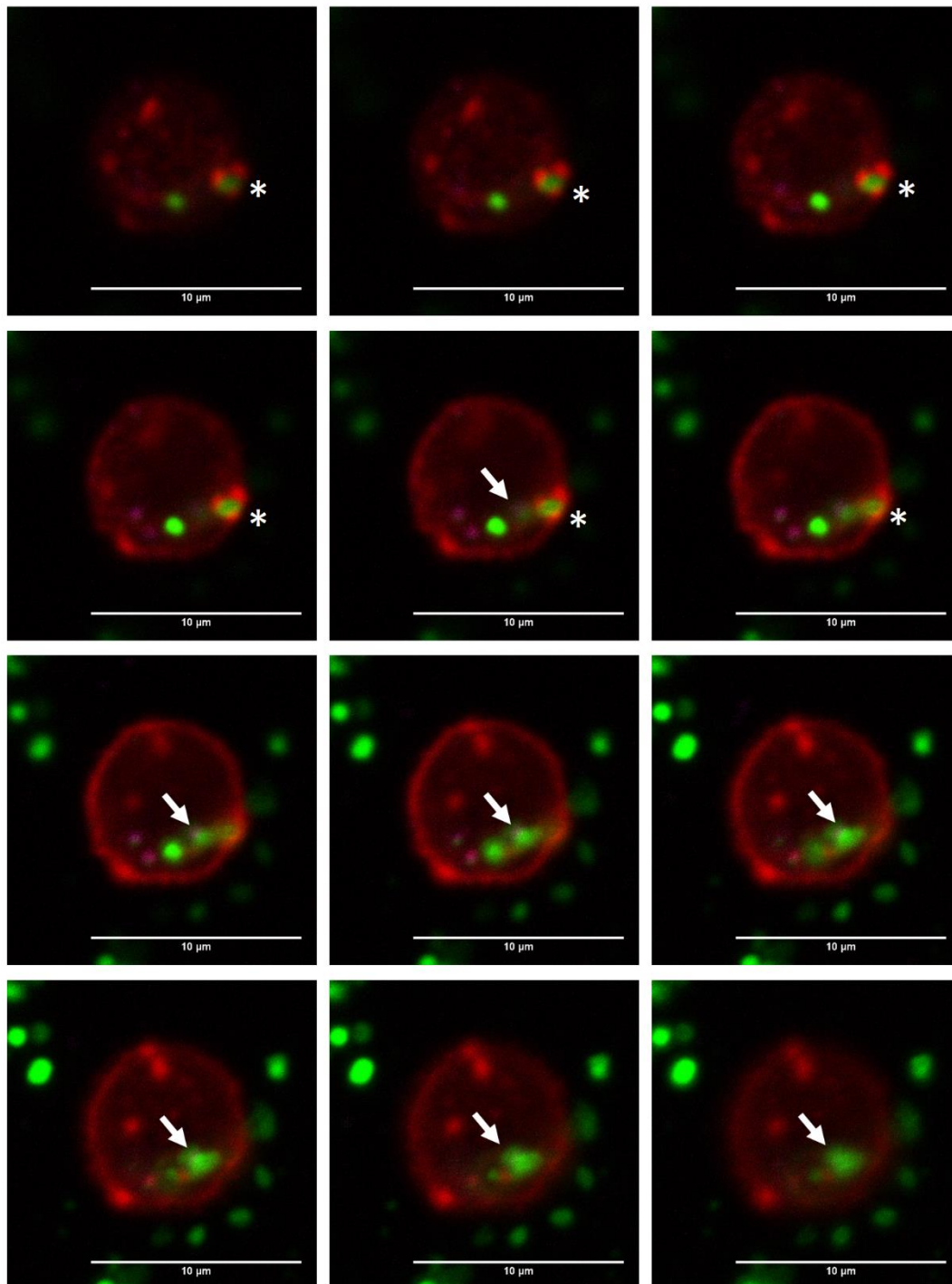


Figure 4.2 – Distinguishing intracellular *E. coli* from surface bound *E. coli* by confocal microscopy z-stacks

Top to bottom z-stacks were taken of freshly isolated $\gamma\delta$ T cells incubated with IgG-opsonised fluorescein-labelled *E. coli*. Individual $\gamma\delta$ T cells can be identified by their fluorescent red cytoskeleton. Punctate $\gamma\delta$ TCR staining can be seen in magenta. Bacteria that appear on the top stacks but disappear when looking inside the cell may be bound but not internalised and are depicted with an asterisk. A white arrow indicates phagocytosed *E. coli* which are not visible on top of the cell but appear in the middle stacks.

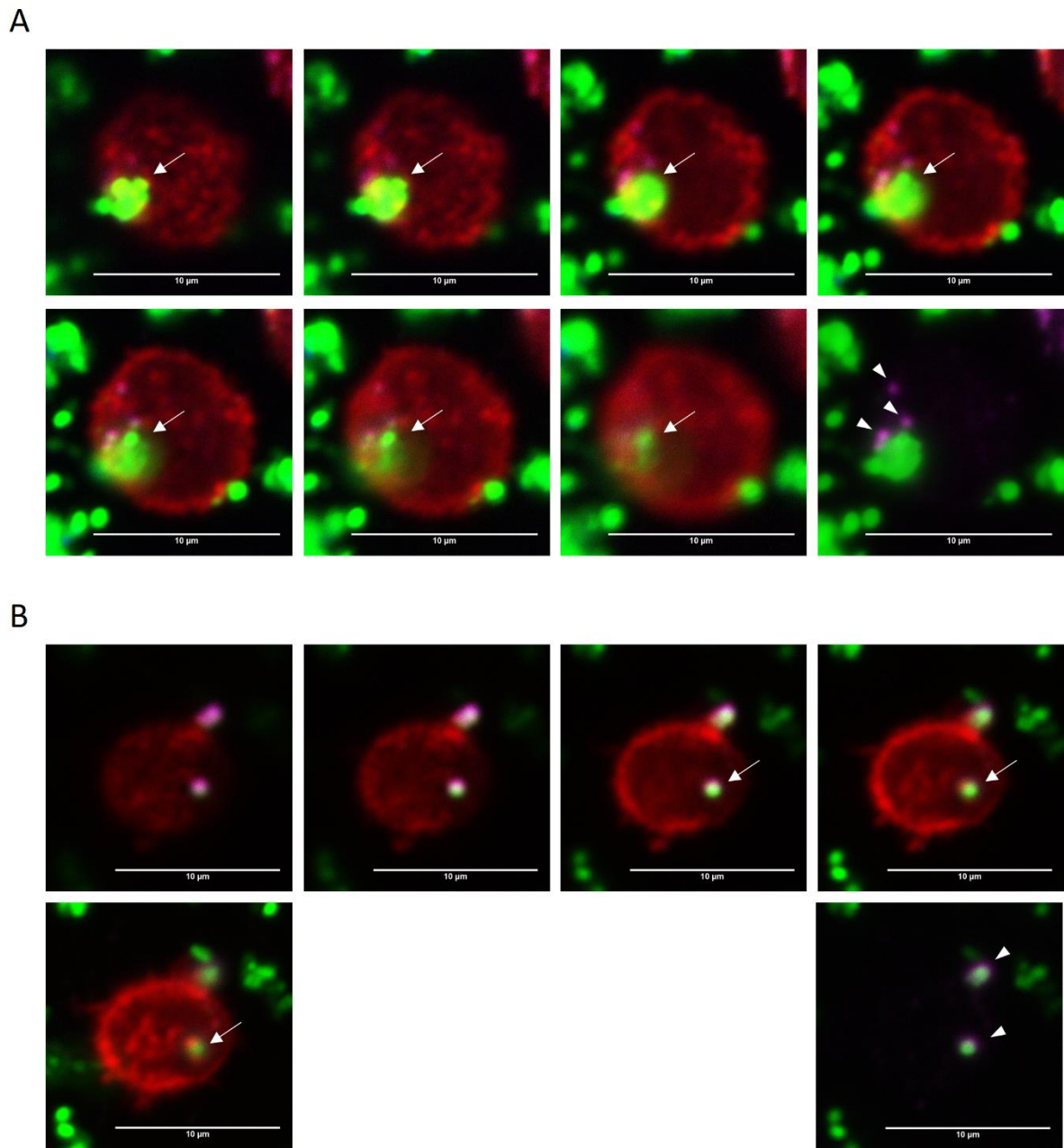


Figure 4.3 – Examples of confocal microscopy z-stacks where the distinction between intracellular *E. coli* and surface bound *E. coli* is ambiguous

Top to bottom z-stacks were taken of freshly isolated $\gamma\delta$ T cells incubated with IgG-opsonised fluorescein-labelled *E. coli*. Individual $\gamma\delta$ T cells can be identified by their fluorescent red cytoskeleton. A white arrow indicates *E. coli*. $\gamma\delta$ TCR staining in magenta is highlighted by removing red cytoskeleton fluorescence in the overlay on the bottom right pictures in A and B. A white arrowhead indicates punctate $\gamma\delta$ TCR staining.

4.4 Quantification of phagocytosis by $\gamma\delta$ T cells using a dual labelling flow cytometry assay

Flow cytometry can be used to quantify phagocytosis using fluorescently labelled bacteria. One caveat is that bacteria adhering to the cell surface but not internalised will still be fluorescent. The fluorescence of externally adhered bacteria can be quenched using the vital dye trypan blue (264-266). This dye is incapable of penetrating intact cell membranes and so does not quench internalised bacteria. However, in initial experiments I found trypan blue quenching to be unreliable as quenched bacteria still appeared visibly green fluorescent under the fluorescent microscope (data not shown). In fact, different brands of trypan blue seem to vary significantly in their quenching abilities (266).

A different option is to use the opposite approach, and fluorescently label only bacteria that are attached to the cell surface by staining with a fluorescently conjugated antibody after phagocytosis has taken place. To quantify phagocytosis I incubated freshly isolated $\gamma\delta$ T cells with opsonised commercially available fluorescein-labelled *E. coli* in two independent experiments, one of which is shown in Figure 4.4. The non-engulfed bacteria were stained with an Alexa Fluor 405 (blue fluorescent) conjugated antibody. Cells that have phagocytosed fluorescein-labelled bacteria would be expected to emit green fluorescence, whereas cells that have only bound but not internalised fluorescein-labelled bacteria should emit both green and blue fluorescence. Samples of Alexa Fluor 405 stained and unstained bacteria were confirmed to fluoresce blue and green, or only green, respectively (Figure 4.4A). These were used to draw theoretical “bound *E. coli*” and “phagocytosed *E. coli*” gates.

Freshly isolated $\gamma\delta$ T cells were incubated with IgG-opsonised fluorescein-labelled *E. coli* for 45 min at 37°C. A control sample was kept on ice. Because phagocytosis is an active cellular process (228;262), low temperatures should significantly impair phagocytic function. By contrast, bacterial binding to the phagocyte surface should be less affected as it is a passive process. The purity of the $\gamma\delta$ T cell fraction and the phagocytosis results are shown in Figure 4.4B. The purity of the fraction was very high (99.58% $\gamma\delta$ TCR+). However, in accordance with the confocal microscopy experiments, very few $\gamma\delta$ T cells were found to phagocytose. Fewer than 2% of $\gamma\delta$ T cells were found to phagocytose using this test. However, one difficulty with this approach is that it is unable to discriminate

between phagocytic cells with bacteria attached and non-phagocytic cells with bacteria attached, as both would be double positive for blue and green. Therefore, phagocytosis might be underestimated. Also, the assay should be validated using a professional phagocyte positive control. In subsequent assays I have compared phagocytic function in $\gamma\delta$ T cells in parallel with other cell types including professional phagocytes.

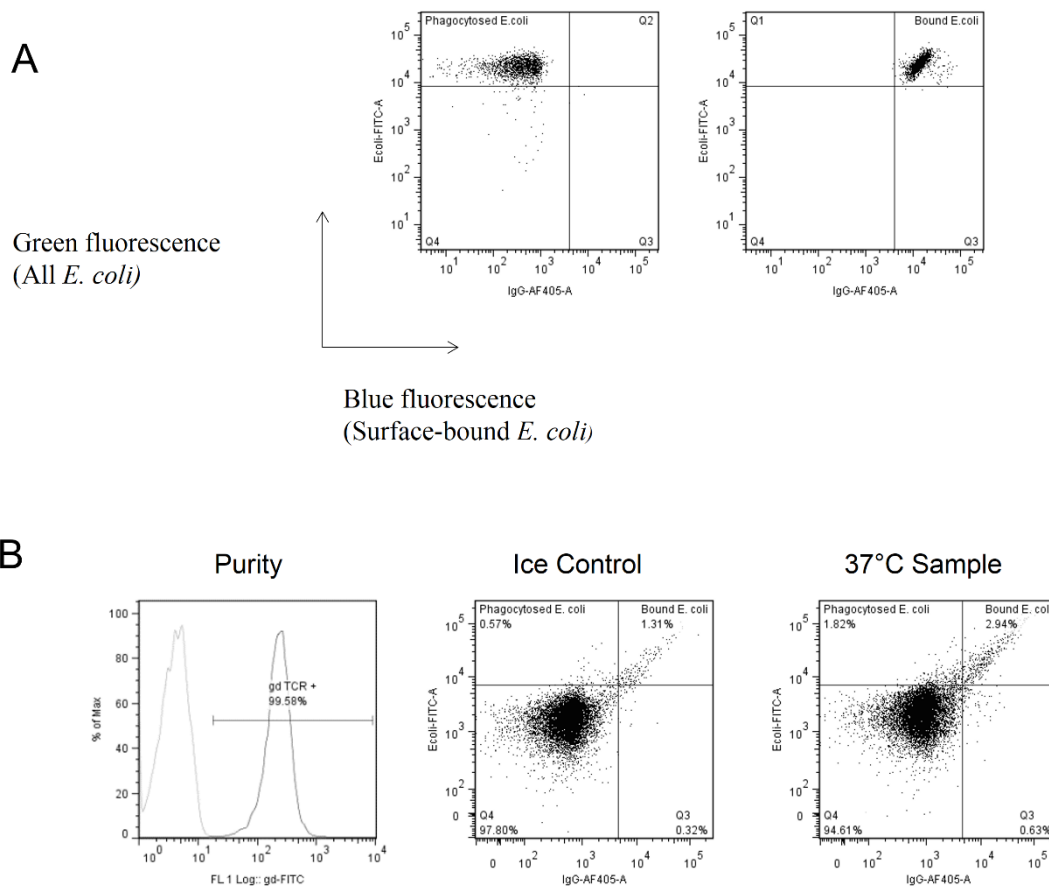


Figure 4.4 – Discrimination between intra and extracellular *E. coli* associated with $\gamma\delta$ T cells using dual fluorescence flow cytometry

To distinguish between phagocytosed bacteria and those bound to the outside of the cell membrane, a dual labelling technique was employed in which fluorescent *E. coli* are counter stained with another fluorochrome after phagocytosis has taken place. (A) Flow cytometry of green fluorescent *E. coli* (left) or of green fluorescent *E. coli* stained with a blue fluorescent antibody (right) in the absence of $\gamma\delta$ T cells. (B) MACS isolated $\gamma\delta$ T cells incubated with opsonised fluorescein-labelled *E. coli* at 37°C. A control sample was kept on ice to prevent phagocytosis. After 45 min co-culture, the non-internalised bacteria were counterstained with a blue fluorescent antibody. The histogram depicts $\gamma\delta$ TCR staining in the MACS sorted fraction with the $\gamma\delta$ T cell fraction in black and unlabelled PBMCs in grey. The dot plots are gated on $\gamma\delta$ T cells and show green and blue fluorescence. $\gamma\delta$ T cells with bacteria attached to the outer cell membrane should fluoresce green and blue (upper right quadrant) whereas $\gamma\delta$ T cells that internalised bacteria but do not have any bacteria bound to their outer membrane should fluoresce only green (upper left quadrant). $\gamma\delta$ T cells with no bacteria should appear in the bottom left quadrant.

4.5 GFP-expressing live *E. coli* can be used to quantify phagocytosis

The commercially available lyophilised and fluorescein-labelled *E. coli* preparation used in the experiments described so far has also been widely used in phagocytosis assays in the literature (267-272). However, a number of drawbacks became evident in the course of my experiments. These green fluorescent *E. coli* bled strongly into the orange-red channels and were so intensely fluorescent that they did not allow for the accurate fluorescence compensation that is needed for multiparameter flow cytometry. In addition, phagocytosis is defined as the receptor-mediated uptake of large particles (228;262), but visualisation of these *E. coli* by confocal microscopy showed that they tend to break down into smaller pieces (Figure 4.1) which is likely to be a consequence of the heat inactivation and lyophilisation processes used during its manufacture. To better evaluate phagocytosis I acquired live *E. coli* expressing *gfpmut3a*, a wavelength-shifted enhanced mutant of wild type green fluorescent protein (GFP) (273;274) which could be grown in the lab before each phagocytosis experiment. I confirmed the morphology and fluorescence of a preparation of opsonised GFP-expressing *E. coli* by confocal microscopy (Figure 4.5A). The bacteria fluoresced green and displayed a rod-like morphology and size typical of intact *E. coli* bacilli.

To ensure standardisation between experiments it is important to add the same ratio of bacteria per mammalian cell each time an experiment is performed, so, it is necessary to have a means of quantifying bacterial cell numbers. The turbidity of bacterial cultures is directly proportional to the bacterial cell concentration during the log phase of expansion. Therefore, I generated a standard curve by measuring the optical density at 600 nm (OD 600) and the number of colony forming units (CFU) from samples taken from a freshly inoculated culture of GFP-expressing *E. coli* every hour for eight hours (Figure 4.5B). Samples were analysed for OD 600 by spectrometry and for colony forming units (CFU) by serial dilution, seeding onto LB agar plates containing ampicillin, and counting colonies the next day. The concentration of the bacterial cultures was calculated from the number of colonies on the plate according to the following equation:

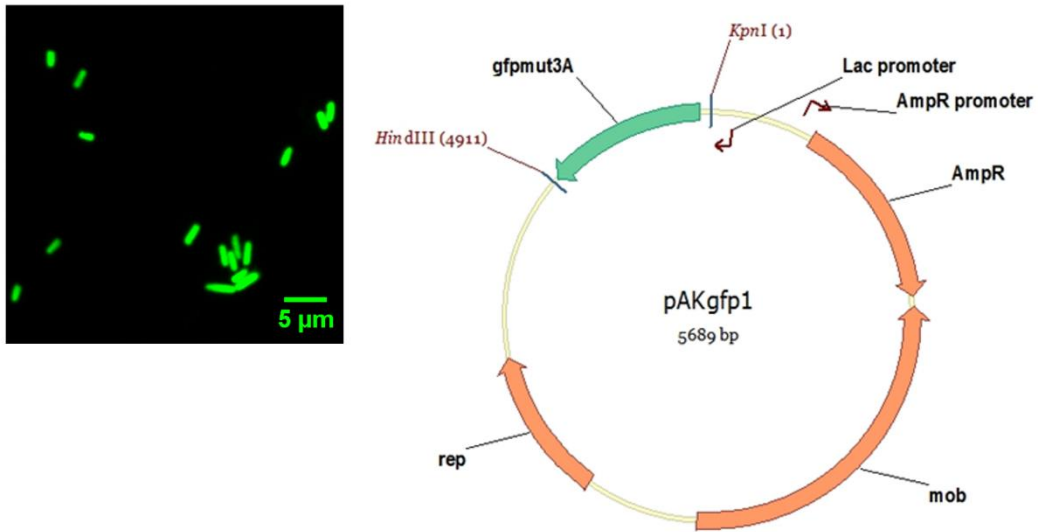
$$\frac{CFU}{ml} = \frac{\text{no. colonies} \times \text{dilution factor}}{\text{volume plated}}$$

By plotting OD 600 vs CFU/ml I generated a standard curve that was used in the following phagocytosis assays to ensure the same number of GFP-expressing *E. coli* was added per sample.

Phagocytosis of lyophilised fluorescein-labelled *E. coli* and GFP-expressing *E. coli* was compared in one donor by a blindly-scored confocal microscopy assay. The two types of *E. coli* were opsonised with IgG and incubated for 45 min with $\gamma\delta$ T cells, $\alpha\beta$ T cells, NK cells and monocytes isolated from PBMC. The slides were then fixed and the cells were stained for F-actin and nuclei, and observed by confocal microscopy. 100 images per cell type were taken. The images were blinded and randomised using the RenameRandom software described in section 4.7 before being scored. The vast majority of monocytes phagocytosed both types of *E. coli*. Although the percentage of phagocytosing monocytes was lower with GFP-expressing *E. coli* than with lyophilised fluorescein-labelled *E. coli* (Figure 4.6A), a larger proportion of monocytes had bacteria bound to the cell surface but not internalised with GFP-expressing *E. coli* (Figure 4.6B). A possible explanation for this observation is that both types of bacteria are subject to phagocytosis but that it takes longer for live GFP-expressing *E. coli* to be engulfed than for the lyophilised fluorescein-labelled *E. coli*. NK cells are known to express high levels of the Fc γ receptor CD16 and were observed to strongly bind both types of IgG coated bacteria suggesting opsonisation with the anti-*E. coli* IgG antibodies was successful. More significantly, the type of *E. coli* used resulted in no observable difference in the number of $\gamma\delta$ T cells undergoing phagocytosis or binding (Figure 4.6).

In conclusion, both types of *E. coli* were strongly phagocytosed by professional phagocytes and equally phagocytosed by $\gamma\delta$ T cells. I decided to replace the commercially available lyophilised fluorescein-labelled *E. coli* used in the previous phagocytosis assays with live GFP-expressing *E. coli* which offer numerous advantages, particularly a more manageable fluorescence intensity that allows for multiparameter flow cytometry and a morphology which better resembles that of the bacteria the immune system is likely to encounter during infection.

A



B

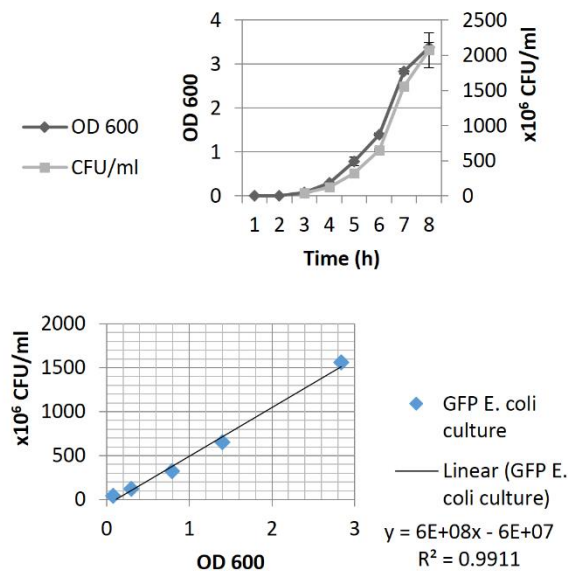


Figure 4.5 – Establishment of live GFP-expressing *E. coli* cultures as an alternative to lyophilised fluorescein-labelled *E. coli* for the study of phagocytosis in $\gamma\delta$ T cells

E. coli containing a plasmid for GFP expression under the control of the LacZ promoter were investigated as an alternative to the lyophilised fluorescein-labelled *E. coli*. (A) *E. coli* cultured overnight in LB broth with IPTG to induce expression of GFP were visualised by confocal microscopy (left). Plasmid map for GFP expression under the control of the LacZ promoter (right). (B) A standard curve was constructed in order to estimate bacterial concentrations from OD 600 readings. Samples were taken from a freshly inoculated culture every hour for eight hours. All samples were tested for OD 600 and then diluted and seeded onto LB agar plates with ampicillin to count colony forming units (CFU). Bacterial growth is shown over time as measured by OD 600 (dark grey line) and CFU/ml (light grey line). Values for OD 600 and CFU/ml were taken from the log phase period and used to build a standard curve. This standard curve was used to calculate the concentration of bacterial cultures in order to standardise phagocytosis assays.

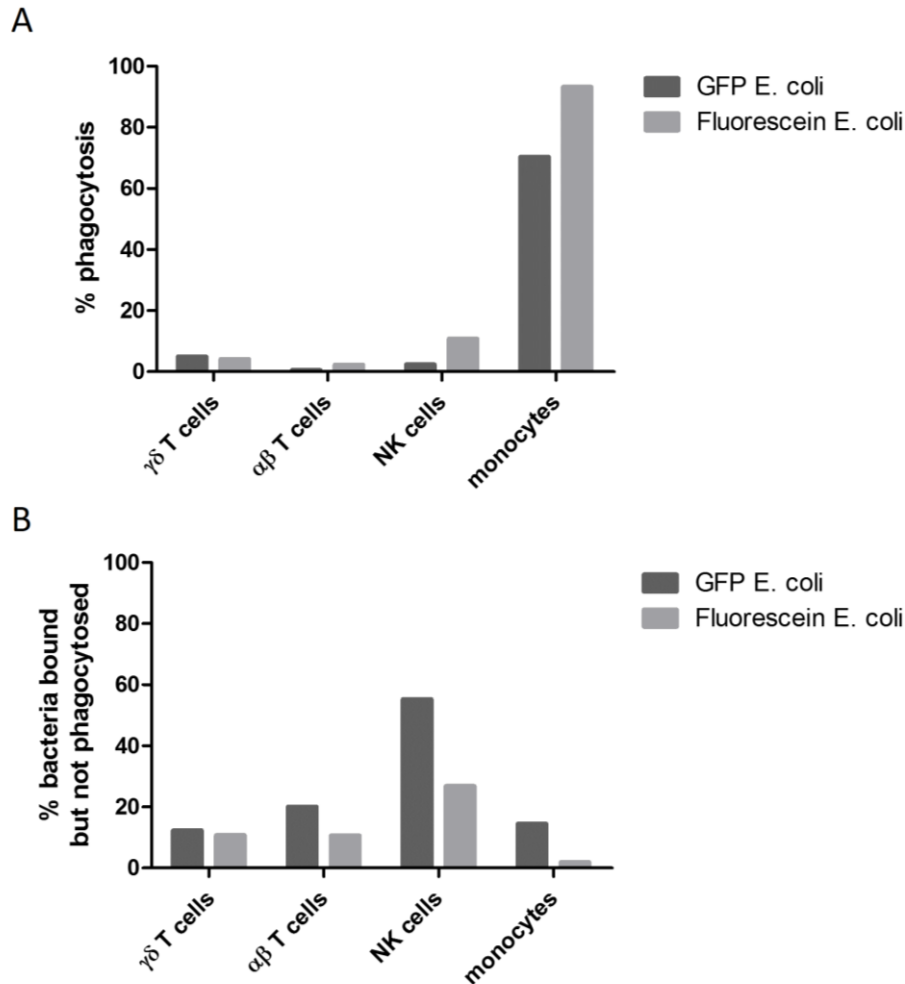


Figure 4.6 – Comparing phagocytosis of lyophilised fluorescein-*E. coli* and live GFP-*E. coli* by confocal microscopy

The phagocytosis assays described in this chapter were performed with either fluorescein-labelled lyophilised *E. coli* (K-12 strain) or live GFP-expressing *E. coli* (DH5 α strain). To test whether the type of *E. coli* used affected the efficiency of phagocytosis both bacteria were tested in parallel in a blindly-scored comparative phagocytosis assay using confocal microscopy. Four cell types were purified from the same donor's PBMCs by MACS. Opsonised *E. coli* were added for 45 min at 37°C. The slides were washed and fixed and stained for F-actin and nuclei. 100 images per slide were taken. The images were blindly-scored using randomising software. Phagocytosed and surface-bound bacteria were counted with the cell counter plugin in the microscopy software Image J. The bar charts show the proportion of cells displaying (A) phagocytosed or (B) surface-bound bacteria.

4.6 Internalisation of opsonised live *E. coli* by $\gamma\delta$ T cells can be detected in a standard gentamicin protection assay

One advantage of using live *E. coli* for phagocytosis experiments is that a wider range of assays can be used. One such is the gentamicin protection assay which is a standard microbiology technique used to measure invasion of mammalian cells by bacteria. This assay takes advantage of the fact that gentamicin efficiently kills Gram-negative bacteria but does not enter most mammalian cells including immune cells. The mechanism by which gentamicin is able to enter some mammalian cells is unclear but appears to be restricted to kidney epithelial cells and inner ear sensory hair cells, leading to kidney failure and hearing loss in some patients on gentamicin (275). In the gentamicin protection assay, internalised bacteria are distinguished from surface-bound bacteria by the addition of gentamicin to the culture media after phagocytosis. The antibiotic kills the bacteria that have not been internalised and hence are not protected from its action.

To confirm bacteria were internalised by $\gamma\delta$ T cells I performed a standard gentamicin protection assay (Figure 4.7). Monocytes were used as a positive control for phagocytosis. Freshly isolated $\gamma\delta$ T cells or monocytes were incubated with opsonised GFP-expressing *E. coli*. Non-phagocytosed bacteria were then killed by adding gentamicin to the culture media. The mammalian cells were pelleted and lysed. The lysed cell pellet was diluted and seeded onto LB agar plates with ampicillin to count bacterial colony forming units (CFU) the next day.

Colonies could be seen both in the $\gamma\delta$ T cell lysates and in the monocyte lysates but not in supernatants containing gentamicin (Figure 4.7A) confirming that non-internalised bacteria were efficiently killed. To understand how the ability of $\gamma\delta$ T cells to phagocytose compares to that of a professional phagocyte I performed experiments varying the ratio of bacteria to phagocyte added. Between 10^4 and 10^7 bacteria were added to 10^5 freshly isolated $\gamma\delta$ T cells or monocytes (a ratio of 0.1-100 bacteria per leukocyte). This experiment was repeated twice with similar results. One such experiment is shown in Figure 4.7B. A dose-dependent response was observed in both monocyte and $\gamma\delta$ T cell wells. The assay could detect phagocytosis with a minimum of 1 *E. coli* per monocyte. However, a ratio of 100 *E. coli* per leukocyte was needed to detect phagocytosis in $\gamma\delta$ T cells. This data can be interpreted in a number of ways. It is possible that $\gamma\delta$ T cells are able to phagocytose but do so with

significantly less proficiency than classical phagocytes. Another possibility is that a small proportion of cells in the $\gamma\delta$ T cell fraction are phagocytic. These phagocytic cells could be contaminating cells that are not $\gamma\delta$ T cells but are present in the highly purified $\gamma\delta$ T cell fraction or alternatively could be a rare and as yet uncharacterised population of phagocytic CD3+ $\gamma\delta$ TCR+ cells. A third possibility is that phagocytic $\gamma\delta$ T cells, like neutrophils, destroy bacteria quickly once internalised and hence would not be detected in the gentamicin protection assay as this only measures viable bacteria.

Three independent experiments using a ratio of 100 bacteria to 1 leukocyte showed phagocytosis in $\gamma\delta$ T cell wells (Figure 4.7C). The first two experiments only show $\gamma\delta$ T cells and monocytes, whereas the third also includes $\alpha\beta$ T cells. Phagocytosis by $\gamma\delta$ T cells was detected in all experiments. On average, lysates from $\gamma\delta$ T cells contained 144 CFU/10⁴ leukocytes whereas monocytes contained 806 CFU/10⁴ leukocytes and $\alpha\beta$ T cells 10 CFU/10⁴ leukocytes. The purity of the fractions as measured by flow cytometry was on average 96.72% \pm 0.65 for $\gamma\delta$ T cells, 96.33% \pm 1.90 for monocytes and 98.74% for $\alpha\beta$ T cells (data not shown). Although the purity of the fractions is high, we cannot rule out the possibility that a phagocytic response could come from the 2.63-3.93 % non-CD3+ $\gamma\delta$ TCR+ flow cytometry events present in the $\gamma\delta$ T cell fraction.

The gentamicin protection assay shows that IgG-opsonised intact bacteria can be internalised by cells in the $\gamma\delta$ T cell fraction as lysates from these cells give rise to bacterial colonies albeit with lower efficiency than monocytes. However, since it is a bulk assay it is not possible to observe whether a small proportion of cells in the $\gamma\delta$ T cell fraction engulfed many bacteria each or whether a larger proportion of cells engulfed a small number of bacteria each. In order to be able to discern this a microscopy or flow cytometry-based method could be used. This assay also confirms that GFP-expressing live *E. coli* can be used reliably to assess phagocytosis in professional phagocytes. Building on these findings, I then developed quantitative microscopy and flow cytometry approaches to quantify the proportion of $\gamma\delta$ T cells that phagocytose.

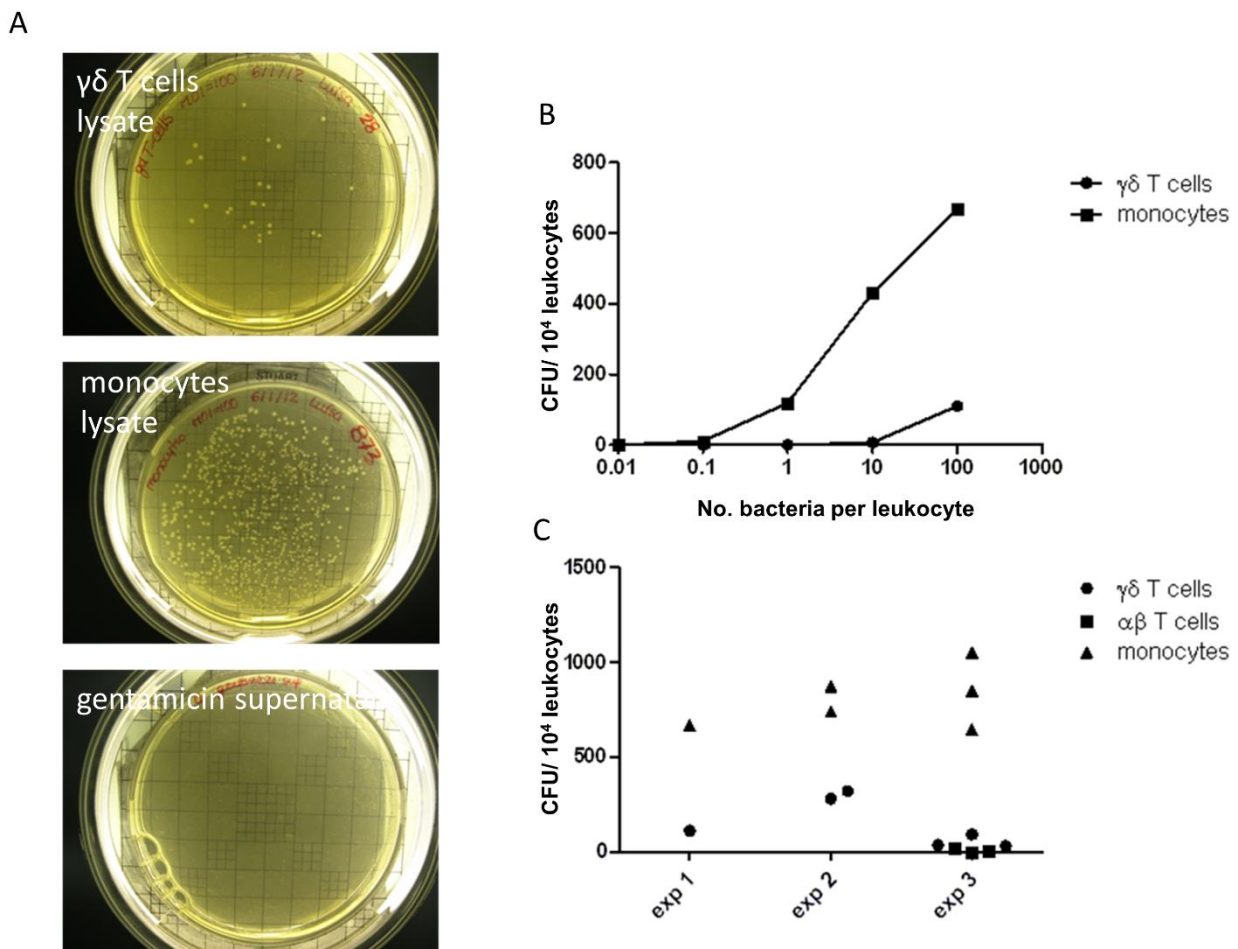


Figure 4.7 – Internalisation of opsonised live *E. coli* by $\gamma\delta$ T cells is detected in a standard gentamicin protection assay

Gentamicin does not penetrate mammalian cells and so can be used to distinguish between non-susceptible bacterial cells inside mammalian cells and susceptible bacterial cells that are attached to the surface. To investigate whether $\gamma\delta$ T cells can internalise live bacteria and to compare their phagocytic ability to that of professional phagocytes, $\gamma\delta$ T cells and monocytes were purified by MACS and assayed in parallel. Leukocytes were incubated with opsonised live bacteria for 45 min, washed and incubated with gentamicin. The leukocytes were washed and lysed and lysates were seeded onto ampicillin LB agar to count bacterial colony forming units (CFU). (A) Example of CFU from a $\gamma\delta$ T cell lysate, a monocyte lysate and the gentamicin-containing supernatant. (B) Varying numbers of bacteria were added to compare the phagocytic ability of $\gamma\delta$ T cells and monocytes and to test for the lower limit of detection of the assay. (C) Three independent assays with the same ratio of 100 bacteria per phagocyte comparing $\gamma\delta$ T cells and monocytes tested in parallel. Experiment 3 also includes $\alpha\beta$ T cells. Each symbol represents CFU from one well.

4.7 Comparative quantification of phagocytosis of highly purified leukocyte fractions using blind scoring of confocal microscopy images

The purity of the cell fraction is a constant concern when assessing phagocytosis in non-classical phagocytes. Direct magnetic isolation through two sequential columns routinely yields very high purities (96-98%) for $\gamma\delta$ T cell preparations but the number of phagocytosing $\gamma\delta$ T cells apparent by confocal microscopy is also very low. Therefore, to assess phagocytosis in a purer preparation of human $\gamma\delta$ T cells, I decided to further purify magnetically isolated cells by FACS sorting before challenging them with bacteria and quantifying phagocytosis by confocal microscopy. Two independent experiments were performed with similar results. Examples from one experiment are shown in Figure 4.8A and 4.8B and the pooled results from the two experiments are shown in Figure 4.8C.

The purity of the cell fractions before FACS sorting was already high: 96.95% for $\gamma\delta$ T cells, 98.26% for $\alpha\beta$ T cells, 88.18% for NK cells and 98.76% for monocytes as measured by flow cytometry (Figure 4.8A). Note FSC x SSC shows absence of monocytes in the $\gamma\delta$ T cell fraction. Unlike the other cell types, NK cells were isolated by negative rather than positive selection hence the comparatively lower purity of the fraction. In order to ensure that adequate numbers of cells were available for the phagocytosis assay I did not measure cell purity after FACS sorting. However, cell purity would be expected to be at least as high after sorting as before.

The cell fractions were incubated with opsonised GFP-expressing *E. coli* at 37°C for 45 min to allow for phagocytosis. Afterwards, the samples were fixed and stained for F-actin (red) and nuclei (blue). Although all lymphocytes were previously stained with antibodies against $\gamma\delta$ TCR, $\alpha\beta$ TCR and CD56 for FACS sorting, the same fluorochrome (PE) was chosen in order to avoid any chance of identifying the cell type during blind scoring of images. Similarly, the Alexa Fluor 555 dye used for F-actin overlaps with PE masking its staining. The dye APC was also chosen for CD3 for FACS sorting as it emits in infrared and therefore can easily be excluded from acquisition on the confocal microscope in this assay.

100 images per cell type were taken in the confocal microscope. The images were anonymised and randomised using the RenameRandom software before being scored.

Each image was scored using the cell counter plugin in the microscopy analysis software Image J (Figure 4.8B shows an example). After scoring, the pictures were cross-referenced back to their original name. This automated blinding was employed in order to prevent observer bias as microscopy techniques are inherently subjective. The software RenameRandom was purpose-built by Flávio J. Saraiva (Department of Informatics Engineering, University of Coimbra, Portugal). During confocal microscopy the user keeps the ZEISS LSM 5 default data file name whilst saving the images, resulting in filenames such as “Image1.lsm”, “Image2.lsm”, and so on. When RenameRandom is run in the directory containing the image files it replaces the numbers in the file names with random numbers and creates a key containing original and randomised file names as a CSV file. The renamed image files are then ordered by name and hence become randomised. The user then manually scores the image files and saves these scores in an Excel spreadsheet. After scoring, the key is pasted into the Excel spreadsheet and the rows are reordered according to the original file names using the “Sort & Filter” command, thereby unblinding the data. This simple bioinformatics tool can be used by individual researchers wishing to score images blindly without the need for two different people to perform data acquisition and scoring.

An average of 923 cells for each cell type was scored (range 722-1292). Average results from two independent experiments are shown in Figure 4.8C. $\gamma\delta$ T cells were not found to phagocytose significantly more frequently than any of the other lymphocytes tested in the same assay. In both donors, a small number of lymphocytes were found to phagocytose (average 2.50% of $\gamma\delta$ T cells, 0.75% of $\alpha\beta$ T cells and 1.70% of NK cells) as well as a large number (average 59.09%) of monocytes. On average, 4143 cells were individually scored per experiment. Of these, an average of 5 $\alpha\beta$ T cells, 16 NK cells, 32 $\gamma\delta$ T cells and 642 monocytes were blindly scored as phagocytic.

Phagocytosis in $\gamma\delta$ T cells may be restricted to a particular subtype of $\gamma\delta$ T cells, for instance, $\gamma\delta$ T cells expressing the CD16 receptor which could mediate binding to IgG opsonised bacteria (223). However, a much greater percentage of $\gamma\delta$ T cells in healthy blood express CD16 than those that were found to phagocytose and NK cells, which stain brightly for CD16 were not phagocytic either.

Another possibility is that mechanical manipulation of the cells by both magnetic isolation and FACS could have negatively impacted the functional activity of the cells. To try to estimate the possible impact of this effect one can look at the literature as monocyte phagocytosis has been extensively characterised. Typically, in tests using opsonised FITC-labelled *E. coli*, researchers have reported between 57.1% and 80% monocyte phagocytosis after only 10 min at 37°C using untouched whole blood samples from healthy adults (276-278). In the assay depicted in Figure 4.8, monocytes phagocytosed between 47.80 and 70.37% after a 45 min incubation and after extensive purification with both MACS and FACS. Therefore, the phagocytosis found for monocytes in this assay is lower than the levels usually reported by other scientists, but not substantially so.

These data suggest that $\gamma\delta$ T cell phagocytosis can be observed but is a rare phenomenon. Because it is so rare it is difficult to confidently ascertain whether this phagocytosis is performed by true $\gamma\delta$ T cells or contaminating cells in the $\gamma\delta$ T cell fraction. However, it should be noted that $\gamma\delta$ TCR staining is visible in the confocal microscopy slides depicting phagocytosis in Figures 4.1-4.3. In order to address the possibility of contaminating cells in the $\gamma\delta$ T cell fraction I decided to test phagocytosis in fresh blood samples without a $\gamma\delta$ T cell isolation step and performed $\gamma\delta$ T cell staining afterwards. This work is described in the following section.

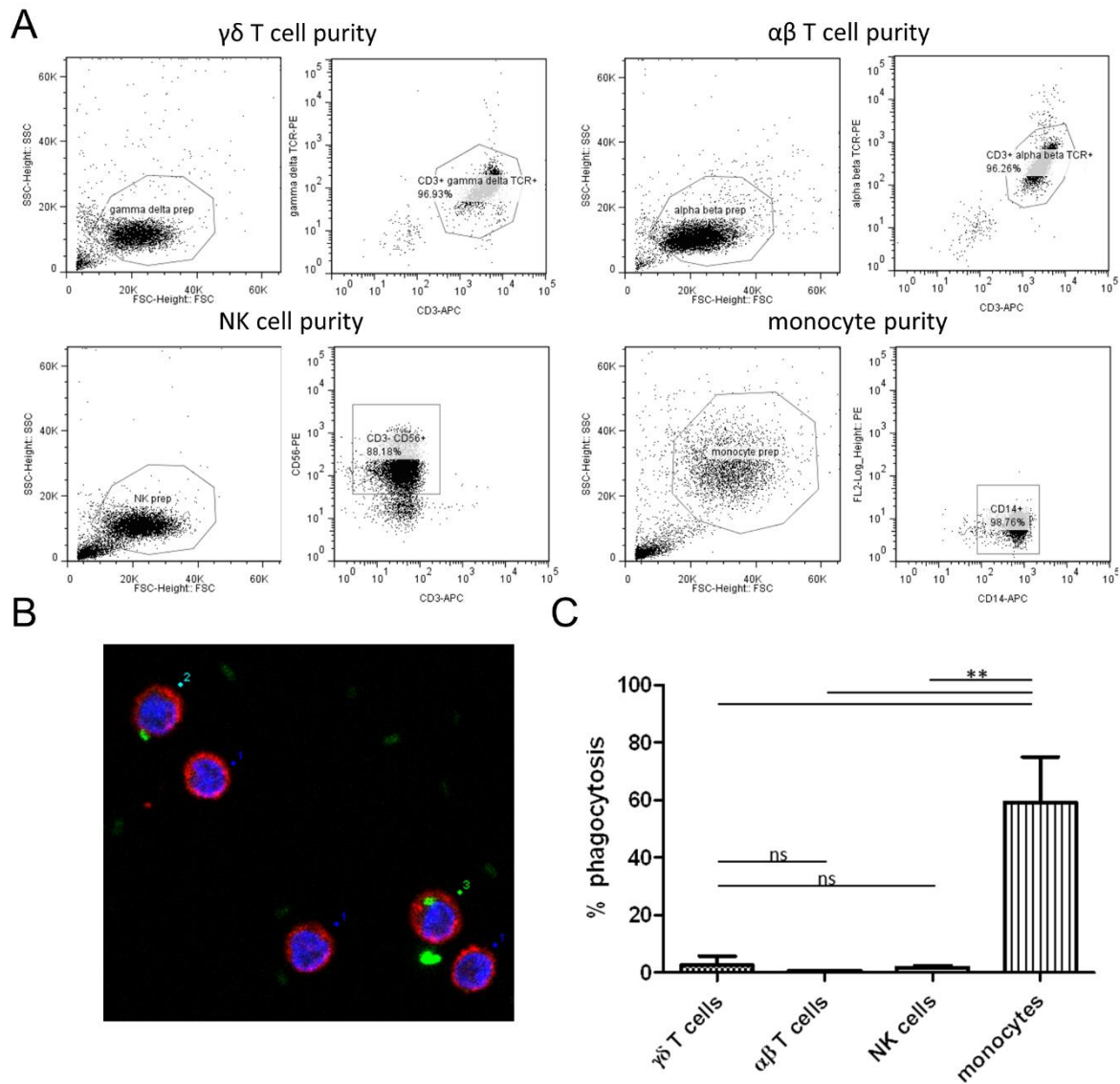


Figure 4.8 – Comparative quantification of phagocytosis of highly purified leukocyte fractions using blind-scored confocal microscopy images

This assay was designed to compare the phagocytic function of $\gamma\delta$ T cells with other lymphocytes and professional phagocytes. $\gamma\delta$ T cells, $\alpha\beta$ T cells, NK cells and monocytes were all isolated by MACS separately from the same donor's PBMCs. (A) Purity of the MACS isolated fractions. The cells were then further purified by FACS. All cell types were co-cultured with opsonised live GFP *E. coli* on slides for 45 min at 37°C. The slides were fixed and stained for F-actin (red) and nuclei (blue). 100 pictures per slide were taken. The pictures were blinded using RenameRandom and scored using the cell counter plugin in Image J. (B) Example of a confocal microscopy image and scoring using the counting plugin. 1 = no phagocytosis, 2 = surface-bound bacteria, 3 = phagocytosis. (C) Phagocytosis by the four different cell types. Average of two independent experiments performed with different donors.

4.8 A population of CD3+ $\gamma\delta$ TCR+ cells in whole blood can phagocytose opsonised GFP-expressing *E. coli*

The results described so far showed that small numbers of $\gamma\delta$ T cells can be found to phagocytose in purified $\gamma\delta$ T cell preparations but that this response is not significantly different from that of other lymphocyte preparations. A possible interpretation of the data is that phagocytosis may be performed by cells in the average 2% contaminating cells present in $\gamma\delta$ T cell preparations that may also presumably be found in $\alpha\beta$ T cell and NK cell preparations. However, the phagocytic $\gamma\delta$ T cells in the images in Figures 4.1-4.3 showed positive $\gamma\delta$ TCR staining.

In order to avoid the problem of contaminating cells in $\gamma\delta$ T cell preparations, a novel assay was developed that tests the phagocytic potential of $\gamma\delta$ T cells in unprocessed blood samples. Since $\gamma\delta$ T cells are only a minor fraction of blood leukocytes (1-5% of PBMC, PBMC are approximately 30% of leukocytes), screening a statistically significant number of $\gamma\delta$ T cells by confocal microscopy would be prohibitively labour-intensive and the samples are analysed instead by flow cytometry. This assay uses whole blood samples that are challenged with bacteria within 30 min of blood collection. 5 ml of blood were drawn from healthy volunteers and separated into five tubes. Opsonised GFP-expressing live *E. coli* and blood were cooled on ice separately for 10 min. Bacteria were then added to all tubes at a ratio of 100 bacteria per leukocyte and four tubes were moved to a 37°C waterbath while the fifth tube was kept on ice. After 30 min incubation at 37°C, all tubes were placed on ice where they were stained with antibodies against the $\gamma\delta$ TCR, $\alpha\beta$ TCR, CD3, CD14 and CD56. All antibodies were directly conjugated to fluorochromes with no spectral overlap to GFP (eFluor450 and APC) in order to prevent false positive results. The samples were fixed and red blood cells were lysed with a one-step RBC lysis reagent from the PHAGOTEST kit (Orpengen, Germany). The samples were run in an LSRII flow cytometer within an hour. The same experiment was repeated a total of five times, each time with a different healthy donor. One representative experiment is shown in Figure 4.9A and the results from all the experiments are pooled in Figure 4.9B.

Figure 4.9A shows a representative experiment. The top plots are from the ice control. On the left is the ice control scatter plot with evidence of 3 populations typically recognisable by light scatter: lymphocytes with smaller FSC and SSC, monocytes with increased FSC

and SSC and granulocytes with the highest SSC. Light scatter in flow cytometry is proportional to the size and granularity of the cell type, with larger cell types having larger FSC and more granular cell types having higher SSC. The histogram next to the ice control scatter plot shows fluorescence in the GFP gate by ungated cells in the ice control and was used to draw a “GFP-*E. coli*+” gate.

The gating strategies and GFP fluorescence of all four cell types assayed are displayed in Figure 4.9A. Gating of $\gamma\delta$ T cells based on CD3+ $\gamma\delta$ TCR+ showed the typical two populations of $\gamma\delta$ T cells in the blood, expressing different levels of TCR (see Figure 5.1 for other examples). A proportion of $\gamma\delta$ T cells (average 12.21%, range 5.00% to 21.32%) appears to have phagocytosed opsonised GFP-expressing *E. coli*. $\alpha\beta$ T cells were gated based on CD3+ $\alpha\beta$ TCR+ and NK cells were gated based on CD3- CD56+. Phagocytosis by $\alpha\beta$ T cells and NK cells was not detected in this assay. Although this assay does not specifically distinguish between bound and internalised bacteria, IgG opsonised *E. coli* only associated weakly with NK cells (average 1.35%, range 0.20% to 2.61%). This suggests that the apparent phagocytosis seen in the $\gamma\delta$ T cell gate should not be a consequence of bacteria bound to the outside of $\gamma\delta$ T cells via CD16 receptors, as otherwise it would be apparent in the NK cell gate as well. Monocytes were gated based on CD14+. Monocytes took up bacteria significantly more frequently than any other cell type (average 74.59%, range 67.20% to 83.05%). Among all lymphocyte populations tested, CD3+ $\gamma\delta$ TCR+ cells in whole blood phagocytosed bacteria significantly more frequently. Interestingly, the MFI of phagocytosing CD3+ $\gamma\delta$ TCR+ cells resembled that of phagocytosing monocytes, suggesting that the number of bacteria taken up per cell was similar. It should be noted that all tests were performed on whole blood, therefore any phagocytosis observed happened in competition with professional phagocytes present in the blood. Therefore, phagocytosis by $\gamma\delta$ TCR+ cells is not only observed when these cells are purified from blood samples and tested in isolation. This whole blood phagocytosis assay has many strengths. Because the cell processing steps have been removed, the cells are assayed very quickly after blood collection which gives us greater confidence that they retain their physiological characteristics. In addition, although the assay does not distinguish between internalised and attached bacteria, it does include an ice control and all the different cell types are tested in parallel. It should also be noted that this assay was adapted from a

clinically-relevant test (PHAGOTEST, Orpengen), which is used at Great Ormond Street Hospital to help diagnose neutrophil disorders in paediatric patients (21;279).

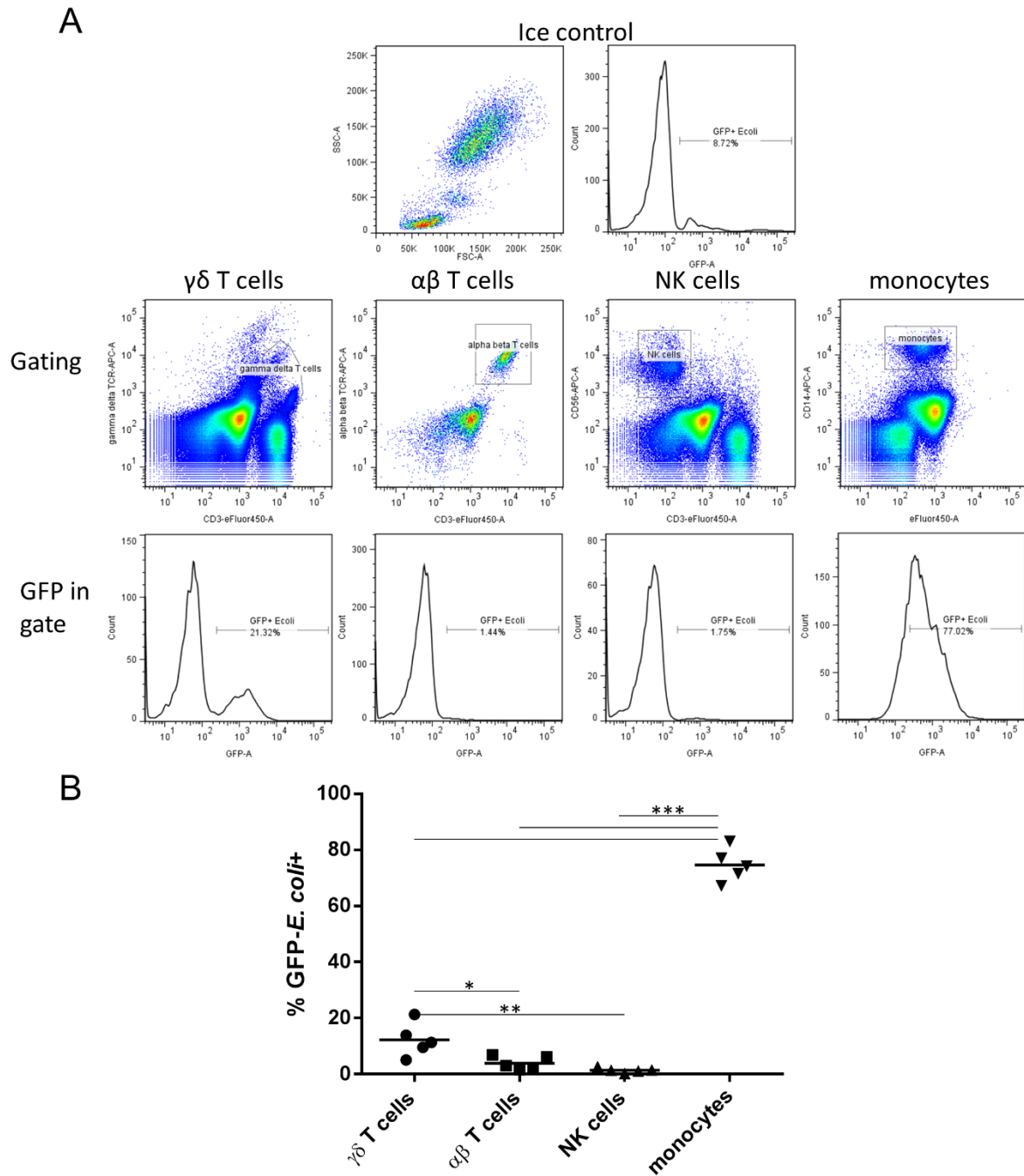


Figure 4.9 – A population of CD3+ $\gamma\delta$ TCR+ cells in whole blood can phagocytose opsonised GFP-expressing *E. coli*

Testing for $\gamma\delta$ T cell phagocytosis under conditions of minimal experimental manipulation of cells. Freshly drawn heparinised blood was separated into 5 FACS tubes to which opsonised GFP-expressing *E. coli* were added. 4 tubes were transferred to a 37°C waterbath. After 30 min, the tubes were placed on ice and stained. Each tube was stained for different markers to identify either $\gamma\delta$ T cells (CD3 and $\gamma\delta$ TCR), $\alpha\beta$ T cells (CD3 and $\alpha\beta$ TCR), NK cells (CD3 and CD56) or monocytes (CD14), except the ice control which was left unstained. Samples were RBC lysed and fixed and analysed by flow cytometry. (A) Example of data analysis from one experiment. Top plots: ice control GFP fluorescence is used to draw the phagocytosis gate. Middle plots: gating strategies for the four cell type. Bottom plots: GFP fluorescence gated on each cell types. (B) Pooled results from five independent experiments with separate donors.

In the flow cytometry experiments depicted in Figure 4.9 a population of CD3⁺ $\gamma\delta$ TCR⁺ cells present in the blood phagocytosed opsonised GFP-expressing *E. coli*. I gated on phagocytic and non-phagocytic CD3⁺ $\gamma\delta$ TCR⁺ cells to see if any differences could be seen between the two in terms of surface staining and light scatter profile (Figure 4.10). CD3⁺ $\gamma\delta$ TCR⁺ cells were gated as shown in Figure 4.9 and divided into non-phagocytic and phagocytic populations based on GFP fluorescence (GFP histogram, Figure 4.10A). Phagocytic and non-phagocytic cells were present in both the CD3⁺ $\gamma\delta$ TCR^{high} and the CD3^{high} $\gamma\delta$ TCR^{low} usual sub-populations of $\gamma\delta$ T cells (CD3 and $\gamma\delta$ TCR histograms, Figure 4.10A; see Figure 6.1 for other examples of $\gamma\delta$ T cell sub-populations). These observations argue against the possibility of the apparent $\gamma\delta$ T cell phagocytosis being a consequence of unspecific granulocyte fluorescent background because the phagocytic $\gamma\delta$ T cells segregated clearly into two populations. In addition, they show that there is no detectable relationship between TCR expression level and the frequency of phagocytosis.

Interestingly, CD3⁺ $\gamma\delta$ TCR⁺ cells in whole blood segregated into two clearly distinct populations by light scatter. The top left dot plot in Figure 4.9A shows the light scatter of an ungated whole blood sample. Typical lymphocyte, monocyte and granulocyte populations are visible with increasingly higher forward scatter (FSC) and side scatter (SSC). This is because FSC is proportional to cell-surface area and SSC is proportional to granularity (280). Therefore, lymphocytes generally appear as small smooth cells, monocytes are larger and granulocytes have abundant intracellular granules that strongly refract light. Figure 4.10 shows all gated CD3⁺ $\gamma\delta$ TCR⁺ cells in a light scatter dot plot. A majority of the cells display the typical light scatter profile of a lymphocyte. However, a significant proportion of CD3⁺ $\gamma\delta$ TCR⁺ cells in whole blood have the same light scattering properties as granulocytes. Gating on “granular CD3⁺ $\gamma\delta$ TCR⁺ cells” and “normal CD3⁺ $\gamma\delta$ TCR⁺ cells” revealed the former were virtually all phagocytic whereas the latter were entirely non-phagocytic (Figure 4.10B).

These results can be interpreted in two ways. Firstly, the cells may appear granular because they have engulfed bacteria. However, phagocytic monocytes did not show a similar increase in SSC (data not shown). Secondly, the cells may indeed be a distinct granular CD3⁺ $\gamma\delta$ TCR⁺ population. The fact that previous experiments in this chapter did not find a significant difference in phagocytosis between different lymphocytes would be in

agreement with granulocyte phagocytic CD3+ $\gamma\delta$ TCR+ cells since these would be excluded from PBMCs, which were used as a source of cells for $\gamma\delta$ TCR+ MACS selection in these previous experiments. Although granulocytes are known to layer with PBMCs in certain situations such as particular disease states (281;282), older blood samples or cryopreserved blood samples (283;284), in general they are excluded from PBMC fractions during density gradient separation.

This assay cannot distinguish between these two possibilities because flow cytometry takes place after phagocytosis. Therefore, it does not inform us as to whether phagocytic CD3+ $\gamma\delta$ TCR+ cells in whole blood are granular cells or appear granular because they have engulfed bacteria. The following experiments attempt to further characterise this phagocytic CD3+ $\gamma\delta$ TCR+ population present in the blood of all donors tested.

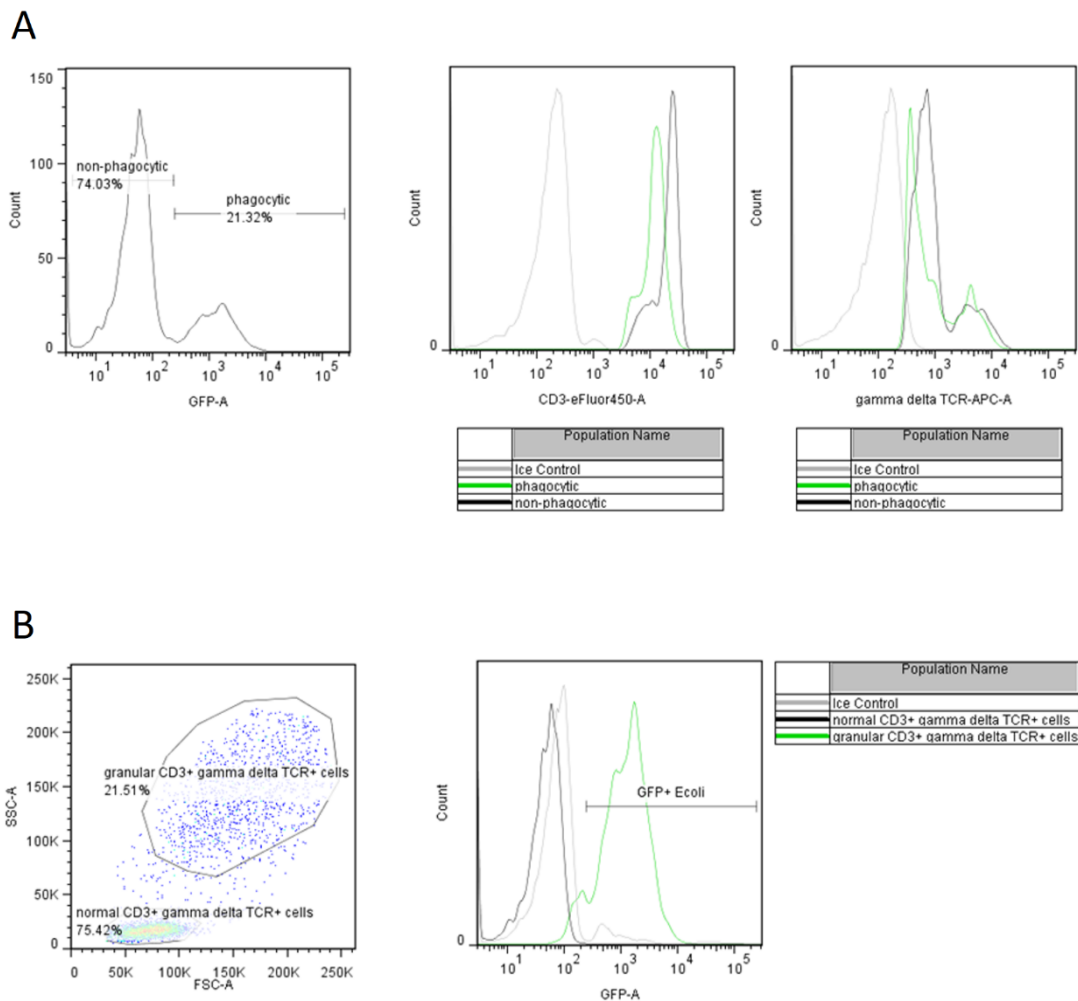


Figure 4.10 – Characteristics of phagocytosing and non-phagocytosing CD3+ $\gamma\delta$ TCR+ cells in the whole blood phagocytosis assay

Further analysis of the flow cytometry data in the $\gamma\delta$ T cell gate in the phagocytosis whole blood assay described in Fig. 4.9. (A) The histogram on the left is gated on $\gamma\delta$ T cells as shown in Fig. 4.9A and shows a negative and a positive population for GFP-*E. coli*, labelled non-phagocytic and phagocytic, respectively. The histograms on the right depict CD3 and $\gamma\delta$ TCR fluorescence. The phagocytic fraction is shown in green and the non-phagocytic fraction in black. (B) The dot plot on the left is gated on $\gamma\delta$ T cells as shown in Fig. 4.9A and shows FSC x SSC. Two populations can be distinguished based on light scatter properties, one labelled “normal CD3+ gamma delta TCR+ cells” in a typical lymphocyte gate and one labelled “granular CD3+ gamma delta TCR+ cells” in a typical granulocyte gate. The histogram on the right depicts GFP-*E. coli* fluorescence in the “normal CD3+ gamma delta TCR+ cells” gate in black and in the “granular CD3+ gamma delta TCR+ cells” in green.

4.9 Phagocytosing CD3+ $\gamma\delta$ TCR+ cells in whole blood produce reactive oxygen species

Professional phagocytes such as macrophages and neutrophils produce reactive oxygen species (ROS) to destroy ingested microbes (285). ROS production is essential for antimicrobial defence. Neutrophils from patients with chronic granulomatous disease (CGD) are deficient in the NADPH oxidase system that generates superoxide and are unable to kill many strains of bacteria, yeast, and fungi. These same patients suffer severe infections (286). CGD is diagnosed by the demonstration of deficient respiratory burst activity in phagocytic cells. The oldest and most widely used assay is the nitroblue tetrazolium (NBT) test (287). The NBT test assays the ability of activated neutrophils to produce superoxide, which reduces the yellow water soluble NBT dye to insoluble blue formazan. Therefore, a functional respiratory burst is demonstrated by the presence of a dark blue precipitate within the cell evident under light microscopy.

To investigate whether phagocytic CD3+ $\gamma\delta$ TCR+ cells were capable of a functional respiratory burst, phagocytic and non-phagocytic CD3+ $\gamma\delta$ TCR+ cells and neutrophils were FACS sorted from the same blood sample and assayed in a functional NBT test. Whole blood was incubated with opsonised GFP-*E. coli* for 30 min at 37°C and then stained on ice for CD3 and $\gamma\delta$ TCR. RBC were lysed with fixative-free ammonium chloride buffer. The cells were directly FACS sorted onto flat 96-well plates containing complete culture media. After FACS sorting, NBT dye was added to the wells and the cells were incubated at 37°C for 30 min. EDTA was added to quench the reaction and pictures were taken by light microscopy (Figure 4.11).

Blue formazan precipitates were clearly visible in phagocytic CD3+ $\gamma\delta$ TCR+ fractions but absent from the non-phagocytic CD3+ $\gamma\delta$ TCR+ fractions. Reactive oxygen species production by phagocytic $\gamma\delta$ T cells was approximately one-third that of neutrophils in the two donors were tested. Overall, these results suggest that the CD3+ $\gamma\delta$ TCR+ population in the blood that is phagocytic towards opsonised *E. coli* is capable of a functional respiratory burst, as would be expected for a professional phagocyte.

NBT positive	Neutrophils	Phagocytic CD3+ $\gamma\delta$ TCR+ cells	Non-Phagocytic CD3+ $\gamma\delta$ TCR+ cells
Donor 1	19.25%	11.92%	0.41%
Donor 2	40.00%	8.20%	0.00%

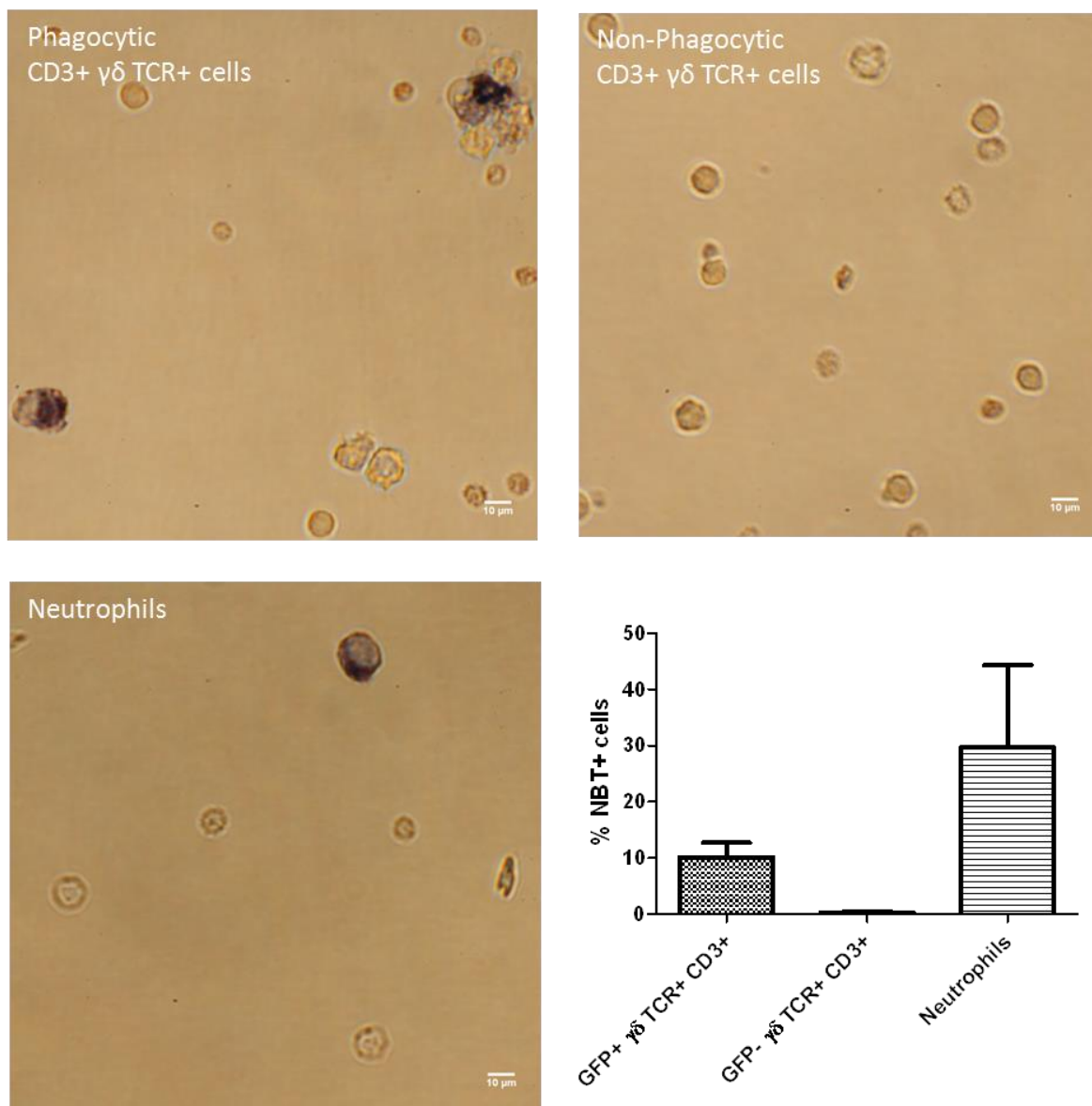


Figure 4.11 – Phagocytosing CD3+ $\gamma\delta$ TCR+ cells in whole blood produce reactive oxygen species

NBT assay to investigate whether phagocytic $\gamma\delta$ T cells have an oxidative burst. Neutrophils, phagocytic and non-phagocytic CD3+ $\gamma\delta$ TCR+ cells were isolated by FACS sorting from whole blood incubated with opsonised GFP-expressing *E. coli*. FACS sorted cells were seeded into flat-bottom 96-well plates with complete media and incubated with NBT dye for 30 min at 37°C. The yellow NBT dye is ingested by the cells and, in the presence of reactive oxygen species, converted to the purple-blue formazan compound. Pictures were taken by light microscopy. The quantification of NBT+ cells is shown. Average of 2 independent donors.

4.10 Phagocytosing CD3+ $\gamma\delta$ TCR+ cells in whole blood have unusual morphology

Histological staining is a simple procedure that enables visual discrimination of cell contents on the basis of different propensities to take up a given stain. The stains typically allow discrimination between the nucleus and the cytoplasm and can also provide information about the content of intracellular granules. Therefore, cell samples can be easily described in terms of nuclear morphology, the size of the cytoplasm, or the presence of specific granules.

In their resting state, human blood $\gamma\delta$ T cells appear smooth and round, are approximately 7-12 μm in diameter, and possess a central circular nucleus surrounded by a small volume of cytoplasm. When activated they appear, as do activated $\alpha\beta$ T cells, much larger with more irregular and granular shapes (288). CD16+ $\alpha\beta$ T cells in the blood of healthy donors have been described as having the appearance of activated lymphocytes with a large granular lymphocyte morphology (289). Skin-resident $\gamma\delta$ T cells also appear larger and show a dendritic-like morphology (290). Rare dendritic-like $\gamma\delta$ T cells have also been described in human blood from healthy donors (223). An example of this was shown earlier in this chapter and is highlighted in Figure 4.12. Dendritic-like extensions are evident by F-actin staining (red) and $\gamma\delta$ TCR staining is also present (magenta).

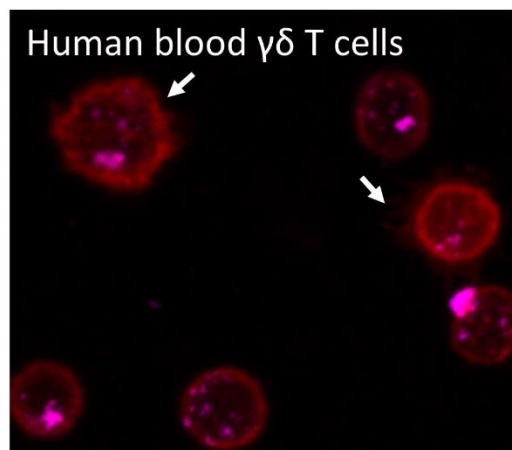


Figure 4.12 - Human blood $\gamma\delta$ T cells include cells with unusual dendritic-like extensions

$\gamma\delta$ T cells freshly isolated from healthy donor PBMCs by MACS. F-actin (red) and $\gamma\delta$ TCR (magenta) staining. White arrows indicate dendritic-like extensions.

To investigate the morphology of phagocytosing and non-phagocytosing CD3⁺ $\gamma\delta$ TCR⁺ cells, whole blood was incubated with opsonised *E. coli*, stained with anti-CD3 and anti- $\gamma\delta$ TCR antibodies and the two populations were FACS sorted. The sorted cells were cytospun onto slides and stained with Diff-Quick. They were then scored as small lymphocytes, large lymphocytes, monocytes or polymorphonucleated cells according to their morphology, specifically nuclear morphology (circular, kidney-shaped or polymorphonuclear) and cytoplasm to nucleus ratio (small or large cells). The images in Figure 4.13 show representative examples. Small lymphocytes include Figure 4.13A and J. Large lymphocytes include Figure 4.13B, F and H. Polymorphonucleated cells are shown in Figure 4.13C, D, E and G, and a monocyte is shown in I. The plots in Figure 4.13K and L show the pooled results of three independent experiments, each with a different healthy donor.

The results from each of the three experiments were strikingly similar. Virtually all non-phagocytic CD3⁺ $\gamma\delta$ TCR⁺ cells had the unequivocal morphology of a lymphocyte, with a round shape containing a nucleus surrounded by a small volume of cytoplasm. However, phagocytic CD3⁺ $\gamma\delta$ TCR⁺ cells were a heterogeneous population. The largest group was composed of polymorphonucleated cells, with either a bi-lobed, tri-lobed or multilobed nucleus. The only cells described in the blood with this nuclear morphology are eosinophils (bi-lobed), basophils (bi-lobed or tri-lobed) and neutrophils (multilobed).

Intriguingly, the presence of a CD3/ $\gamma\delta$ TCR has been described in polymorphonucleated cells before. Puellmann et al showed the presence of various components of the TCR complex including each of the TCR α , β , γ and δ constant regions by RT-PCR and Western blot in human granulocyte preparations containing 97% neutrophils (291). Other granulocytes like eosinophils are also present in granulocyte fractions isolated with the same method (Figure 4.17). Indeed, a subsequent paper by a different group found no CD3/ $\gamma\delta$ TCR on neutrophils purified from granulocyte preparations but did find a functional CD3/ $\gamma\delta$ TCR complex in eosinophils from the same donors (292). Puellmann recently reported again the expression of a CD3/ $\gamma\delta$ TCR receptor in human monocytes and macrophages (293).

Only 1% of the phagocytic CD3+ $\gamma\delta$ TCR+ cells showed monocyte morphology, as shown in Figure 4.13I, with a kidney shaped nucleus. The largest group (41.67%) of phagocytic CD3+ $\gamma\delta$ TCR+ cells were polymorphonucleated cells. Additionally, 20.33% of the phagocytic cells observed had a round nucleus and a large cytoplasmic body, similar to activated T cells. It should be noted that the phagocytosis experiment takes place less than 30 min after the blood was drawn and the FACS sorting takes place around 2h30 after the start of the experiment, so these cells have been cultured *ex vivo* for a minimal amount of time and should have phenotypes similar to those of cells circulating in healthy blood. Finally, 24.87% of the phagocytic cells resembled normal T cells, with a round nucleus and a small cytoplasmic volume, but with bacteria evident in the cytoplasm. These may correspond to the rare phagocytic $\gamma\delta$ T cells present in PBMCs that have been observed to phagocytose previously (223) and in experiments described in this chapter (Figures 4.1-4.2, 4.6) but that do not do so significantly more than other lymphocytes (Figure 4.8).

In conclusion, in all donors tested CD3+ $\gamma\delta$ TCR+ cells with the normal morphology of a T cell could be found with phagocytosed bacteria clearly evident inside the cytoplasm. However, a majority of the phagocytic CD3+ $\gamma\delta$ TCR+ cells did not have lymphocyte morphology. These results can be interpreted in two ways. They either suggest the purity of the sort was very low, with over 40% contaminating granulocytes, or, alternatively, that a CD3/ $\gamma\delta$ TCR complex is indeed expressed in a fraction of polymorphonucleated cells. Both possibilities were addressed and are shown in detail in the following sections.

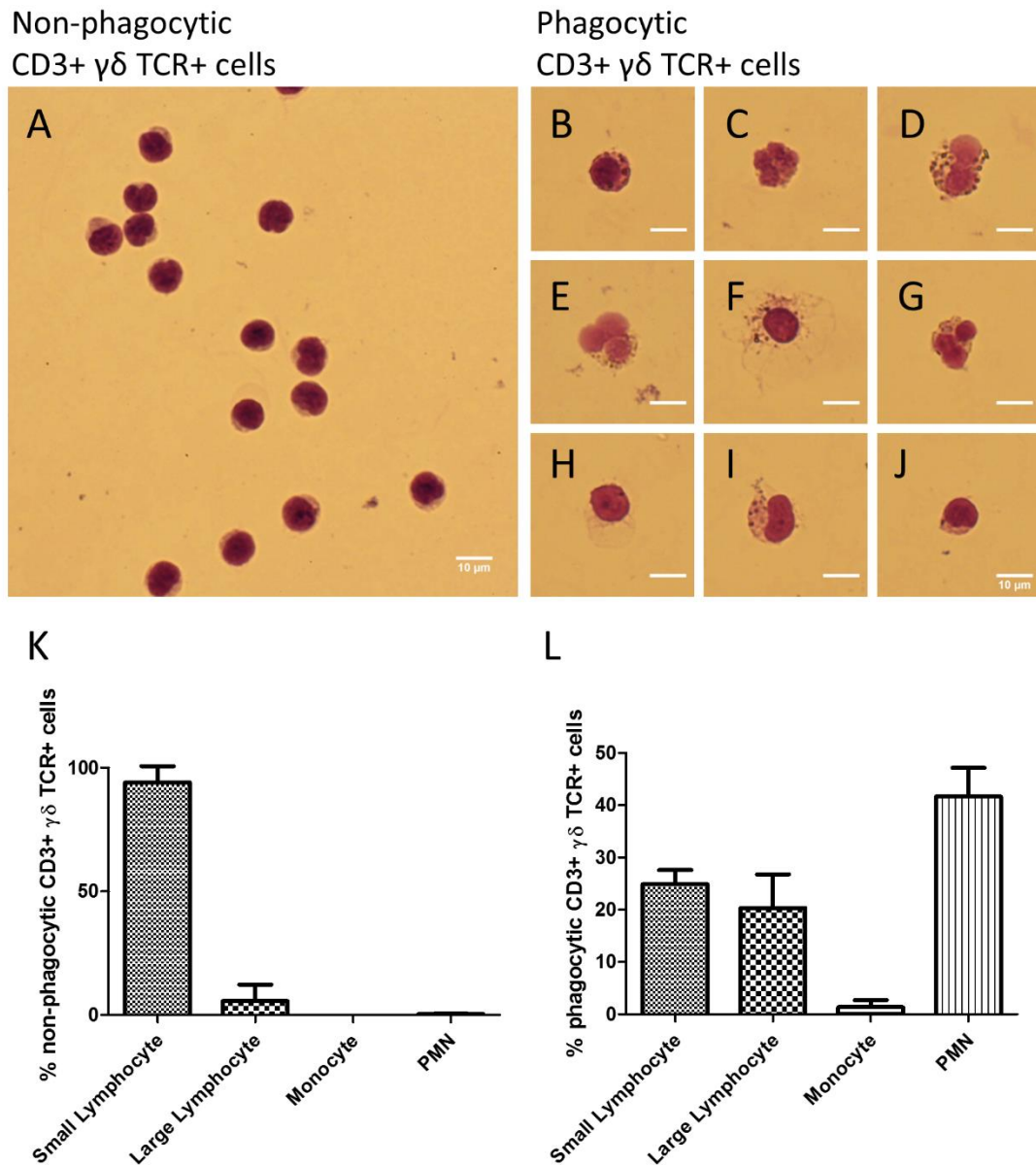


Figure 4.13 – Phagocytosing CD3+ $\gamma\delta$ TCR+ cells in whole blood have unusual morphology

Comparison between the morphology of phagocytic and non-phagocytic CD3+ $\gamma\delta$ TCR+ cells isolated by FACS sorting from whole blood incubated with opsonised GFP-expressing *E. coli*. FACS sorted fractions were cytopun onto slides and stained with Diff-Quick. The nucleus stains darker than the cytoplasm highlighting nuclear morphology. Bacteria are apparent as dark dots in the cytoplasm. (A) Cells from the non-phagocytic fraction. (B) to (J) Cell from the phagocytic fraction. All cells were scored according to size and nuclear morphology. Plots show average of 3 independent donors. PMN= polymorphonucleated cell. (K) Non-phagocytic fraction. (L) Phagocytic fraction.

4.11 Purity assessment of FACS sorted fractions of CD3+ $\gamma\delta$ TCR+ cells

In order to characterise phagocytic CD3+ $\gamma\delta$ TCR+ cells present in whole blood, the assay described in section 4.8 was performed followed by FACS sorting of the GFP+ CD3+ $\gamma\delta$ TCR+ and GFP- CD3+ $\gamma\delta$ TCR+ fractions. The FACS sorted fractions were then tested for ROS production (Figure 4.11) or inspected using histological stains (Figure 4.13). The purity of the sort was assessed by running a small sample of unsorted and FACS sorted cells through a flow cytometer immediately after the sort.

The normal range of $\gamma\delta$ T cells in healthy adults is 55 000 – 120 000 $\gamma\delta$ T cells per ml of blood. This range is taken from T cell phenotyping studies in a large cohort of 352 peripheral blood samples (294). Assuming an average frequency of phagocytosis of approximately 10% of $\gamma\delta$ T cells (Figure 4.9), I would expect to recover around 5 000 to 10 000 phagocytic $\gamma\delta$ T cells per 1 ml blood sample tested. However, FACS sorting is less efficient at isolating very rare subsets of cells (295) and the number of cells actually recovered was somewhat smaller averaging around 10 000 non-phagocytic CD3+ $\gamma\delta$ TCR+ cells and 300-500 phagocytic CD3+ $\gamma\delta$ TCR+ cells per 1 ml blood sample tested. In order to ensure that sufficient cells of the phagocytic fraction would be available for the experiments for which they were being FACS sorted (the NBT test or the histological staining), the purity of the sort was always assessed using a sample from the non-phagocytic fraction, as both samples were FACS sorted simultaneously from the same sample.

In addition, it should be noted that in the earlier quantification experiments, PE was deliberately avoided because of the known spectral overlap with GFP fluorescence. However, the FACS sorting machine available has a smaller range of lasers than the LSRII flow cytometer used for sample analysis and because of this the fluorochromes eFluor450 and APC used in the initial quantification experiments were replaced with PE and APC for the characterisation experiments that followed. Therefore, before FACS sorting, compensation was set using a GFP single stained control.

Figure 4.14 shows an example of the proportion of CD3+ $\gamma\delta$ TCR+ cells before and after FACS sorting. The unsorted cells were used to draw a generic cell gate by FSC x SSC and then a second CD3+ $\gamma\delta$ TCR+ region gated on the cell gate. The graph underneath shows the purities of the individual experiments depicted in Figures 4.11 and 4.13. The purity as

measured by the proportion of CD3+ $\gamma\delta$ TCR+ cells in the collected non-phagocytic fraction was very high with an average of 97.30% CD3+ $\gamma\delta$ TCR+ cells.

In one donor a sample containing 192 phagocytic CD3+ $\gamma\delta$ TCR+ cells was also tested for purity in parallel with the non-phagocytic fraction. The results are shown in Figure 4.15. The purity of the two fractions was very different, even though they were isolated from exactly the same sample simultaneously. The sorted non-phagocytic CD3+ $\gamma\delta$ TCR+ fraction showed a high purity of 98.83% CD3+ $\gamma\delta$ TCR+ cells (Figure 4.15B) and these cells were completely negative for GFP (Figure 4.15C). Surprisingly only 6.25% of cells in the sorted phagocytic CD3+ $\gamma\delta$ TCR+ fraction were CD3+ $\gamma\delta$ TCR+ cells, as assessed by flow cytometry immediately after the sort (Figure 4.15D). The majority of the contaminating cells (54.69%) were CD3- cells with high fluorescence in the PE channel.

Compensation was set before the sort with a GFP single stained control. Therefore, high fluorescence in the PE channel should not be a result of “fluorescent spillover” of the GFP fluorescent cells into the PE channel. However, high autofluorescence is a characteristic of granulocytes, particularly eosinophils (296), and hence these cells may appear PE+. In fact, autofluorescence alone has been used by some researchers as a tool to FACS sort unstained eosinophils (297). The remaining contaminants in the phagocytic CD3+ $\gamma\delta$ TCR+ fraction appeared to be $\alpha\beta$ T cells (CD3+ $\gamma\delta$ TCR-) that were surprisingly present in greater numbers (39.06%) than CD3+ $\gamma\delta$ TCR+ cells (6.25%). Therefore, the phagocytic FACS sorted fraction was composed of CD3+ $\gamma\delta$ TCR+ cells, CD3+ $\gamma\delta$ TCR- cells and CD3- $\gamma\delta$ TCR- cells (Figure 4.15D).

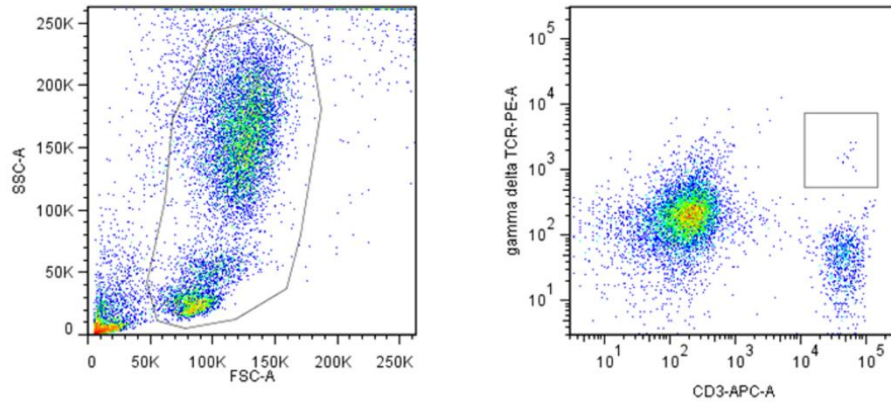
Further analysis of the phagocytic FACS sorted fraction (Figure 4.15E) revealed that it contained both GFP+ and GFP- cells. Plotting each of the populations apparent in the CD3 x $\gamma\delta$ TCR dot plot (Figure 4.15D) on a GFP histogram revealed that CD3+ $\gamma\delta$ TCR+ cells displayed a small GFP-*E. coli*+ peak, CD3+ $\gamma\delta$ TCR- cells were negative for GFP and CD3- $\gamma\delta$ TCR- cells were almost all positive for GFP (Figure 4.15F). By plotting all the individual 192 cells from the phagocytic CD3+ $\gamma\delta$ TCR+ fraction in a GFP x CD3 dot plot it is clear that the contaminating $\alpha\beta$ T cells were non-phagocytic, the majority (all except 8 out of 103 cells) of contaminant CD3/ $\gamma\delta$ TCR double negative cells were phagocytic and 1 out of a total of 12 true CD3+ $\gamma\delta$ TCR+ cells was phagocytic (Figure

4.15G). Clearly, many phagocytic cells that are not $\gamma\delta$ T cells are present in the sorted fraction. However, the low number of $\gamma\delta$ T cells present in this sample (12 cells) makes it difficult to determine whether or not this population is significantly phagocytic.

Earlier in this chapter, I presented microscopy evidence of phagocytosis in $\gamma\delta$ T cells isolated from PBMCs. However, the frequency of phagocytosis by these $\gamma\delta$ T cells was not significantly different from that of other lymphocytes tested and was very small. When testing whole blood, $\gamma\delta$ T cells appeared to be significantly more phagocytic than other lymphocytes. These cells were able to produce reactive oxygen species following phagocytosis. However, many of these cells had a granular appearance by flow cytometry light scatter and were polymorphonucleated. In addition, testing the purity of the FACS sorted fractions by re-running them in a flow cytometer revealed a high purity of $\gamma\delta$ T cells in the non-phagocytic fraction and a low purity in the phagocytic fraction, even though these were both sorted simultaneously from the same sample. It may be that the fact that phagocytic $\gamma\delta$ T cells seemed to be 10-fold rarer than their non-phagocytic counterparts amplifies the effect of any error during sorting. For example, if 1 cell out of every 10^6 in the sample is incorrectly sorted into one of the collection wells it will have a disproportionately higher effect on the phagocytic $\gamma\delta$ T cell fraction. This is because the incorrectly sorted cells will be diluted out by the non-phagocytic $\gamma\delta$ T cells (total number of cells in fraction around 10^4) much more than in the phagocytic $\gamma\delta$ T cell fractions (total number of cells in fraction around 300-500).

An alternative explanation for the presence of granulocytes in FACS sorted phagocytic CD3+ $\gamma\delta$ TCR+ fractions could be the presence of granulocytes expressing a CD3/ $\gamma\delta$ TCR complex in whole blood. Experiments to test for their presence are described in the following section.

Before FACS sorting



After FACS sorting

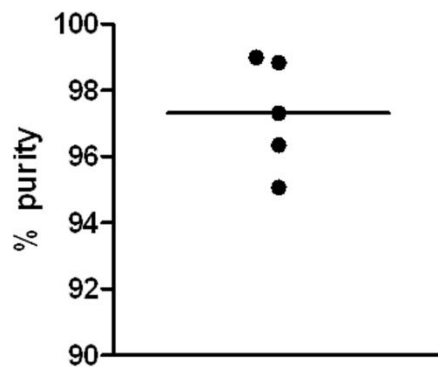
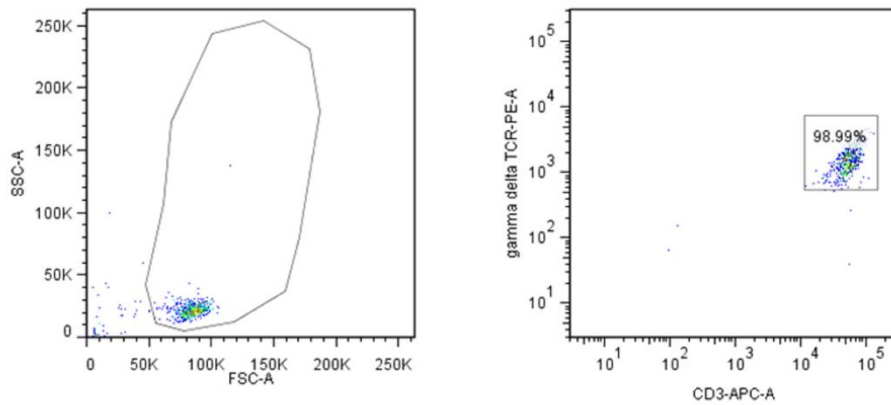


Figure 4.14 – Purity assessment of FACS sorted $\gamma\delta$ T cells by flow cytometry

Purity assessment of the FACS sorted cells used in the experiments shown in Figure 4.11 and Figure 4.13. A sample of cells was taken from the FACS sorted GFP- CD3+ $\gamma\delta$ TCR+ cells and immediately tested for purity by flow cytometry in all five assays. Representative plots from one experiment are shown. A graph with purity results for all the experiments is shown.

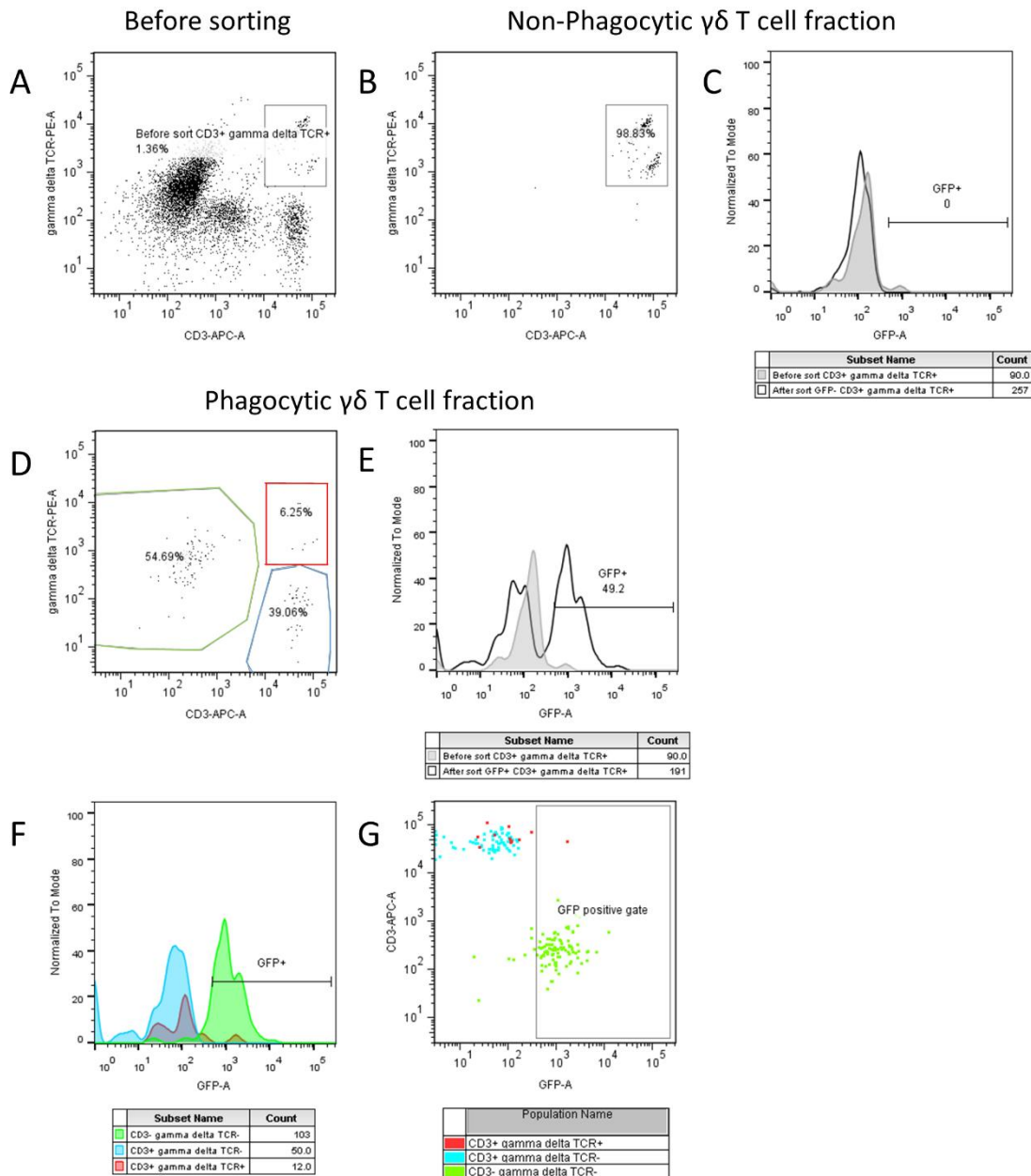


Figure 4.15 – Purity of non-phagocytic and phagocytic FACS sorted $\gamma\delta$ T cells

Non-phagocytic and phagocytic fractions of $\gamma\delta$ T cells were sorted simultaneously from the same sample for the assays described in Figure 4.11 and 4.13. Purity was routinely assessed using the non-phagocytic $\gamma\delta$ T cell fraction due to the scarcity of the phagocytic fraction. To test whether the purity of one fraction could be used as a surrogate for the other, a sample containing 192 phagocytic CD3+ $\gamma\delta$ TCR+ cells was tested for purity in one experiment. (A) Dot plot showing CD3 x $\gamma\delta$ TCR fluorescence in the original sample. (B) Purity of the non-phagocytic fraction by CD3 x $\gamma\delta$ TCR dot plot and (C) GFP histogram. (D) Purity of the phagocytic fraction by CD3 x $\gamma\delta$ TCR dot plot. 3 separate cell populations are evident. (E) Phagocytic fraction GFP histogram. (F) GFP histogram gated on the 3 separate populations shown in (D). (G) GFP x CD3 dot plot for the 3 populations gated in (D).

4.12 The $\gamma\delta$ TCR is not expressed on polymorphonucleated fractions in whole blood

Recent studies in myeloid immune cells have challenged the dogma that rearranged T cell receptors are an exclusive feature of T cells. Puellmann and colleagues demonstrated that a proportion of peripheral blood neutrophils from healthy humans express rearranged T cell receptors (291). On average, 5-8% of neutrophils in circulation were found to express variable immune receptors composed of α and β TCR chains. They also reported the presence of γ and δ TCR chains in bulk neutrophil preparations by RT-PCR and Western blot. However, what researchers commonly refer to as “neutrophil preparations” are actually the polymorphonucleated cell fractions (PMN) of blood samples. The method Puellmann et al used is commonly found in neutrophil literature and involves an initial dextran sedimentation step to remove RBC followed by a density gradient centrifugation step which separates PBMC and PMN fractions. Because neutrophils are by far the most common type of leukocyte present in the blood (50 to 70% of total leukocytes) they will constitute the vast majority of cells in PMN fractions. However, other granulocytes may also be present. Although eosinophils (1 to 3% of leukocytes) and basophils (0.5 to 1% of leukocytes) are rare when expressed as a percentage of total leukocytes, they will be enriched in PMN fractions. Accordingly, when Legrand et al replicated this work but additionally separated the granulocyte fractions into CD16+ (neutrophils and basophils) and CD16- (eosinophils), they found only the eosinophil fractions expressed a CD3/ $\gamma\delta$ TCR complex (292).

I investigated the presence of a CD3/ $\gamma\delta$ TCR complex in PMN fractions by flow cytometry in two different donors and Western blot in one additional donor. For flow cytometry, a blood sample was freshly drawn and stained for CD3, $\gamma\delta$ TCR and CD16. Granulocytes have a high refractive index due to the abundance of intracellular granules and consequently exhibit high side scatter (SSC) profiles evident by flow cytometry. A scatter plot of a fresh blood sample lysed for red blood cells will typically distinguish lymphocyte, monocyte and granulocyte populations (Figure 4.16A). I gated on lymphocytes and then on CD3+ cells to draw a CD3+ $\gamma\delta$ TCR+ gate. In addition, neutrophil and eosinophil populations were gated based on expression of CD16 together with high SSC (Figure 4.16D) as previously described (298).

Gated neutrophils (Figure 4.16E) and eosinophils (Figure 4.16F) had no significant expression of CD3 and $\gamma\delta$ TCR, as defined previously with T cells in the lymphocyte gate. This was true for both donors tested with an average CD3+ $\gamma\delta$ TCR+ of 0.29% for neutrophils and 0.64% for eosinophils. Interestingly, a small number of neutrophils but not eosinophils seemed to be CD3+ $\gamma\delta$ TCR- perhaps corresponding to the $\alpha\beta$ TCR+ neutrophils reported previously by Puellmann (291).

Intracellular staining of whole blood was not informative due to high unspecific fluorescence and the fact that permeabilising cells changes their light scatter profile (data not shown). Eosinophil cytoplasmic granules in particular are known to strongly bind some fluorescent molecules like FITC (299). In addition, unstained eosinophils exhibit unusually high autofluorescence due to the presence of native fluorescent intracellular flavins which are excited by blue-green light and emit over a broad range of wavelengths (297). High eosinophil autofluorescence is evident in Figure 4.16F. This property alone has been exploited in the past to FACS sort unstained eosinophils (297).

In previous experiments, highly autofluorescent granulocytes appeared to have been incorrectly FACS sorted into the phagocytic CD3+ $\gamma\delta$ TCR+ fractions leading to polymorphonucleated cells making up over 40% of phagocytic FACS sorted fractions (Figure 4.13). However, in the experiments described in this section no significant expression of CD3 and $\gamma\delta$ TCR was detected in neutrophils and eosinophils. Two other effects possibly worked together to result in a low purity specifically in the FACS sorted phagocytic $\gamma\delta$ T cell fraction:

- 1) Rarity – the rarer the cell type, the lower the purity of the fraction. This is due to the cumulative effect of small errors during cell sorting. The order of cell type frequency in whole blood is: granulocytes > $\alpha\beta$ T cells > monocytes \approx NK cells > $\gamma\delta$ T cells > phagocytic $\gamma\delta$ T cells.
- 2) Granulocytes autofluorescent in the CD3 and $\gamma\delta$ TCR channels will tend to be GFP+ as they will be strongly phagocytic for GFP-*E. coli*. Therefore, they will preferentially be sorted into the phagocytic CD3+ $\gamma\delta$ TCR+ fraction as opposed to the non-phagocytic CD3+ $\gamma\delta$ TCR+ fraction.

A possible solution to the problem of incorrectly FACS sorting granulocytes into the phagocytic $\gamma\delta$ T cell fraction could be to repeat the same assay using CD15 to exclude granulocytes from the $\gamma\delta$ T cell gate. CD15 is expressed on neutrophils, eosinophils and monocytes. However, although not usually found on T cells, it can be expressed on late stage activated T cells (300) and so could potentially also exclude phagocytic $\gamma\delta$ T cells. A better solution would be to repeat these experiments using PBMC fractions from healthy donors since these typically contain no granulocytes. This approach would be necessary to validate the results in Figure 4.9 that showed that an average of 12% of $\gamma\delta$ T cells in the blood (range 5.00% to 21.32%) phagocytosed opsonised *E. coli*.

Finally, even though CD3/ $\gamma\delta$ TCR complexes could not be found on the surface of neutrophils or eosinophils, it is still conceivable that intracellular stores of these markers could be mobilised to the cell surface during the bacterial assay. To investigate whether intracellular $\gamma\delta$ TCR is present in polymorphonucleated cells, PMN and PBMC fractions were isolated from one donor (Figure 4.17). Diff-Quick staining of the PMN fraction demonstrated that the fraction was rich in neutrophils, identified by their multilobed “C-shaped” nuclei and light cytoplasm, and eosinophils, with bi-lobed nuclei and strong eosin staining. As positive and negative controls for $\gamma\delta$ TCR expression, $\gamma\delta$ T cells and monocytes were purified from PBMC by direct magnetic isolation. $\gamma\delta$ TCR expression could not be detected in the PMN fraction by Western blot. A strong $\gamma\delta$ TCR signal was detected in the purified $\gamma\delta$ T cells. Curiously, a small $\gamma\delta$ TCR signal was also found in monocytes isolated with magnetic beads bound to CD14 antibodies as previously reported (293).

In conclusion, I did not find evidence that a CD3/ $\gamma\delta$ TCR complex is expressed by either neutrophils or eosinophils using flow cytometry and Western blot. However, this does not exclude the possibility that the strong autofluorescence of these cells caused them to be FACS sorted together with true CD3+ $\gamma\delta$ TCR+ cells.

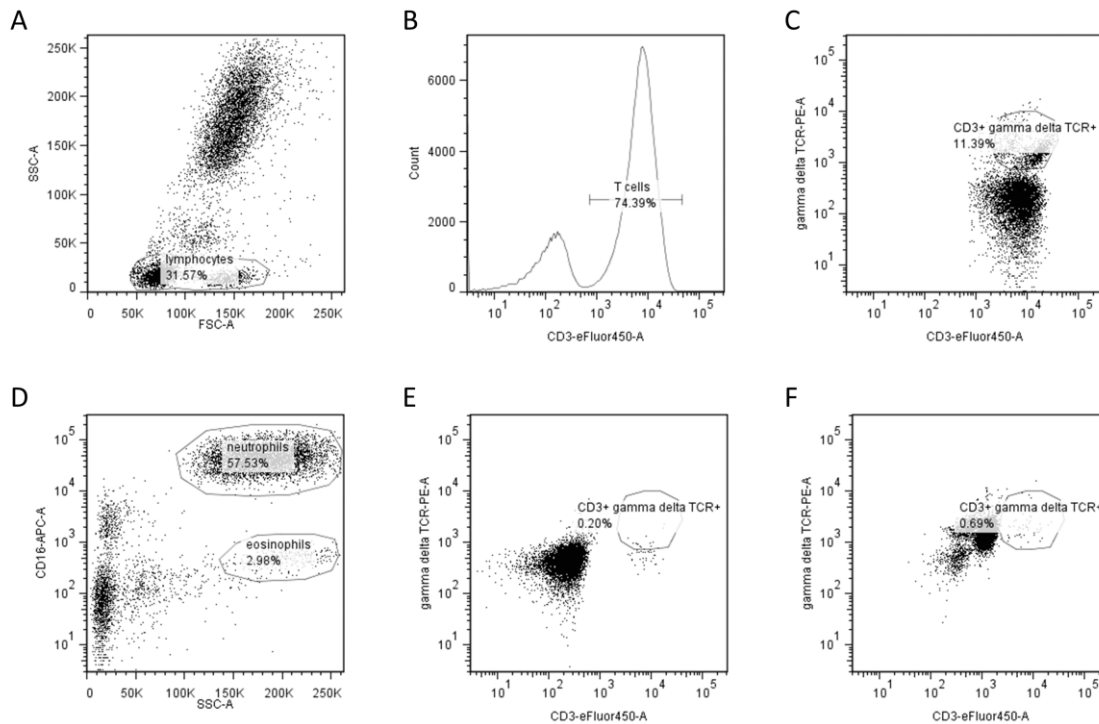


Figure 4.16 – The CD3/ $\gamma\delta$ TCR complex is not expressed in human neutrophils or eosinophils

Investigation into the possible presence of CD3/ $\gamma\delta$ TCR expressing granulocytes in whole blood. Whole blood was stained with CD3, CD16 and $\gamma\delta$ TCR antibodies. The samples were RBC lysed and fixed and analysed by flow cytometry. $\gamma\delta$ T cells were gated using sequential gating. (A) A generic lymphocyte gate was set based on FSC x SSC properties. Activated lymphocytes apparent by FSC x SSC were also included in this gate. (B) CD3+ cells in the lymphocyte gate were selected to draw a T cell gate. (C) The cells in the T cell gate were plotted on a CD3 x $\gamma\delta$ TCR dot plot to draw a CD3+ $\gamma\delta$ TCR+ region. This region was later used to probe for CD3/ $\gamma\delta$ TCR expression in granulocyte populations. (D) Dot plot of an ungated whole blood sample is used to identify neutrophils and eosinophils based on high SSC and the presence or absence of CD16. (E) CD3/ $\gamma\delta$ TCR expression in gated neutrophils. (E) CD3/ $\gamma\delta$ TCR expression in gated eosinophils.

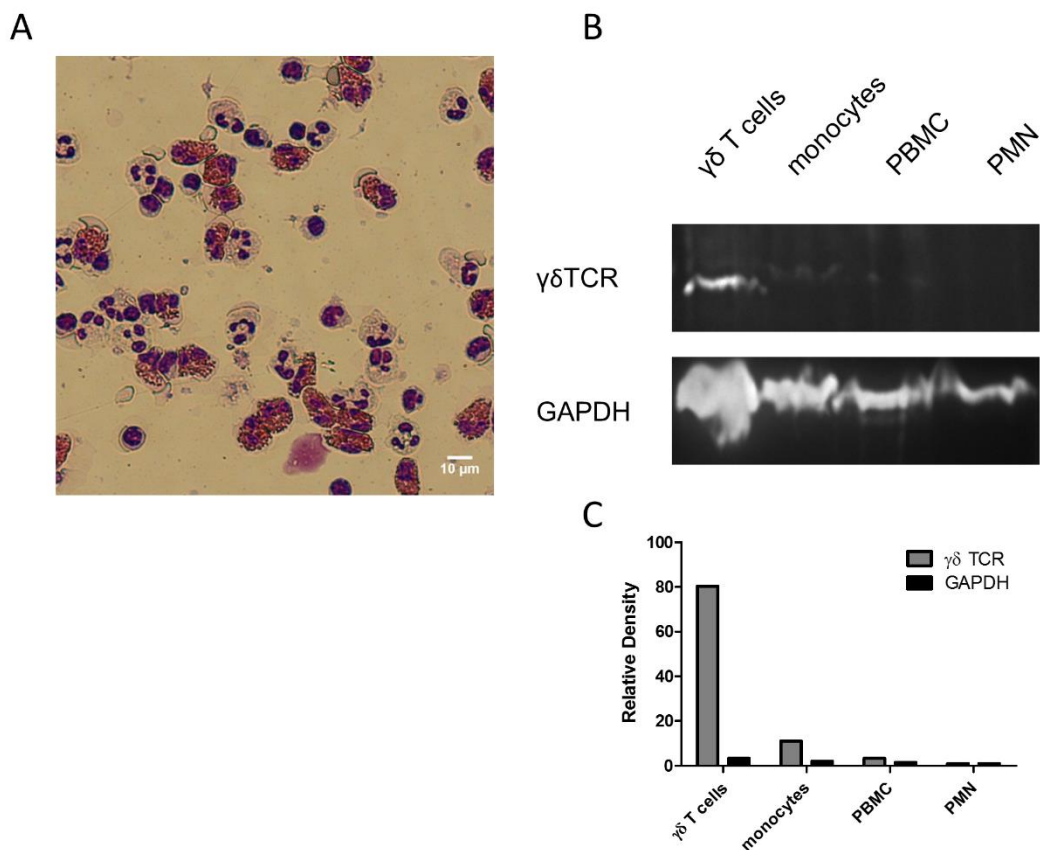


Figure 4.17 – The $\gamma\delta$ TCR is not expressed by polymorphonucleated cells

Investigation into the possible presence of $\gamma\delta$ TCR expressing granulocytes in whole blood. PMN and PBMC fractions were isolated from whole blood using dextran and density gradient separations. (A) A sample of the PMN fraction was stained with Diff-Quick. Red, eosinophil granules; dark violet, nuclei; pale pink, cytoplasm. (B) $\gamma\delta$ T cells and monocytes were purified by MACS from PBMC. The cell fractions were analysed by Western blot. The membrane was probed for $\gamma\delta$ TCR using GAPDH as a loading control. (C) A density plot of the bands is shown.

4.13 Summary

- $\gamma\delta$ T cell phagocytosis of *E. coli* was observed by confocal microscopy
- Fewer than 2% of $\gamma\delta$ T cells were identified as phagocytic using a flow cytometry assay that discriminates between intracellular and extracellular bacteria.
- Internalisation of live opsonised *E. coli* by $\gamma\delta$ T cell fractions was detected using a gentamicin protection assay. 100 bacteria per leukocyte were needed to detect phagocytosis in $\gamma\delta$ T cell fractions whereas 1 bacteria per leukocyte was sufficient to detect phagocytosis in monocyte fractions tested in parallel.
- In a blindly-scored confocal microscopy phagocytosis assay, phagocytosis was detected in 2.50% of $\gamma\delta$ T cells, which was a lower rate than that observed in monocytes (59.09%) and not significantly different from $\alpha\beta$ T cells (0.75%) and NK cells (1.70%).
- In a whole blood phagocytosis assay by flow cytometry, phagocytosis was detected in 12.21% of $\gamma\delta$ T cells and was significantly different from $\alpha\beta$ T cells (3.85%) and NK cells (1.35%). 74.59% of monocytes tested in parallel phagocytosed.
- GFP-*E. coli*+ CD3+ $\gamma\delta$ TCR+ fractions FACS sorted following a whole blood phagocytosis assay produced reactive oxygen species when tested in a NBT assay.
- Histological staining and light microscopy inspection revealed only 58.33% of GFP-*E. coli*+ CD3+ $\gamma\delta$ TCR+ fractions FACS sorted following a whole blood phagocytosis assay had a mononuclear morphology whereas the remainder were polymorphonucleated cells.
- GFP-*E. coli*- CD3+ $\gamma\delta$ TCR+ fractions could be FACS sorted following a whole blood phagocytosis assay to high purity (97.30% CD3+ $\gamma\delta$ TCR+) but GFP-*E. coli*+ CD3+ $\gamma\delta$ TCR+ fractions FACS sorted simultaneously from the same sample had a much lower purity (6.28% CD3+ $\gamma\delta$ TCR+)
- A CD3/ $\gamma\delta$ TCR complex was not detected in PMN cells by flow cytometry or by western blot.

This chapter described experiments investigating phagocytosis by human blood $\gamma\delta$ T cells. These experiments aimed to clarify the role that $\gamma\delta$ T cell phagocytosis may play in the immune response by addressing questions that have not been studied in the field. In